



Brain reorganization in an experimental model of intrauterine growth restriction

Elisenda Eixarch Roca

ADVERTIMENT. La consulta d'aquesta tesi queda condicionada a l'acceptació de les següents condicions d'ús: La difusió d'aquesta tesi per mitjà del servei TDX (www.tdx.cat) ha estat autoritzada pels titulars dels drets de propietat intel·lectual únicament per a usos privats emmarcats en activitats d'investigació i docència. No s'autoritza la seva reproducció amb finalitats de lucre ni la seva difusió i posada a disposició des d'un lloc aliè al servei TDX. No s'autoritza la presentació del seu contingut en una finestra o marc aliè a TDX (framing). Aquesta reserva de drets afecta tant al resum de presentació de la tesi com als seus continguts. En la utilització o cita de parts de la tesi és obligat indicar el nom de la persona autora.

ADVERTENCIA. La consulta de esta tesis queda condicionada a la aceptación de las siguientes condiciones de uso: La difusión de esta tesis por medio del servicio TDR (www.tdx.cat) ha sido autorizada por los titulares de los derechos de propiedad intelectual únicamente para usos privados enmarcados en actividades de investigación y docencia. No se autoriza su reproducción con finalidades de lucro ni su difusión y puesta a disposición desde un sitio ajeno al servicio TDR. No se autoriza la presentación de su contenido en una ventana o marco ajeno a TDR (framing). Esta reserva de derechos afecta tanto al resumen de presentación de la tesis como a sus contenidos. En la utilización o cita de partes de la tesis es obligado indicar el nombre de la persona autora.

WARNING. On having consulted this thesis you're accepting the following use conditions: Spreading this thesis by the TDX (www.tdx.cat) service has been authorized by the titular of the intellectual property rights only for private uses placed in investigation and teaching activities. Reproduction with lucrative aims is not authorized neither its spreading and availability from a site foreign to the TDX service. Introducing its content in a window or frame foreign to the TDX service is not authorized (framing). This rights affect to the presentation summary of the thesis as well as to its contents. In the using or citation of parts of the thesis it's obliged to indicate the name of the author.



UNIVERSITAT DE BARCELONA



DOCTORAL THESIS

Programa de Doctorat en Medicina

Universitat de Barcelona

BRAIN REORGANIZATION IN AN EXPERIMENTAL MODEL OF INTRAUTERINE GROWTH RESTRICTION

AUTHOR: ELISENDA EIXARCH ROCA

DIRECTORS: EDUARD GRATACÓS SOLSONA

FRANCESC FIGUERAS RETUERTA

Universitat de Barcelona

Divisió de Ciències de la Salut

Facultat de Medicina

Departament d'Obstetrícia i Ginecologia, Pediatria, Radiologia i Medicina Física.

Programa de Doctorat de Medicina RD 1393/2007

A thesis submitted by Elisenda Eixarch Roca for the PhD degree (Doctor in Medicine, Faculty of Medicine, University of Barcelona) including the mention of "European Doctor" under the direction of Eduard Gratacós Solsona, Professor of Obstetrics and Gynecology at Barcelona University and Francesc Figueras Retuerta, Associate Professor of Obstetrics and Gynecology at Barcelona University.

Elisenda Eixarch Roca

Barcelona, September 2011.

Professor Eduard Gratacós Solsona

Professor Francesc Figueras Retuerta

Department of Maternal-Fetal Medicine, Hospital Clínic

Department of Obstetrics and Gynecology, Pediatrics, Radiology and Pathology,

Faculty of Medicine, University of Barcelona

We confirm that Elisenda Eixarch Roca has conducted under our supervision the studies presented in the thesis “Brain reorganization in an experimental model of intrauterine growth restriction”. The present thesis has been structured following the normative for PhD theses as a compendium of publications for the degree of Doctor of European Doctor in medicine, and that the mentioned studies are ready to be presented to the Tribunal.

Eduard Gratacós Solsona

Francesc Figueras Retuerta

Barcelona, September 2011

PRESENTATION

This thesis project has been structured following the normative for PhD thesis as a compendium of publications. The studies included in the thesis belong to the same research line leading to three papers already published or submitted for publication in international journals:

1. Eixarch E, Hernandez-Andrade E, Crispi F, Illa M, Torre I, Figueras F, Gratacos E. **Impact on fetal mortality and cardiovascular Doppler of selective ligation of uteroplacental vessels compared with undernutrition in a rabbit model of intrauterine growth restriction.** Placenta. 2011 Apr; 32(4):304-9.

State: published

Impact factor: 3.060

Quartile: 1st

2. Eixarch E, Figueras F, Hernández-Andrade E, Crispi F, Nadal A, Torre I, Oliveira S, Gratacós E. **An Experimental Model of Fetal Growth Restriction Based on Selective Ligation of Uteroplacental Vessels in the Pregnant Rabbit.** Fetal Diagn Ther. 2009; 26(4):203-11.

State: published

Impact factor: 0.962

Quartile: 4th

3. Eixarch E, Batalle B, Illa M, Muñoz-Moreno E, Arbat A, Amat-Roldan I, Figueras F, Gratacos E. **Neonatal neurobehavior and diffusion MRI changes in brain reorganization due to intrauterine growth restriction in a rabbit model.** PLoS ONE. Submitted

State: submitted, under review

Impact factor: 4.610

Quartile: 1st

TABLE OF CONTENTS

1. Introduction	
1.1. Intrauterine growth restriction: consequences in neurodevelopment	15
1.2. Placental insufficiency and brain damage of prenatal origin	16
1.3. Animal models of IUGR	17
1.4. Evaluation of brain damage in experimental models	19
1.5. From animal to clinics: relevance of this project	21
2. Hypotheses	25
3. Objectives	29
4. Material and methods	
4.1. Project 1	33
4.2. Project 2	35
4.3. Project 3	37
4.4. Description of research methodology	
4.4.1. Surgical protocol	39
4.4.2. Undernutrition protocol	40
4.4.3. Ultrasound evaluation	41
4.4.4. Neurobehavioral evaluation	44
4.4.5. Diffusion MRI	45
5. Results	
5.1. Project 1	51
5.2. Project 2	55
5.3. Project 3	59

6. Discussion	
6.1. General overview	67
6.2. Project 1	69
6.3. Project 2	75
6.4. Project 3	81
7. Conclusions	93
8. References	97
9. Acknowledgments	119
10. Annexes	
10.1. Project 1: Ethic committee approval	125
10.2. Project 2: Ethic committee approval	126
10.3. Project 3: Ethic committee approval	127
11. Papers:	
11.1. Project 1: a copy of published paper	131
11.2. Project 2: a copy of published paper	141
11.3. Project 3: a copy of submitted paper	153

1. INTRODUCTION

1.1. Intrauterine growth restriction: consequences in neurodevelopment

Intrauterine growth restriction (IUGR) due to placental insufficiency affects 5-10% of all pregnancies. This condition is associated with an increased risk of stillbirth, perinatal morbidity and neonatal mortality [1]. In addition, IUGR is also a risk factor for brain damage after birth [2] and cognitive disorders later in childhood [3].

The association between IUGR and short [4, 5] and long-term [4, 6-12] neurodevelopmental and cognitive dysfunctions has been extensively described. In the neonatal period, neurodevelopmental dysfunctions have been reported in IUGR babies, being attention, habituation, regulation of state, motor and social-interactive competencies the most affected [5]. Regarding long-term effects, many studies have found associations between preterm IUGR and later behavioural [7, 13, 14], sensorial [12, 15], and cognitive [8-11] dysfunctions. Long-term outcomes for such infants reveal a specific profile of neurocognitive difficulties, with poor executive functioning, cognitive inflexibility, poor creativity, and language problems [8, 10]. Furthermore, suboptimal neurodevelopment with cognitive disadvantages [4, 16, 17], increase risk of attention deficit/hyperactivity disorder [18], and social skills [6] have also been described in term IUGR.

Changes in brain structure of IUGR children have also been consistently demonstrated by magnetic resonance imaging (MRI) [13, 19-22]. In neonatal period, decreased volume in gray matter (GM) [13] and hippocampus [19], and major delays in cortical development [20] have been reported in neonates with IUGR. These structural changes have also been described in childhood, when it has been demonstrated reduced GM volumes [21] and decreased fractal dimension of both GM and white matter (WM) [22].

1.2. Placental insufficiency and brain damage of prenatal origin

Placental insufficiency occurring in IUGR produces a reduction of placental blood flow resulting in chronic exposure to hypoxemia and undernutrition [23] and this has consequences on the developing brain [24]. Chronic hypoxia in IUGR is mainly due to reduction of maternal-fetal oxygen exchange as a result of abnormal placental development [25]. In most cases, the fetus tries to adapt to hypoxic conditions by reducing his growth and activity and redistributing blood flow to the principal organs, such as the brain and heart [23]. This blood flow redistribution to brain in IUGR fetuses, which is called “brain sparing”, follows a regional pattern with increased perfusion in frontal area in early stages followed by a decrease in frontal area and increase in basal ganglia perfusion when fetal deterioration occurs [26]. However, evidence of the protective effect of this mechanism is controversial. Recent studies have demonstrated that 15-20% of term SGA fetuses with normal umbilical artery Doppler have vasodilation in the MCA, and that this sign is associated with poorer perinatal outcome [27] and increased risk of abnormal neurobehavior neonatally [28, 29] and at two years of age [6].

This regionality described in the “brain sparing” mechanism supports the hypothesis that brain damage of prenatal origin due to chronic hypoxia has also a regional distribution. Human and animal studies have demonstrated that fetal brain damage is related to the onset, severity and extent of the hypoxic insult. Animal models of acute hypoxia in early pregnancy have shown an increased vulnerability of Purkinje cells in the cerebellum, pyramidal cells in the hippocampus and cortical neurons [30]. Late in pregnancy, acute hypoxia produces neuronal death in the cerebral cortex and striatum [31], whereas

hippocampal and cerebellar neurons do not appear to be affected at the gross level. In term pregnancies, the white matter is damaged but less extensively than when insults are delivered earlier in gestation; this appears to be due to the vulnerability of immature oligodendrocytes to hypoxemia [32]. Experimental models of chronic hypoxia have also demonstrated a regional pattern of brain damage development with decreased myelination of white matter axons and reduced number of neurons [33]. Clinical studies showed that in term infants exposed to intrauterine hypoxia neurological damage is mainly expressed in neurons while in premature infants is presented as a reduction in glial cells and white matter damage [24]. In fact, as previously described, long-term follow up of IUGR infants have demonstrated abnormalities in specific developmental areas which correlate with specific brain areas including, frontal and temporal cortex [6, 8, 9, 18], hippocampus [19], and striatum [34].

1.3. Animals models of IUGR

While it is well established that placental insufficiency occurring in IUGR produces changes in brain development, the pathophysiological pathways leading to adverse neurodevelopmental outcome and brain reorganization among growth restricted babies remain poorly understood [35]. The use of animal models is essential to advance in the understanding of brain injury in IUGR, but reproducing the features of the human condition in an experimental model is challenging.

Animal models described so far have been based either in maternal food restriction or in surgical reduction of placental mass and/or blood supply [36, 37]. Food restriction models do not involve a decrease in fetal oxygen supply, which

may be a critical factor in the pathogenesis of brain injury [24]. Uteroplacental embolization [38, 39] and bilateral uterine artery ligation [40] result in massive, non-predictable reductions of placental blood supply [41]. A systematic review of the latter technique concludes that it lacks of efficacy in reproducing the growth restriction in the offspring [42]. The uterine vasculature in some animal models allows selective ligation of a proportion of the vessels supplying each gestational sac, which should theoretically allow to achieve a gradable and more reproducible model of growth restriction. As an alternative, methods based on ligation of utero-placental vessels [43-46] are proposed as more appropriate models to achieve a combined restriction of nutrients and oxygen, and to better assess the impact of IUGR on fetal and neonatal brain [47].

Choosing the appropriate animal model to extrapolate to the clinical condition of placental insufficiency requires similarities in the involved organs. Firstly, human placenta is hemochorial, in which maternal blood is in direct contact with the chorion. Secondly, brain maturation in humans is characterized by beginning in second trimester and continuing during the first years of life, that is, a perinatal maturation [48]. The association between hypoxic insult and neural damage has been previously documented in the hypoxic lamb model at the later third of gestation [49]. However, sheep have an epitheliochorial placenta [50] and prenatal brain maturation and by the time of birth, most of the white-matter tracts are myelinated [51]. Rodents have also been extensively used as a model for placental insufficiency [36] and brain damage [52]. Nevertheless, myelination begins postnatally in rats and mice [53] and the paucity of white matter in these species does not allow to replicate human neurological lesions [52]. Rabbit model has been proposed before to study intrauterine growth restriction [44] and acute

brain damage [51, 54, 55]. This model has several advantages compared with rodents and sheep. First, the placenta of the rabbit is discoid, villous, and hemodichorial [50], much similar to the human placenta. Second, there is a possibility to graduate the reduction of blood flow to each gestational sac [44] and to compare control and case fetuses obtained from the same pregnancy. Finally, rabbits resemble humans more closely than other species in terms of the timing of perinatal brain white matter maturation [54]. Because myelination in rabbits starts around term, rabbits may be more appropriate models for demonstrating neonatal brain injury from insults occurring in the perinatal period [51].

1.4. Evaluation of brain damage in experimental models of IUGR

Contrary to acute perinatal events, IUGR is a chronic condition that induces brain reorganization and abnormal maturation rather than gross tissue destruction [33]. In order to reveal these subtle differences in brain development, different approaches to characterize these changes should be used.

At the cellular level, regional consequences could be assessed evaluating expression of histological markers of brain injury and proliferation. S100 β is a calcium-binding protein which is mainly present in the cytosol of glial cells of the central and peripheral nervous system [56]. “In vitro” studies have demonstrated that S100 β is actively secreted by astrocytes under hypoxic conditions [57] and serum levels of this protein are increased in several forms of brain injury. Thus, this parameter has been suggested as a biochemical marker of brain damage [58]. In clinical studies, increased values of S100 β have been demonstrated after neonatal asphyxia [59], but also in neonates with IUGR, especially in those with “brain sparing” [60]. Ki-67 is a nuclear protein that is expressed by proliferating

cells [61] and this protein is present during all active phases of the cell cycle, but is absent from resting cells. Changes in cell proliferation in the central nervous system have been previously described in response to either acute [62, 63] or chronic hypoxic damage [64]. Thus, regional differences in expression of these two proteins; S100 β and Ki-67, could be useful to assess effects of IUGR in brain development.

Changes in brain organization could also be assessed by means of magnetic resonance imaging (MRI). Diffusion MRI measures the diffusion of water molecules in tissues and obtains information about brain microstructure and the disposition of fiber tracts [65]. White matter fibers are organized in bundles, consequently water molecules diffuse more freely along the direction of the fibers but are restricted in their movement perpendicular to the fibers (anisotropic diffusion). In order to describe tissue characteristics two main parameters are used: Apparent Diffusion Coefficient (ADC) that gives information about overall magnitude of water diffusion and Fractional anisotropy (FA) which indicates the degree of anisotropic diffusion [66]. Diffusion MRI has been consistently shown to be highly sensitive to changes after acute hypoxia in adults [67, 68] and fetuses [66, 69]. Aside from reflecting acute injury, diffusion MRI parameters seem to correlate well with brain maturation and organization in fetal and early postnatal life [66, 69]. In addition, preliminary clinical results suggests that diffusion MRI could also be suitable to detect maturational changes occurring in chronic fetal conditions, including fetal cardiac defects [70] and IUGR [71]. Use of diffusion MRI in experimental models allows to perform MRI with long acquisition periods in fixed whole brain preparations. This approach allows high resolution images which can reveal submillimetric structures, particularly in the

gray matter, which is difficult to measure in the *in vivo* images [72]. Such high quality would be difficult to achieve *in vivo* due to motion artifacts and limited acquisition times.

Brain reorganization could also be revealed by demonstrating changes in neurobehavioral performance. The behavioral repertoire of newborn rabbits is somewhat limited. Compared with humans, rabbits are slightly more capable in motor development at birth [73] and at postnatal day 1, but sensory development is about the same as that of humans [51]. Based on the capabilities of the rabbit newborn pup, objective and standardized evaluation of neurobehavior can be performed in neonatal period [54]. Previous studies suggest the ability of the rabbit model to illustrate the neonatal effects of acute severe prenatal conditions. Thus, hypoxic-ischemic injury and endotoxin exposure produce hypertonic motor deficits [54, 74], reduced limb movement [75] and olfactory deficits [76] in this model.

1.5. From animal to clinics: relevance of this project

As previously mentioned, IUGR affects 5-10% of all newborns worldwide and it is a well-recognized cause of abnormal neurodevelopmental outcome during childhood. Prediction of neurodevelopmental outcome during infancy and childhood is a recognized clinical need. However, there is limited understanding of brain organization processes behind the restriction of oxygen and nutrients brought about by intrauterine growth restriction. In order to advance in this direction, is essential the use of animal models.

The studies included in this project are part of a research line on the development of imaging biomarkers of brain reorganization in IUGR to predict

1. INTRODUCTION

abnormal neurodevelopment. Developing the appropriate animal model, describing regional pattern depending on severity and onset of injury and describing functional and structural effects in neonatal period, could be useful information which will contribute to the understanding of brain reorganization under chronic prenatal conditions. In addition, the studies included in this project provide a new experimental setting to develop future studies to test the impact of interventions aimed at improving neurodevelopmental outcomes.

2. HYPOTHESES

Intrauterine growth restriction induces brain injury and reorganization in an experimental model on the fetal rabbit, and this model can be used to describe in detail the anatomical patterns of brain reorganization by MRI and to describe their neurobehavioral correlates

Specific hypotheses

1. An animal model based in selective ligation of uteroplacental vessels in the pregnant rabbit is a suitable model of intrauterine growth restriction, which reproduces better the human disease in comparison with an undernutrition model.
2. The regional pattern and severity of brain damage depends on severity and onset of placental insufficiency in a surgical model of intrauterine growth restriction in the pregnant rabbit.
3. Neurobehavioral abnormalities produced by intrauterine growth restriction are correlated with changes in brain reorganization demonstrable by high-resolution magnetic resonance imaging diffusion techniques

3. OBJECTIVES

To develop a suitable experimental model of intrauterine growth restriction in fetal rabbits, in order to conduct a detailed MRI description of the neurostructural brain abnormalities associated with this disease and their neurobehavioral correlates.

Specific objectives

1. To evaluate the best experimental model of intrauterine growth restriction in fetal rabbits by comparing selective ligature of uteroplacental vessels with a model based on maternal undernutrition in pregnant rabbit.
2. To demonstrate the effects of different timings and severity of intervention in the best performing model, in terms of fetal mortality, biometrical restriction and histological markers of brain injury.
3. To describe the anatomical pattern of fetal brain maturation changes and their neurobehavioral correlates by developing a high-resolution magnetic resonance imaging diffusion approach.

4. MATERIAL AND METHODS

To achieve the main and specific objectives, three different projects were planned and performed as explained below.

4.1. Project 1: Comparison of two experimental models of IUGR: undernutrition versus. selective ligation of uteroplacental vessels

Study design: Controlled laboratory study.

Study population: New-Zealand rabbits at 25 days gestation were included in a surgical (ligature 40-50%) or undernutrition protocol (reduction 70% of normal diet) and three different groups were obtained:

- a. Growth restricted rabbits by surgical protocol
- b. Growth restricted rabbits by undernutrition
- c. Control rabbit

Interventions:

- Prenatal induction of IUGR at 25 days of gestation: surgical and undernutrition protocol
- Ultrasound evaluation before delivery
- Cesarean section at 30 days gestation
- Sacrifice and samples collection

Measures:

- a. **Prenatal ultrasound evaluation:**
 - i. Abdominal perimeter

- ii. Pulsed Doppler: Umbilical artery pulsatility index (UAPI) and Middle cerebral artery pulsatility index (MCAPI).
- iii. Echocardiography: Ductus venosus pulsatility index (DVPI), Aortic isthmus pulsatility index (AoIPI), isovolumetric contraction time (ICT), ejection time (ET), isovolumetric relaxation time (IRT) and myocardial performance index (MPI).

b. Delivery data: neonatal and placental weight, crown-rump length, anterior-posterior cranial diameter, transverse cranial diameter and brain weight.

Outcome variables: Mortality, neonatal and placental weight, crown-rump length, cephalic perimeter, brain weight, UAPI, MCAPI, DVPI, AoIPI, ICT, ET, IRT and MPI.

4.2. Project 2: Evaluation of different timings and severity of the intervention: comparison of the effects of late versus early onset, and of various proportions of vessels ligated in a model of IUGR based on selective ligation of uteroplacental vessels

Study design: Controlled laboratory study.

Study population: New-Zealand rabbits were included at two different moments of pregnancy: 21 or 25 days gestation. Within each group, surgical protocol was performed with two degrees of ligation (20-30% (mild) or 40-50% (severe)) obtaining six different groups:

- a. 21 D Controls
- b. 21 D Mild reduction
- c. 21 D Severe reduction
- d. 25 D Controls
- e. 25 D Mild reduction
- f. 25 D Severe reduction

Interventions:

- Prenatal induction of IUGR at 21 or 25 days of gestation by means of mild or severe reduction
- Cesarean section at 30 days gestation
- Sacrifice, samples collection and processing: S100 β and Ki-67 immunohistochemistry staining

4. MATERIAL AND METHODS

- Quantification of positive cells for S100 β and Ki-67 immunohistochemistry staining

Measures:

- a. Delivery data:** neonatal and placental weight, crown-rump length, anterior-posterior cranial diameter, transverse cranial diameter and brain weight.
- b. Immunohistochemistry:** ratios of positive cells over total number of cells for S100 β and Ki-67.

Outcome variables: Mortality, neonatal and placental weight, crown-rump length, cephalic perimeter, brain weight, ratio S100 β positive cells and ratio Ki67 positive cells.

4.3. Project 3: Development of a high-resolution brain MRI diffusion approach to describe the anatomical patterns of brain reorganization induced by IUGR and to describe the postnatal neurobehavioral correlates of the neurostructural changes.

Study design: Controlled laboratory study.

Study population: New-Zealand rabbits at 25 days gestation were included in a surgical protocol and two different groups were obtained:

- a. Growth restricted rabbits
- b. Control rabbits

Interventions:

- Prenatal induction of IUGR at 25 days of gestation: surgical protocol
- Cesarean section at 30 days gestation
- Neurobehavioral evaluation
- Sacrifice and samples collection
- Diffusion MRI acquisition
- Global and regional analysis of diffusion parameters

Measures:

- a. **Delivery data:** neonatal weight.
- b. **Neurobehavioral evaluation**
- c. **Diffusion MRI:** Apparent diffusion coefficient (ADC), Fractional anisotropy (FA), axial and radial diffusivity and coefficients of linearity, planarity and sphericity.

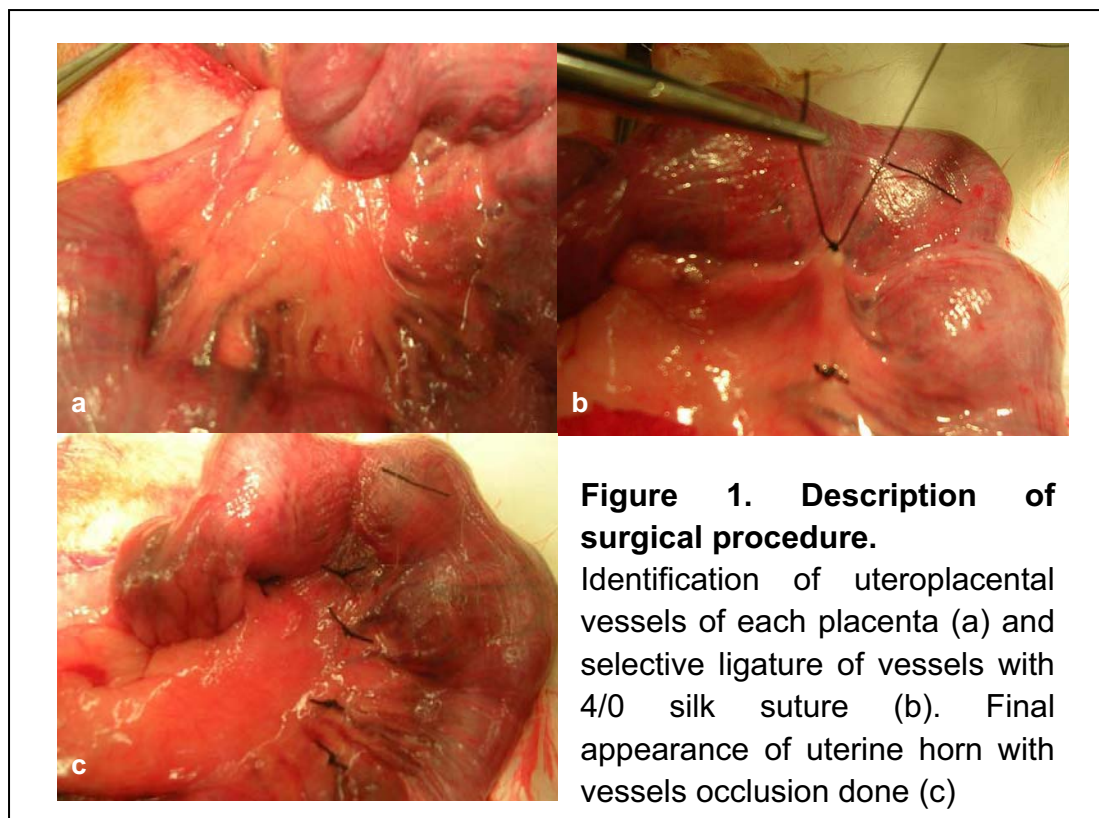
4. MATERIAL AND METHODS

Outcome variables: Neonatal weight, neurobehavioral evaluation scores, ADC and FA.

4.4. Description of research methodology

4.4.1. Surgical protocol

Prior to surgery, progesterone 0,9 mg/kg was administered intramuscularly for tocolisis. A peripheral ear venous catheter was placed and antibiotic prophylaxis (Penicillin G 300.000 UI) was administered. Ketamine 35 mg/kg and Xylazine 5mg/kg were given intramuscularly for anesthetic induction. Inhaled anesthesia was maintained with a mixture of 1-5% isoflurane and 1-1.5 L/min oxygen. Maternal heart rate, oxygen saturation, central temperature and blood pressure were monitored during the procedure (Pluto Veterinary Medical Monitor, Bionics corp.). An abdominal midline laparotomy was performed and both uterine horns were exteriorized. Gestational sacs of both horns were counted and numbered and each fetus was identified taking into account the fetal position within the bicornuate uterus. The fetus at the ovarian end was considered to be the first fetus. At random, one horn was assigned as the case horn and the other horn was considered as the control horn (no procedure was performed). In the case horn, part of the uteroplacental vessels of all gestational sacs were ligated in a proportion of 20-30% or 40-50%, according to the experimental group. Ligatures were performed with silk sutures (4/0) (Figure 1). The exteriorized sacs were continuously rinsed with warm ringer lactate solution. After the procedure the abdomen was closed in two layers with a single suture of silk (3/0). Animals were kept under a warming blanket until they awoke and became active, and received intramuscular meloxicam 0.4 mg/kg/24 h for 48 h, as postoperative analgesia. The animals were again housed and their well-being was controlled daily.

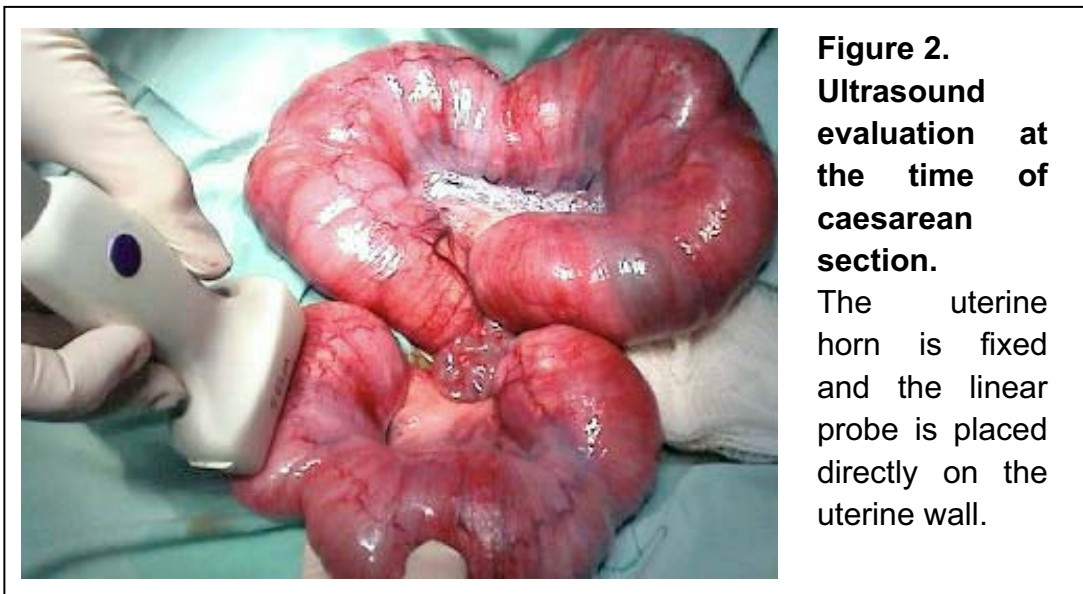


4.4.2. Undernutrition protocol

At 25 days of gestation, a sham-surgery following the surgical protocol previously described was performed. Briefly, after the abdominal midline laparotomy, the gestational sacs of both horns were counted and numbered. Then, both uterine horns were placed back into the abdominal cavity and abdomen was closed in two layers with a single silk suture (3/0). Postoperative analgesia was administered and animals were again housed and well-being was controlled each day. After surgery, severe undernutrition was induced by restricting 70% of the normal diet (45 g/day of standard chow) for 5 days until delivery.

4.4.3. Ultrasound evaluation

Ultrasound evaluation (US) was performed using a Siemens Sonoline Antares (Siemens Medical Systems, Malvern, PA, USA) with a 14-10 MHz linear probe. The US examination was performed under anesthesia placing the probe directly on the uterine wall before fetal extraction at the time of the caesarean section (Figure 2). The angle of insonation was $<30^\circ$ in all measurements and a 70 Hz high pass filter was used to avoid slow flow noise.



Parameters included in the US evaluation are depicted in Figure 3:

- Abdominal perimeter measured in a transverse view of the fetal abdomen at the level of the intrahepatic umbilical vein.
- Umbilical artery pulsatility index (UAPI) was calculated in a free-floating portion of the umbilical cord.

- Middle cerebral artery pulsatility index (MCAPI) was measured in a transverse view of the fetal skull at the level of the circle of Willis.
- Ductus venosus pulsatility index (DVPI) was obtained in a midsagittal or transverse section of the fetal abdomen positioning the Doppler gate at its isthmic portion.
- Aortic isthmus pulsatility index (AoIPI) was also obtained in a sagittal view of the fetal thorax with a clear view of the aortic arch, placing the sample volume between the origin of the last vessel of the aortic arch and the aortic joint of the ductus arteriosus.
- Myocardial performance index (MPI) was evaluated in the left fetal cardiac ventricle, as previously described [12]. Briefly, Doppler sample volume was placed on the lateral wall of the ascending aorta in an apical 4-chamber view. The time-periods were then estimated as follows: isovolumetric contraction time (ICT) from the closure of the mitral valve to the opening of the aortic valve, ejection time (ET) from the opening to the closure of the aortic valve, and isovolumetric relaxation time (IRT) from the closure of the aortic valve to the opening of the mitral valve (Figure 3). The final MPI was calculated as: $(ICT+IRT)/ET$.

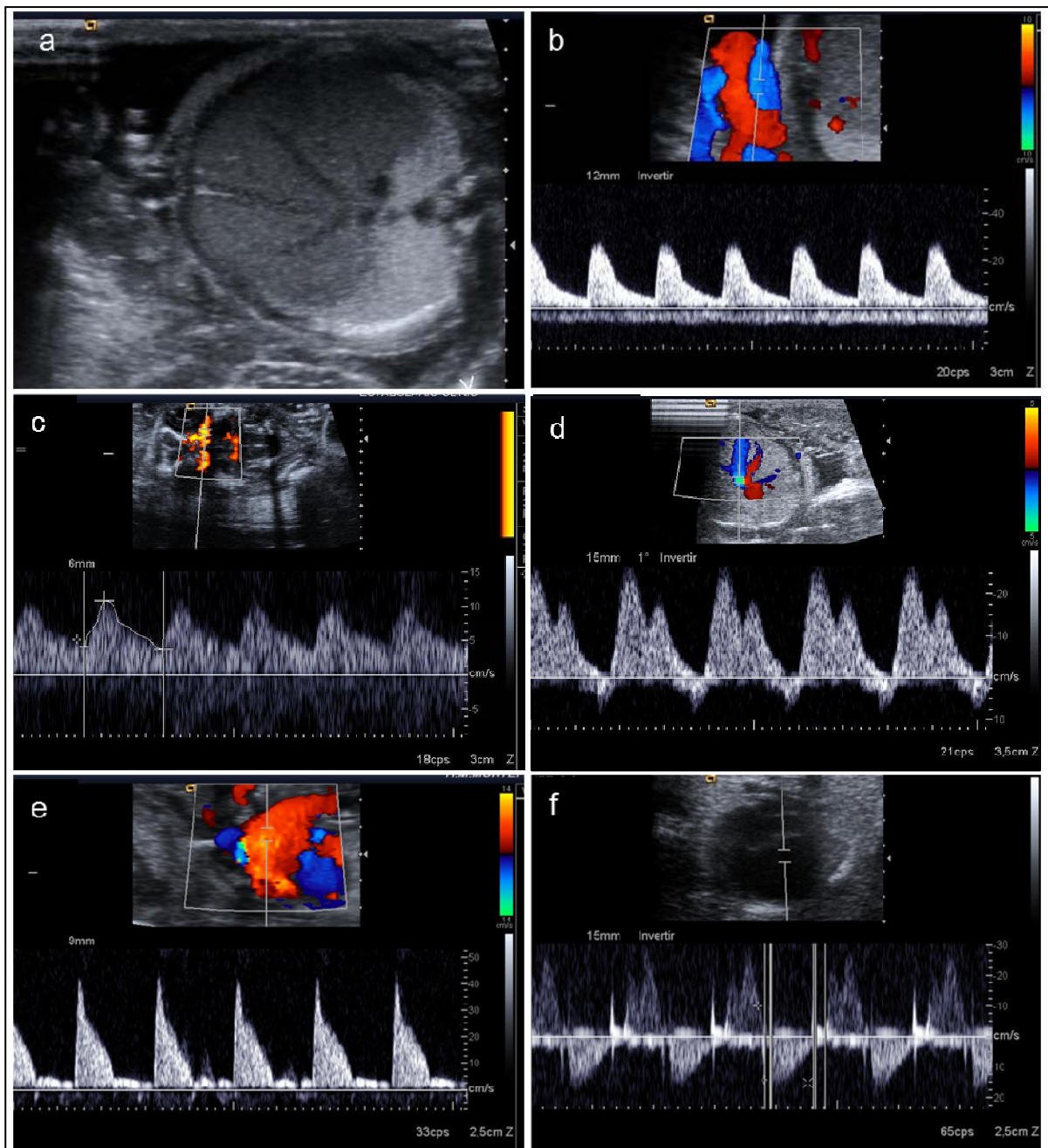
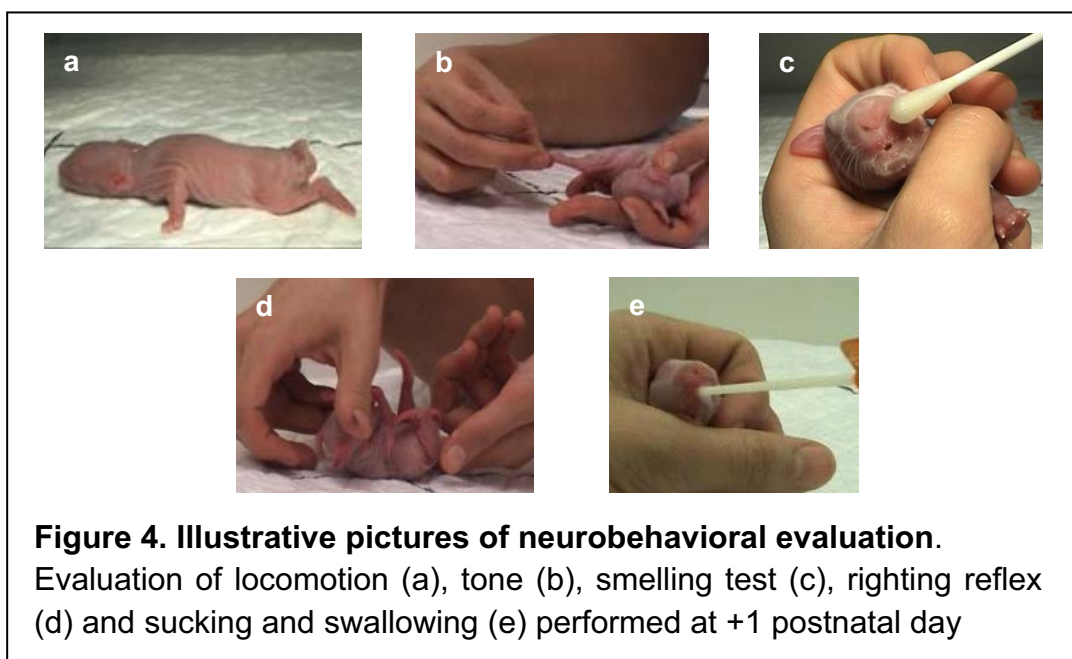


Figure 3. Biometric and Doppler measurements.

(a) abdominal perimeter measured in a transverse view of the fetal abdomen, (b) UAPI obtained in a free-floating portion of the umbilical cord, (c) MCAPI obtained in a transverse view of the fetal skull at the level of the circle of Willis; (d) DVPI acquired in a midsagittal section of the fetal abdomen (e) AoIPI obtained in a sagittal view of the fetal thorax; (f) MPI evaluated in an apical 4-chamber view.

4.4.4. Neurobehavioral evaluation

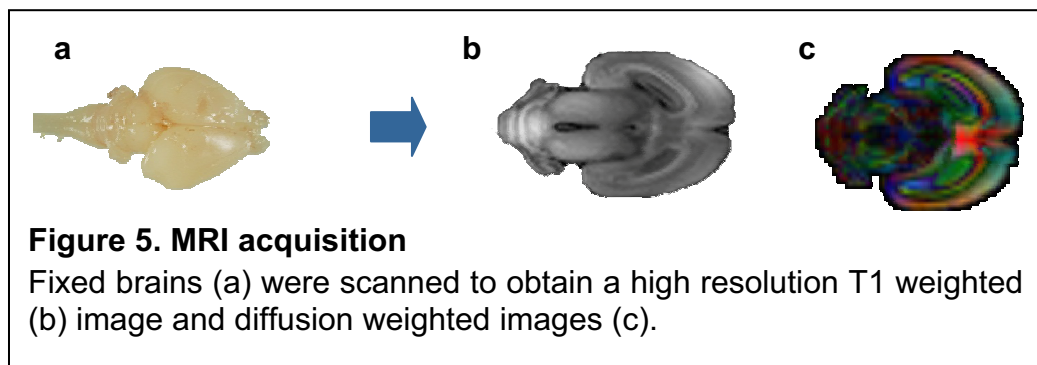
Neurobehavioral evaluation was performed at postnatal day +1 following methodology previous described by Derrick et al. [35]. For each animal, the testing was videotaped and scored on a scale of 0–3 (0, worst; 3, best) by a blinded observer. Locomotion on a flat surface was assessed by grading the amount of spontaneous movement of the head, trunk, and limbs. Tone was assessed by active flexion and extension of the forelimbs and hindlimbs (0: No increase in tone, 1: Slight increase in tone when limb is moved, 2: Marked increase in tone but limb is easily flexed, 3: Increase in tone, passive movement difficult, 4: Limb rigid in flexion or extension). The righting reflex was assessed when the pups were placed on their backs and the number of times turned prone from supine position in 10 tries was registered. Suck and swallow were assessed by introduction of formula (Lactadiet with omega 3; Royal Animal, S.C.P.) into the pup's mouth with a plastic pipette. Olfaction was tested by recording time to aversive response to a cotton swab soaked with pure ethanol.



4.4.5. Diffusion MRI

4.4.5.1. Acquisition

MRI was performed on fixed brains (4% paraformaldehyde phosphate-buffered saline for 24 hours at 4 °C) using a 7T animal MRI scanner (Bruker BioSpin MRI GMBH). High-resolution three-dimensional T1 weighted and diffusion weighted images (DWI) were acquired. Specifically, DWI was acquired by using a standard diffusion sequence covering 126 gradient directions with a b-value of 3000 s/mm² together with a reference (b=0) image.



4.4.5.2. Processing

As a first step, the brain was segmented from the background. The 126 weighted image (iDWI) that was used to create a binary mask to segment the brain from the background, in a similar way as previously described [77]. In brief, iDWI of each subject was min-max normalized, and non-brain tissue values were estimated to have values below 5% of the maximum of the iDWI normalized volume. After applying the threshold, internal holes in the mask were filled by 3D morphological closing and isolated islands were removed by 3D morphological opening. This mask was used to estimate brain volume and constrain the area where the diffusion related measures were analyzed.

Tensor model of diffusion MRI was constructed by using MedINRIA 1.9.4 [78] (available at www-sop.inria.fr/asclepios/software/MedINRIA/). Once the tensors were estimated at each voxel inside the brain mask, a set of measures describing the diffusion were computed: apparent diffusion coefficient (ADC), fractional anisotropy (FA), axial and radial diffusivity and the coefficients of linearity, planarity and sphericity [65, 79]. They are all based on the three eigenvalues of each voxel tensor (λ_1 , λ_2 , λ_3). ADC measures the global amount of diffusion at each voxel, whereas axial diffusivity measures the diffusion along the axial direction, that is, along the fiber direction. On the other hand, radial diffusivity provides information of the amount of diffusion orthogonal to the fiber direction. The other parameters are related to the shape and anisotropy of the diffusion. FA describes the anisotropy of the diffusion, since diffusion in fibers is highly anisotropic its value is higher in areas where fiber bundles are [65]. Linearity, planarity and sphericity coefficients describe the shape of the diffusion; higher values of the linear coefficient indicates that diffusion occurs mainly in one direction; higher planarity involves that diffusion is performed mostly in one plane, and higher values of sphericity are related to isotropic diffusion [79].

4.4.5.3. Analysis

4.4.5.3.1. Global analysis

The parameters described in the previous section were computed at each voxel belonging to the brain mask, and their value was averaged in the whole brain, in order to perform a global analysis of the differences between controls and IUGR. In addition, so as to avoid potential confounding values produced

by GM and cerebrospinal fluid (CSF), a second mask was applied to analyse the changes in the WM.

4.4.5.3.2. Regional analysis

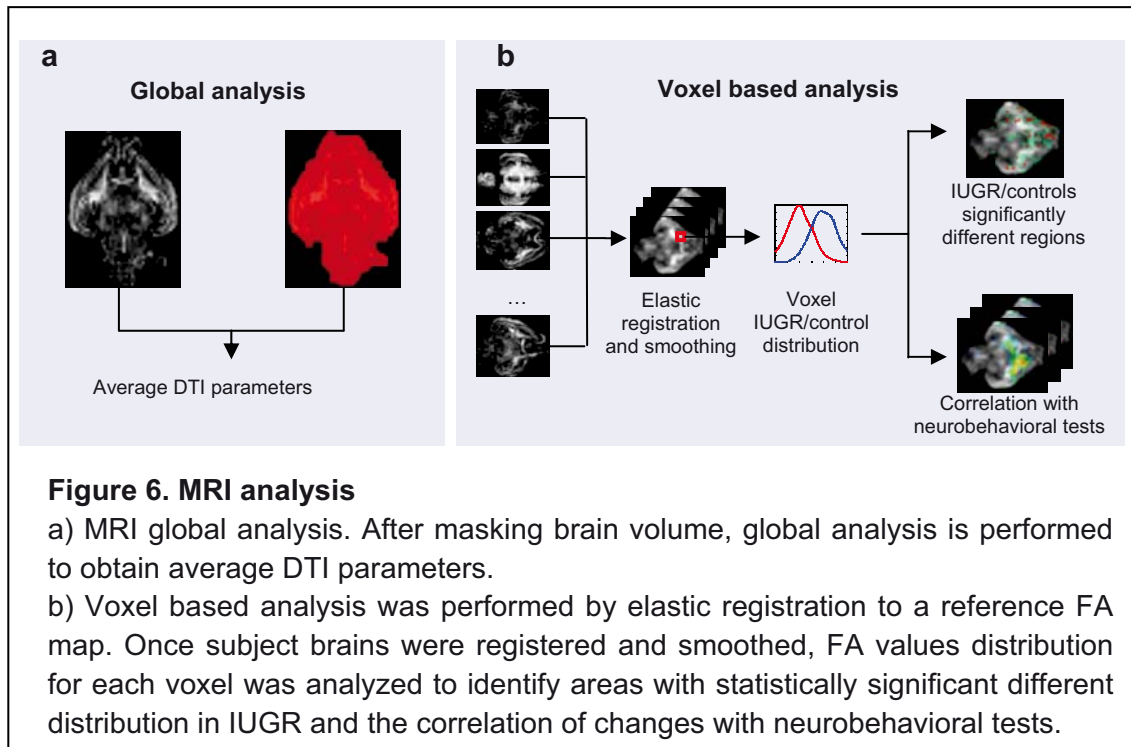
Manual delineation

Manual delineation of GM regions of interest (ROIs) was performed in T1 weighted images including thalamus, putamen and caudate nucleus, prefrontal cortex, cerebellar hemispheres and vermis structures of each hemisphere. WM ROIs (corpus callosum, fimbria of hippocampus, internal capsule and corona radiata) were delineated directly in FA map. GM ROIs were co-registered to DWI by applying a previously calculated affine transformation of the T1 weighted images to DWI space. Mean diffusion related measures were obtained including ADC, axial and radial diffusivities, FA, linearity, planarity and sphericity coefficients.

Voxel based analysis

All rabbit brains were registered to a reference brain using their FA volumes [80]. Once the images are aligned to the reference, it can be assumed that the voxels in the same location in all the registered images belong to the same structure, and therefore, they can be compared. Voxel-wise t-test was performed, obtaining the voxels with a statistically significant different distribution of diffusion related parameters between controls and IUGR. Moreover, in this study, the Pearson correlation between the diffusion parameters and the neurobehavior test outcome at each voxel was also computed, to identify which regions were related to the observed changes in neurobehavioral tests. In order to increase the reliability of the results

obtained, the procedure was repeated using all the subjects as the reference in the elastic warping, allowing to discard variability produced by the arbitrary choice of the reference template.



5. RESULTS

5.1. Project 1: Comparison of two experimental models of IUGR: undernutrition versus. selective ligation of uteroplacental vessels

The results of this project have been published in:

Eixarch E, Hernandez-Andrade E, Crispi F, Illa M, Torre I, Figueras F et al. Impact on fetal mortality and cardiovascular Doppler of selective ligation of uteroplacental vessels compared with undernutrition in a rabbit model of intrauterine growth restriction. *Placenta* 2011 Apr; 32(4):304-9.

And presented in the following congresses:

19th World Congress of Ultrasound in Obstetrics and Gynecology in Hamburg, October 2009 (oral communication: E. Eixarch; F. Figueras; E. Hernandez; F. Crispi; M. Illa; E. Gratacós. *Selective ligation of the uteroplacental vessels in the pregnant rabbit is a more suitable model of intrauterine growth restriction than hyponutrition*)

7th World Congress in Fetal Medicine in Sorrento, June 2008 (oral communication: Eixarch, E Hernández-Andrade, F Figueras, A Nadal, F Crispi, I Torre, B Wojtas, E Gratacós. *Rabbit model for Fetal growth restriction*).

5.1.1. Study population

A total of 153 fetuses were included (70 controls and 83 ligated fetuses) in the surgical group, 98 of which were alive at delivery (60 controls and 38 ligated fetuses), while a total of 20 fetuses were included in the undernutrition group, 19 being alive at delivery.

5.1.2. Mortality and biometric data

Table 1 depicts the mortality and biometric outcome of the study groups. Fetal mortality rate in control and undernutrition did not show any difference. On the

5. RESULTS

contrary, the ligature group showed a significantly higher mortality rate than the control and the undernutrition groups. Neonatal biometrics decreased significantly across the experimental groups.

Table 1. Mortality and biometric measurements in experimental groups.

	Control (n=60)	Undernutrition (n=19)	Ligature (n=38)	p*	p**	p***
Mortality rate	14.3 (10/70)	5.0 (1/20)	54.2 (45/83)	<0,001	n.s.	<0,001
Neonatal weight (g)	45.9 (8.5)	37.9 (9.7)	33.2 (9.5)	<0,001	0.003	0.000
Placental weight (g)	6.8 (1.8)	5.3 (1.1)	6.1 (1.8)	n.s.	0.006	n.s.
Crown-rump length (mm)	9.52 (0.99)	9.16 (0.87)	8.84 (1.16)	0,002	n.s.	0.006
Cephalic perimeter (mm)	8.08 (0.57)	7.75 (0.84)	7.43 (0.65)	<0,001	n.s.	0.000
Brain weight (g)	1.45 (0.14)	1.38 (0.16)	1.28 (0.15)	0,002	n.s.	0,001
Brain/neonatal weight ratio	0.020 (0.004)	0.038 (0.008)	0.037 (0.006)	0,004	0,001	0,001

Values are mean and standard deviation (mean (sd)) or rate (%(n/total)).

g: grams; mm: millimetres

p* linear trend ; p** control vs undernutrition; p*** control vs ligature

5.1.3. Ultrasound evaluation

Results are shown in Figure 7 and Table 2. DVPI and IRT were significantly different and changed across the experimental groups. However, only ligature group showed significant changes when compared with control. Interestingly, none of the controls or undernourished fetuses showed reverse flow during atrial contraction, whereas a 33,3% (5/15) of the cases in the ligature group had a reverse flow (p=0.010). AoIPI showed a significant increase in the study groups.

However, neither the undernutrition nor the ligature group significantly differed from the control group. UAPI and MCAPI did not show significant differences between groups.

Figure 7. Pulsatility index of ultrasound parameters in experimental groups.

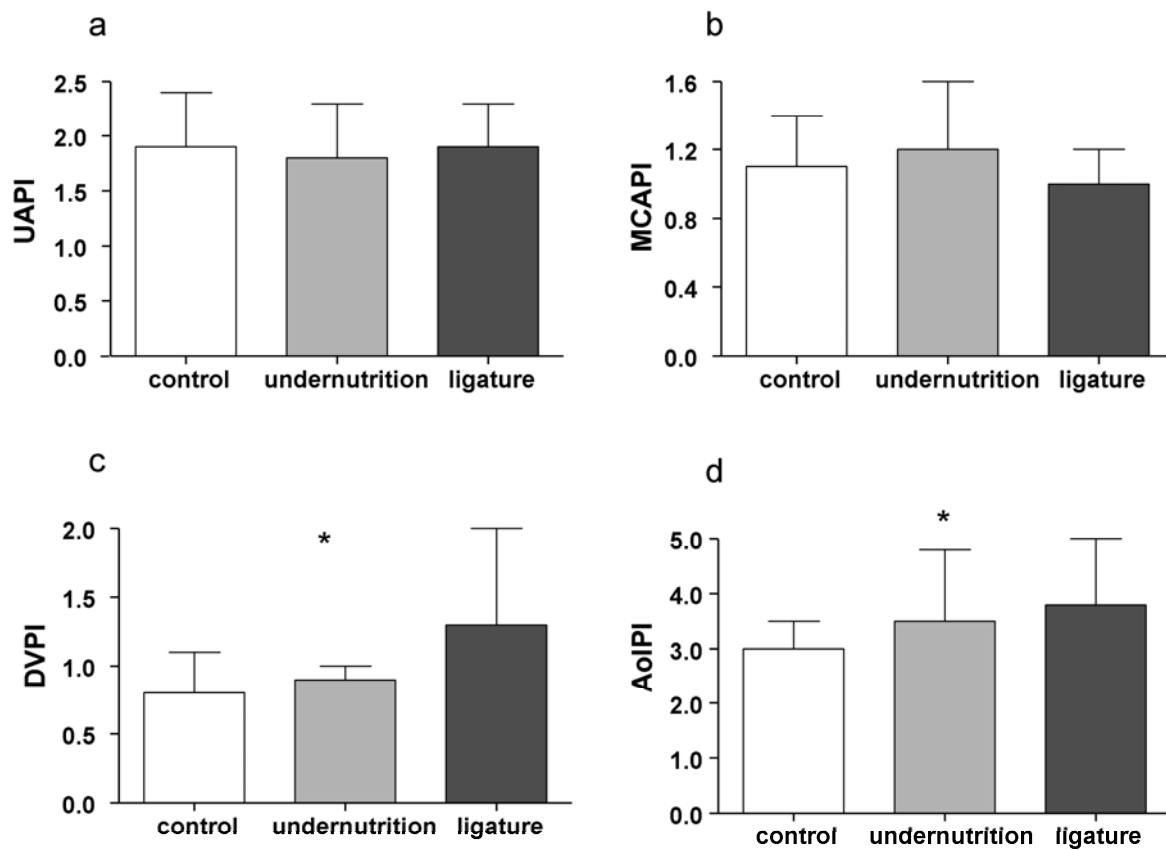


Table 2. Ultrasound parameters in experimental groups.

Values are mean and standard deviation (mean (sd))

	Control (n=15)	Undernutrition (n=9)	Ligature (n=15)	p*	p**	p***
Abdominal perimeter (mm)	79.0 (5.5)	70.4 (5.5)	68.3 (8.8)	0.004	0.031	0.006
UAPI	1.9 (0.5)	1.8 (0.5)	1.9 (0.4)	n.s.	ns	ns
MCAPI	1.1 (0.3)	1.2 (0.4)	1.0 (0.2)	n.s.	ns	ns
DVPI	0.8 (0.3)	0.9 (0.1)	1.3 (0.7)	0.003	ns	0.009
AoIPI	3.0 (0.5)	3.5 (1.3)	3.8 (1.2)	0.029	ns	ns
ICT (ms)	25.5 (9.5)	29.1 (6.3)	25.5 (8.1)	n.s.	ns	ns
IRT (ms)	38.1 (7.7)	42.0 (8.5)	50.1 (12.4)	0.003	ns	0.008
ET (ms)	149.2 (220.6)	150.6 (11.6)	155.9 (21.8)	n.s.	ns	ns
MPI	0.44 (0.10)	0.48 (0.07)	0.49 (0.08)	n.s.	ns	ns

UAPI: Umbilical artery pulsatility index, MCAPI: Middle cerebral artery pulsatility index, DVPI: Ductus venosus pulsatility index, AoIPI: Aortic isthmus pulsatility index, ICT: isovolumetric contraction time, IRT: isovolumetric relaxation time, ET: ejection time, MPI: myocardial performance index

p* linear trend ; p** control vs undernutrition; p*** control vs ligature

5.2. Project 2: Evaluation of different timings and severity of the intervention: comparison of the effects of late versus early onset, and of various proportions of vessels ligated in a model of IUGR based on selective ligation of uteroplacental vessels

The results of this project have been published in:

Eixarch E, Figueras F, Hernández-Andrade E, Crispi F, Nadal A, Torre I et al. An Experimental Model of Fetal Growth Restriction Based on Selective Ligation of Uteroplacental Vessels in the Pregnant Rabbit. *Fetal Diagn Ther* 2009; 26(4):203-11.

And presented in the following congresses:

28th Annual Meeting of The Society for Maternal-Fetal medicine in Dallas, January 2008 (poster: E Eixarch, E Hernández- Andrade, F Figueras, S Oliveira, F Crispi, E Gratacós. *Hypoxic brain damage as measured by fetal blood and amniotic fluid levels, and immunohistochemical brain expression of S100 β in a rabbit model of intrauterine growth restriction*)

17th World Congress on ultrasound in Obstetrics and Gynaecology in Firenze, October 2007 (oral communication: E Eixarch, E Hernandez- Andrade, F Figueras, E Gratacos. *Selective ligation of uteroplacental vessels in the pregnant rabbit: a novel experimental model of intrauterine growth restriction*)

5.2.1. Study population

In the 21D protocol a total of 101 fetuses were included (36 controls; and 29 and 36 in the mild and severe reduction groups, respectively). Of these 101 fetuses, 62 were alive at delivery (32 controls, 19 mild reduction and 11 severe reduction).

In the 25D protocol a total of 145 fetuses were included (67 controls, 17 mild reduction and severe reduction). Of these 145 fetuses, 94 were alive at delivery (57 controls; and 15 and 22 in the mild and severe reduction groups, respectively).

5.2.2. Mortality and biometric data

All experimental groups showed significantly higher mortality rates than sham controls except for the 25D mild reduction group. There was a linear increase in mortality rates across the experimental groups when ordered by gestational age and severity (Linear-by-linear $p < 0.001$) (Figure 8).

Figure 8. Mortality rates across the study groups.

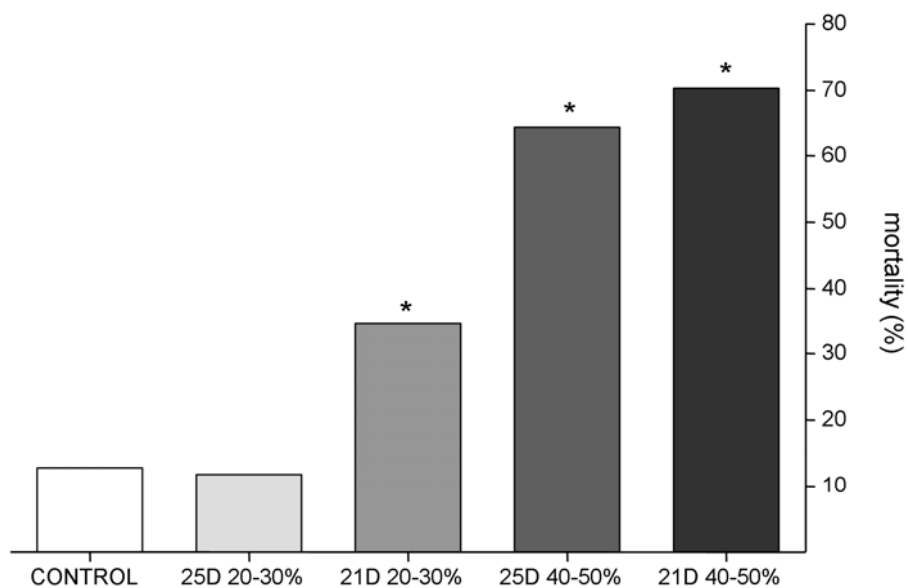


Table 3 details the biometrical outcome in the study groups. Birth weight, crown-rump length and brain weight decreased significantly across the experimental groups (control, mild and severe reduction) both at 21D and 25D. Additionally,

brain/birth weight ratio increased throughout the study groups in both 21D and 25D protocols. Placental weight showed no significant differences among experimental groups in either protocol.

Table 3. Biometric measurements obtained from the different experimental groups.

21D	Control n=32	20-30% n=19	40-50% n=11	p	Linear trend
Birth weight (g)*	23.1 (4.2)	21.5 (3.7)	18.2 (5.6)	0.008	0.002
Placental weight (g) **	5.3 (1.7)	4.4 (1.7)	4.6 (2.2)	0.261	
Crown-rump length (mm) *	7.7 (0.5)	7.3 (0.5)	7.1 (0.6)	0.002	0.002
Cephalic perimeter (mm)*	6.3 (0.4)	6.2 (0.4)	6.1 (0.6)	0.190	0.074
Brain weight (g) *	0.8 (0.07)†	0.8 (0.08)	0.7 (0.06)	0.005	0.007
Brain/birth weight ratio*	0.032 (0.003)	0.038 (0.006)	0.044 (0.012)	0.004	0.001
25D	Control n=57	20-30% n=15	40-50% n=22	p	Linear trend
Birth weight (g) *	45.5 (8.5)	36.4 (8.9)	35.4 (8.6)	<0.001	<0.001
Placental weight (g) **	6.5 (2.2)	5.5 (2.3)	5.9 (2.6)	0.108	
Crown-rump length (mm)*	9.5 (1)	9.4 (1.4)	8.8 (0.8)	0.014	0.004
Cephalic perimeter (mm)**	8 (0.8)	7.6 (1.1)	7.4 (0.6)	0.009	
Brain weight (g) *	1.4 (0.1)†	1.2 (0.1)	1.3 (0.1)	0.005	0.072
Brain/birth weight ratio *	0.028 (0.003)	0.035 (0.007)	0.038 (0.005)	0.002	0.001

* Values are mean and standard deviation, ANOVA test

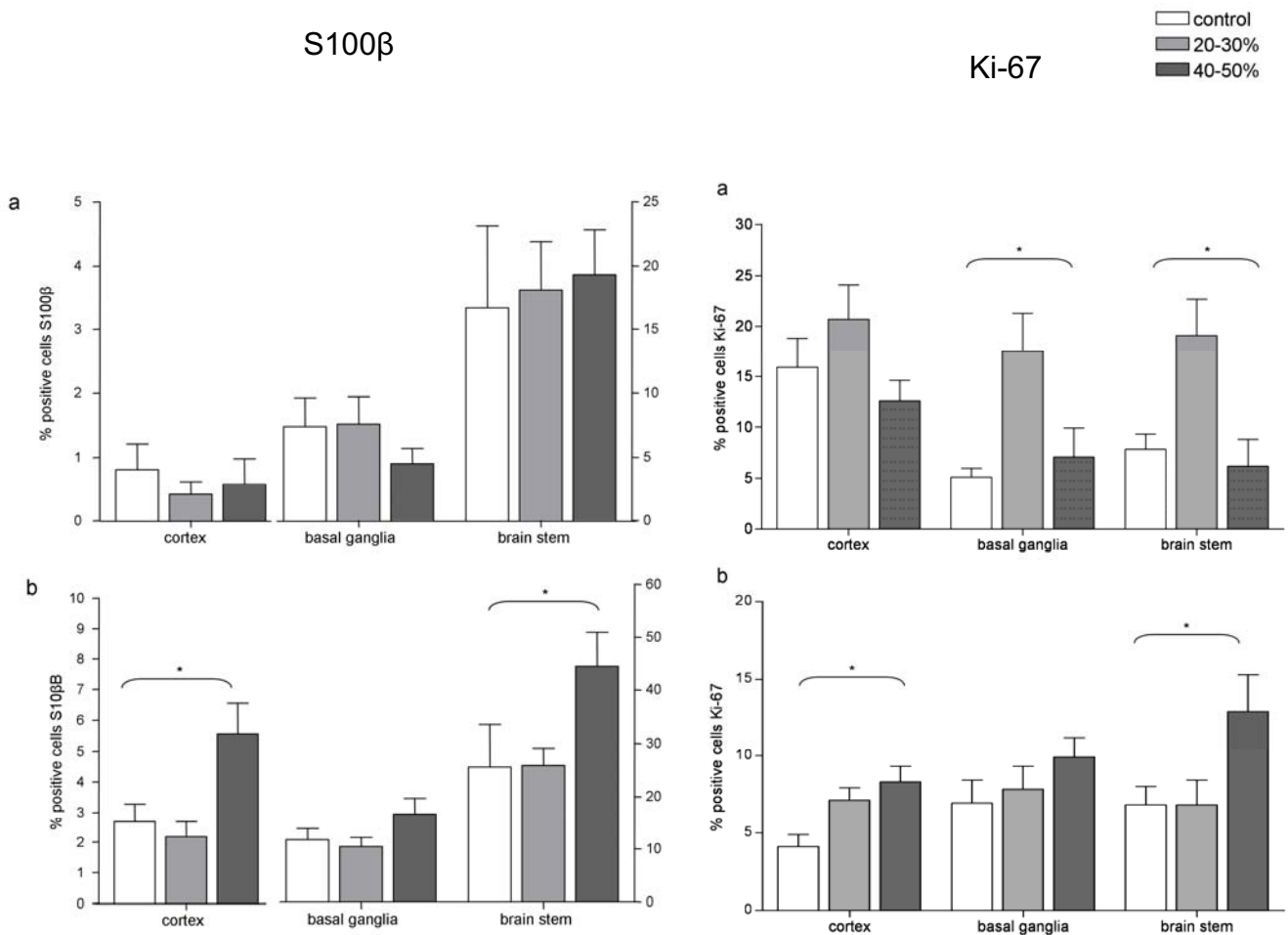
** Values are median and interquartile range, Kruskal-Wallis test

† Data were available in only 10 fetuses

5.2.3. Immunohistochemistry results

Figure 9 displays immunohistochemistry results. In the 25D protocol, S100- β expression was significantly higher in the severe reduction group in cortical and brainstem regions. In the 21D protocol, Ki-67 expression was significantly higher in the cortex and brain stem regions of the mild reduction group. In contrast, in the 25D protocol, Ki-67 expression was significantly higher in the cortex and brain stem regions of the severe reduction group.

Figure 9. S100 β and Ki-67 expression in fetal brain regions.



5.3. Project 3: Development of a high-resolution brain MRI diffusion approach to describe the anatomical patterns of brain reorganization induced by IUGR and to describe the postnatal neurobehavioral correlates of the neurostructural changes

The results of this project have been submitted for publication in:

Eixarch E, Batalle B, Illa M, Muñoz-Moreno E, Arbat A, Amat-Roldan I et al. Neonatal neurobehavior and diffusion MRI changes in brain reorganization due to intrauterine growth restriction in a rabbit model. PLoS ONE, submitted.

And presented in the following congresses:

10th World Congress in Fetal Medicine in St Julien, Malta, June 2011 (oral communication: M.Illa, E.Eixarch, D.Batalle, A.Arbat, R.Acosta-Rojas, F.Figueras, E.Gratacos. *Fetal growth restriction: Evaluation of the fetal rabbit as a model to evaluate neurostructural and neurodevelopmental changes*).

5.3.1. Study population

A total of 10 control and 10 growth restricted neonates were included. Birth weight was significantly lower in cases than in controls (30.4 ± 12.2 g. vs. 47.0 ± 9.3 g., $p=0.007$).

5.3.2. Neurobehavioral results

Neurobehavioral test results are shown in Table 4. Growth restricted pups showed poorer results in all parameters, reaching significance in righting reflex, tone of the limbs, locomotion, lineal movement, forepaw distance, head turn during feeding and smelling response.

Table 4. Neurobehavioral test results in study groups

	<i>Control</i> <i>n=10</i>	<i>IUGR</i> <i>n=10</i>	<i>p</i>
Posture, score*	3.0 (0)	3.0 (1)	0.143
Righting reflex, number of turns	8.7 (1.5)	6.3 (3.0)	0.035
Tone, score*	0 (0)	1.0 (1.5)	0.019
Locomotion, score*	3.0 (0)	2.0 (2)	0.005
Circular motion, score*	2.0 (1)	2.0 (1)	0.247
Intensity, score*	3.0 (0)	2.5 (2)	0.089
Duration, score*	2.0 (0)	1.5 (1)	0.052
Lineal movement, line crosses in 60 sec	2.8 (1.4)	1.1 (1.1)	0.009
Fore–hindpaw distance, mm †	0.7 (1.9)	7.6 (5.4)	0.007
Sucking and swallowing, score*	3.0 (1)	1 (2)	0.075
Head turn, score*	3.0 (1)	2.0 (1)	0.043
Smelling test, score *†	3.0 (1)	1.0 (0)	0.006
Smelling test time, sec †	4.0 (1)	8.5 (5)	0.021

Values are mean and standard deviation (mean (sd)) or median and interquartile range (median (IQ)) when appropriate.

*U Mann-Whitney

†Data available for 7 controls and 8 cases.

5.3.3. Diffusion MRI results

a) Global analysis

Table 5 depicts the results of global analysis of diffusion related parameters. Whole brain analysis revealed non-significantly higher ADC values and significantly lower FA and linearity values in the growth restricted group. When the WM mask was applied, FA significantly differed between cases and controls.

Table 5. Whole brain and white matter global analysis of diffusion parameters

	<i>Control</i> <i>n=10</i>	<i>IUGR</i> <i>n=10</i>	<i>p</i>
<i>Whole brain</i>			
Fractional anisotropy	0.16 (0.02)	0.15 (0.02)	0.048
Apparent Diffusion Coefficient ($\times 10^{-3} \text{mm}^2/\text{s}$)*	0.44 (0.08)	0.47 (0.10)	0.353
Axial diffusivity ($\times 10^{-3} \text{mm}^2/\text{s}$)*	0.52 (0.10)	0.54 (0.11)	0.393
Radial diffusivity ($\times 10^{-3} \text{mm}^2/\text{s}$)*	0.41 (0.07)	0.43 (0.10)	0.393
Sphericity (C_s)	0.74 (0.02)	0.76 (0.02)	0.061
Linearity (C_l)	0.16 (0.02)	0.15 (0.02)	0.044
Planarity (C_p)	0.10 (0.01)	0.10 (0.01)	0.368
<i>White matter (threshold FA>0.2)</i>			
Fractional anisotropy	0.27 (0.01)	0.26(0.00)	0.019
Apparent Diffusion Coefficient ($\times 10^{-3} \text{mm}^2/\text{s}$)*	0.42(0.08)	0.44(0.11)	0.353
Axial diffusivity ($\times 10^{-3} \text{mm}^2/\text{s}$)*	0.55 (0.10)	0.58 (0.15)	0.393
Radial diffusivity ($\times 10^{-3} \text{mm}^2/\text{s}$)*	0.36 (0.06)	0.38 (0.09)	0.247
Sphericity (C_s)	0.60 (0.02)	0.61 (0.01)	0.033
Linearity (C_l)	0.29 (0.02)	0.28 (0.02)	0.201
Planarity (C_p)	0.11 (0.02)	0.11 (0.03)	0.877

Values are mean and standard deviation (mean (sd)) or median and interquartile range (median (IQ)) when appropriate.

*U Mann-Whitney

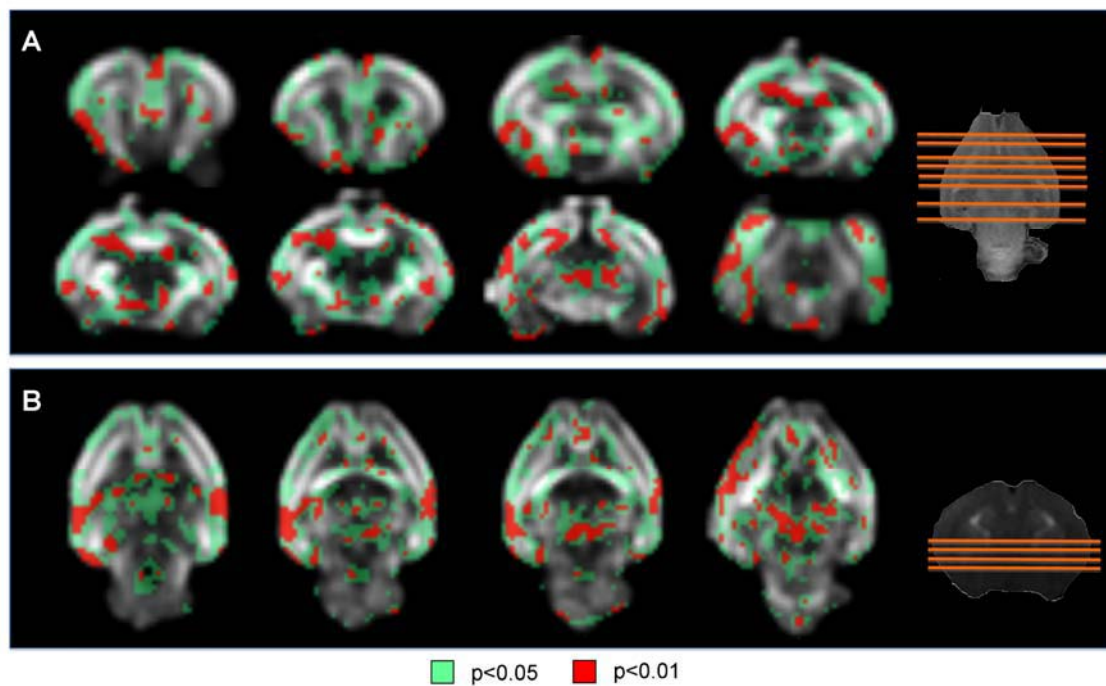
b) Regional analysis

ROIs analysis of diffusion parameters only found differences in right fimbria of hippocampus, showing decreased values of FA in IUGR. When VBA analysis was applied, statistically significant differences were found in FA distribution between cases and controls in multiple structures such as different cortical regions (frontal, insular,

5. RESULTS

occipital and temporal), hippocampus, putamen, thalamus, claustrum, medial septal nucleus, anterior commissure, internal capsule, fimbria of hippocampus, medial lemniscus and olfactory tract (Figure 10).

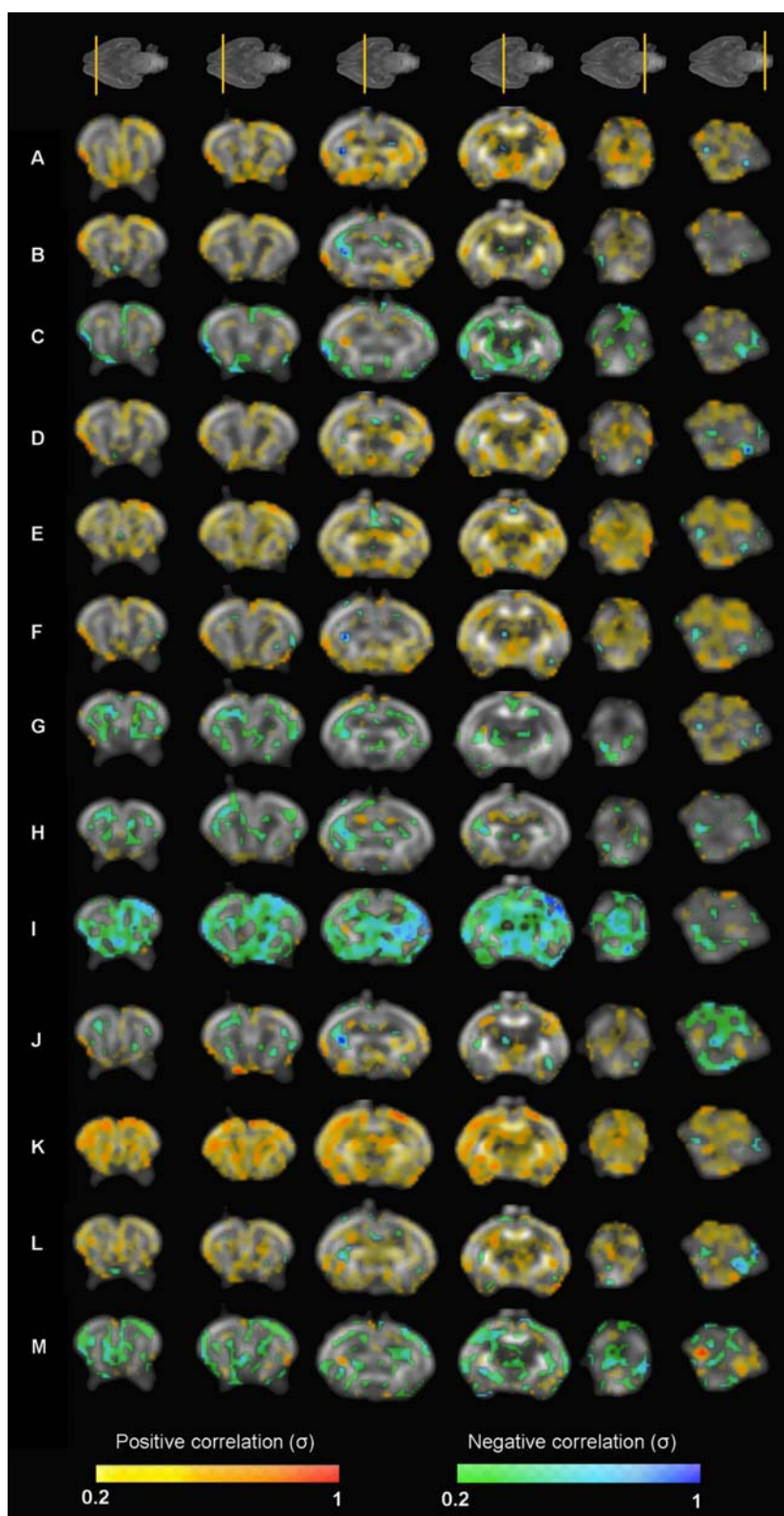
Figure 10. Fractional anisotropy values: regions showing statistically significant differences between cases and controls.



c) Correlation between MRI diffusion and neurobehavioral outcome

FA map showed multiple areas correlated with most of neurobehavioral domains, being posture, locomotion, circular motion, intensity, fore-hindpaw distance and head turn the domains showing more statistically significant correlated areas (Figure 11). Subcortical GM areas were mainly significantly correlated with posture, locomotion and head turn and WM structures essentially with posture and locomotion parameters. Within WM structures, both anterior commissure and fimbria of hippocampus were the areas correlated with a bigger amount of neurobehavioral items.

Figure 11. Correlation maps between neurobehavioral test items and fractional anisotropy values.



(A) Posture, (B) Righting reflex, (C) Tone, (D) Locomotion, (E) Circular motion, (F) Intensity, (G) Duration, (H) lineal movement, (I) Fore-hindpaw distance, (J) Sucking and swallowing, (K) Head turn, (L) Smelling test, (M) Smelling test time

6. DISCUSSION

6.1. General overview

This study provides evidence supporting the concept that a surgical model of IUGR in pregnant rabbits is suitable to evaluate the effects of placental insufficiency on brain development. The results showed that chronic reduction of placental supply, which implies a reduction of both oxygen and nutrients, reproduces the human features of IUGR better than reduction of nutrients produced by undernutrition models. Changes in brain development produced by placental insufficiency showed different patterns according to the onset and severity of growth restriction induction. An early onset insult produces changes in proliferation on subcortical areas without changes in S100 β expression, whereas late onset insults increase proliferation and S100 β expression in both cortical and subcortical areas. The correlation between abnormal neurobehavior and microstructural changes demonstrated by diffusion MRI in neonatal period illustrates that sustained intrauterine restriction of oxygen and nutrient induces a complex pattern of maturational changes. The model developed may be a powerful tool to correlate functional and structural brain information with histological, molecular and other imaging techniques.

6.2. Project 1: Comparison of two experimental models of IUGR: undernutrition versus. selective ligature of uteroplacental vessels

The results of this project demonstrated that, despite the fact that both surgical and undernutrition models in the pregnant rabbit result in a reduction of biometric parameters, only selective ligature of uteroplacental vessels was associated with an increase in fetal mortality and remarkably more pronounced changes in Doppler cardiovascular parameters

Mortality and biometric data

Selective ligature of uteroplacental vessels has previously been used in rabbits [43, 44], guinea pigs [45] and rats [46] resulting in a reduction in fetal weight and increased mortality [43-46]. Undernutrition has mainly been reported in rodents by means of either caloric restriction or low-protein diet leading to a



Figure 12. Illustrative image of neonatal size differences between growth restricted and controls pups

decrease in birth weight [37]. We found that both experimental models resulted in a significant reduction in fetal weight, with lower values in the surgical model. In keeping with previously reported data [37], maternal food restriction did not increase fetal mortality. This could be explained by the fact that undernutrition generates fetal

hypoglycemia producing hypoinsulinemia, whereas reduced blood flow through placenta generates fetal hypoxemia and increase of lactate [36], producing

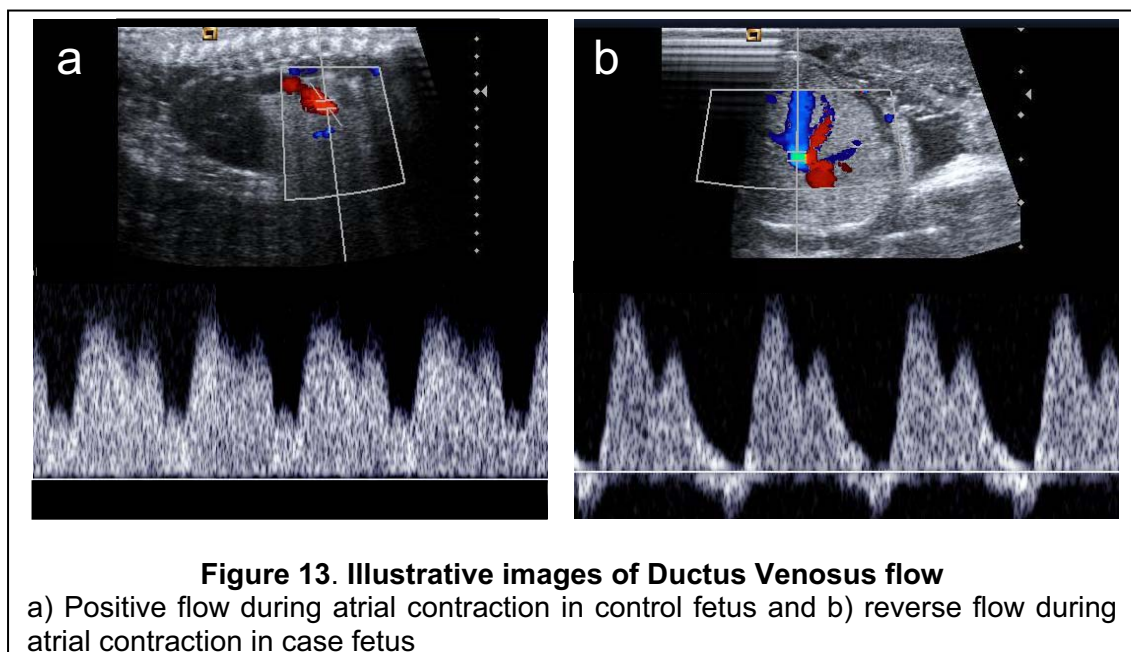
acidosis that could lead eventually to circulatory failure and fetal death [81]. Our finding supports the notion that hypoxia is an essential mechanism in the cascade of events leading to the increased risk of fetal death in IUGR [81]

Ultrasound evaluation

In this project both of the two evaluated experimental models failed to induce changes in umbilical artery Doppler. This observation is in line with a previous study in Guinea pigs [45]. In humans, increased pulsatility index in the UA is thought to result from profound changes in placental vasculature, including a reduction of over 30% of the placental mass [82] and severe vasoconstriction phenomena in the fetal-sided tertiary stemvilli [25]. Since models based on uteroplacental vessel occlusion do not alter placental micro-anatomy, the absence of changes in the umbilical artery is not surprising. Indeed, previous experiments in sheep have shown that only direct embolization of placental tissue from the fetal side is capable of inducing changes in umbilical artery Doppler [38, 83, 84]. Umbilical flow has been previously assessed in normal grown rabbits by means of pulsed Doppler [85], reporting pulsatility index values that were significantly lower than those observed in the present study. This could be explained by the fact that we performed our examinations placing linear probe directly to uterine wall, whereas they perform examination transabdominally, without laparotomy.

The ductus venosus has a central role in regulating the distribution of oxygen and nutrients in fetal life [86] and has been anatomically demonstrated in several species [87] including rabbits [88]. In IUGR, ductus venosus flow velocity during atrial contraction is progressively reduced as hypoxemia and acidemia

progress, with a consequent increase in pulsatility index [89]. In our rabbit model we reproduced these changes with a significant increase in pulsatility index in ligature fetuses only in the ligature group, with the presence of reverse flow during atrial contraction in most severe cases (Figure 13). In addition, there was a remarkable increase in isovolumetric relaxation time, with increasing values in the study groups. IRT is used in the calculation of the MPI in fetuses and is an early marker of fetal cardiac dysfunction [90].



Concerning MPI which has been reported to be increased in early and late onset IUGR fetuses [91-93], we could only demonstrate a non-significant trend for increased values. We hypothesize that the lack of significance may have been due to our limited sample size. Overall, changes in cardiovascular Doppler were substantially more pronounced and statistically significant in the surgical ligation group. However, the undernutrition model was associated with a trend for increased values in isovolumetric relaxation time. This observation should be confirmed in a large sample size, although this finding is in line with previous data

demonstrating postnatal changes in cardiac structure and hypertension in the offspring of rats exposed to undernutrition during pregnancy [94-97]. In conclusion, while we can not exclude a modest effect of undernutrition on cardiac function parameters, uteroplacental vessel ligation induced more pronounced cardiovascular Doppler changes supporting the suitability of this experimental model for future research on cardiac dysfunction in IUGR.

Increased values of the aortic isthmus pulsatility index across the study groups were demonstrated in this study, with more pronounced differences being observed in the surgical model. The aortic isthmus plays an important role in redistributing blood flow to the brain under hypoxic conditions [98]. The aortic isthmus pulsatility index has been demonstrated to increase as placental insufficiency progresses in growth restricted fetuses [99] and this has been correlated with abnormal postnatal neurodevelopment [100, 101]. Consistently with our findings, a previous study using a growth restriction model in rabbits has also reported changes in maturation of cortical astrocytes [43]. However, we failed to demonstrate changes in blood flow in middle cerebral artery. In human fetuses with IUGR, the key sign to identify cerebral blood flow redistribution is a reduction in the pulsatility index in the MCA and this sign has been found to be associated with increased risk of abnormal neurobehavior [6, 28]. The lack of changes in fetal rabbits could be due to fundamental anatomical differences with human fetuses. However, since ultrasound examinations were done under anaesthetic drugs, which are associated with brain vasodilatation [102], we can not exclude a systematic bias induced by the experimental setting.

Limitations

Firstly, the high mortality rate in the ligature group may have biased our results, since biometric and ultrasound evaluations could only be performed in the surviving fetuses. However, it is likely to be a conservative bias as only the less affected fetuses would have been analysed, attenuating the differences between groups. Secondly, all ultrasound examinations were done under anaesthetic conditions that produce haemodynamic changes in rabbit brain [102], and we can not exclude that this may have prevented the observation of differences in fetal Doppler brain parameters.

Conclusion

Selective ligation of uteroplacental vessels in the pregnant rabbit partially reproduces the haemodynamic features of IUGR of human fetuses, particularly with regards to changes in cardiovascular function. In this respect, this model seems to be a better approach to mimic the human condition than undernutrition models.

6.3. Project 2: Evaluation of different timings and severity of the intervention: comparison of the effects of late versus early onset, and of various proportions of vessels ligated in a model of IUGR based on selective ligation of uteroplacental vessels

The results obtained in this study show that selective ligation of uteroplacental vessels in the pregnant rabbit induces different degrees of fetal growth restriction associated with progressive increases in mortality and biometrical restriction and differences in brain histological response to hypoxia.

Mortality and biometric data

This model has previously been used by Bassan et al. in an experimental study to assess the impact of fetal growth restriction on renal development [44]. The authors used a 20-30% ligation at 25 days of gestation and demonstrated a decrease in biometrical measurements and a deleterious effect on kidney development. Partial occlusion of uteroplacental vessels has also been used in guinea pigs and rats producing a decrease in body weight and an increase in mortality [45] [46]. In the present project we have further developed this experimental approach and evaluated the capability of the model to induce different degrees of growth restriction by modulating the timing and the proportion of vessels ligated.

We obtained a linear decrease in mortality rate across experimental groups suggesting that gestational age and severity of blood flow reduction have a key role in fetal survival. In addition, linear changes in biometric measurements and in brain/birth weight ratio were obtained in both protocols, 21D and 25D, in a similar proportion to those obtained in previous studies [44, 45]. Thus, these

results support our hypothesis that it is possible to induce a progressive model of fetal growth restriction. It could be argued that fetal position in the uterine horn, which is a “natural model” of fetal growth restriction [103-109], could have influenced these results. However, we have found that in our model, mortality rate and biometrics of growth restricted fetuses is not influenced by uterine position (Figure 14).

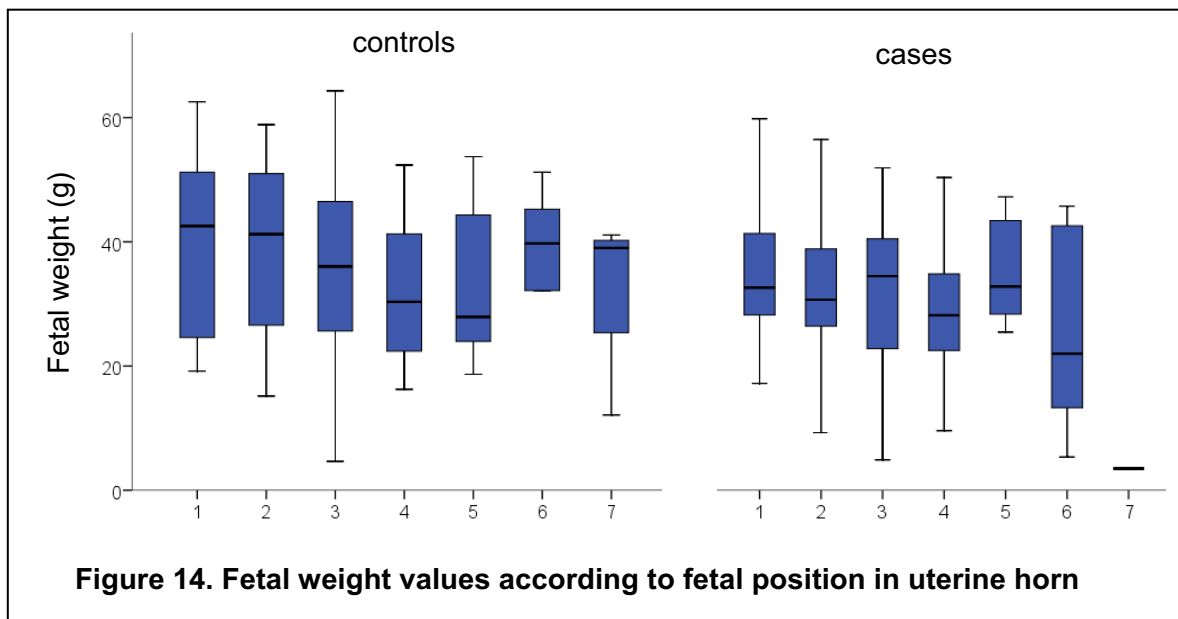


Figure 14. Fetal weight values according to fetal position in uterine horn

Immunohistochemistry results

Brain damage was evaluated by means of S100 β that has been suggested as a biochemical marker of brain damage [58, 110-112]. We demonstrated an increase of S100 β expression in 25D severe reduction group in cortex and brain stem, while at 21 days no differences were observed. This could be speculatively explained by the fact that this protein is a marker of astrocyte maturation during development [113]. It could then be argued that the central nervous system at an earlier gestational age has less capability to increase S100 β expression in the presence of an injury. Another explanation could be that placental insufficiency at

21 days of gestation induces a transient increase in S100 β expression that is later inhibited. Indeed, “in vitro” studies have demonstrated that chronic hypoxia induces a transient increase in S100 β mRNA expression, followed by rapid downregulation with a sustained reduction of protein release [57].

Regional changes in proliferation by means of Ki-67 expression were found in our model: while at 21D only the mild occlusion group showed signs of increased proliferation in basal ganglia and brain stem, at 25 days this phenomenon was only observed in the severe occlusion group in cortex and brain stem. The data support the notion that the impact of chronic hypoxia on brain proliferation may differ depending on gestational age and severity of the insult [24]. Preterm birth is associated with white matter injury and neuronal damage in cortical and subcortical areas [114]. We could hypothesize that, at 21 days of gestation, mild chronic hypoxia enhances proliferation in order to protect subcortical areas, while severe hypoxia inhibits this proliferation because of higher intensity. On the other hand, cortical neurons are predominantly injured after hypoxic insult in term neonates [24]. Actually, when we analyzed the stained tissue we discovered that in most cases proliferating cells were found in subventricular zone as reported before [62-64]. Thus, these differences observed in brain histological changes at different gestational ages illustrate the potential usefulness of the model to explore the neurological impact of growth restriction at different gestational ages.

Strengths and limitations

The rabbit model described in this project may have several advantages compared to previously used models of intrauterine growth restriction. Firstly, the model allows adjusting the timing and the severity of fetal growth restriction. As

illustrated by the progression in biometrical reduction and mortality rates observed in our study, different degrees of reduction in the uteroplacental blood flow may be achieved with a technically feasible and reproducible surgical procedure, which allows establishing comparisons among different severity groups. Thirdly, although the fetal size in the rabbit does not allow us to place vascular catheters or sensors as sheep models [115], it still may allow us to perform certain manipulations more easily and reproducibly than in rodents, for example obtaining *in vivo* fetal biological samples or performing Doppler investigations [116]. Finally, the rabbit model may present some advantages with respect to other models to evaluate the impact of intrauterine growth restriction in basic aspects of brain development and maturation. Similar to humans, rabbits start the maturation process of white matter in the last period of pregnancy and continues postnatally [51] while in lambs and rodents such maturation occurs predominantly in fetal or postnatal life, respectively [52].

Our study has some limitations. Firstly, as previously mentioned, the high mortality rate in the more severe occlusion groups reduces the number of fetuses available for analysis and it may have biased our results, since biometrical and immunohistochemical measurements could only be performed in the surviving fetuses. Secondly, although S100 β has been described as a serological marker of brain damage, it is unclear whether and how chronic hypoxia could modulate S100 β expression. Brain histological markers in this study were used to demonstrate that the progressive experimental model described here resulted in different histological brain changes, but the study was not designed to draw any pathophysiological conclusion on the impact of IUGR on brain injury.

Conclusion

In conclusion, selective ligation of uteroplacental vessels in the pregnant rabbit may be used to create a gradable model of fetal growth restriction that reproduces in a progressive manner different clinical manifestations of the human condition. In addition, this model demonstrated that changes in the severity and the onset of placental insufficiency produces different patterns of histological changes in fetal brain.

6.4. Project 3: Neurobehavioral and neurostructural effects of IUGR in neonatal period

In this project we demonstrated that rabbit model of IUGR was associated with brain regional changes in brain diffusivity, which were significantly correlated with neurobehavioral impairments. To the best of our knowledge, this is the first study that demonstrates that chronic reduction of uteroplacental blood flow in an animal model produces changes in brain diffusivity and in neurobehavioural function.

Neonatal neurobehavior

It is well-known that IUGR in humans is associated with neonatal neurodevelopmental dysfunctions [4, 5], being attention, habituation, regulation of state, motor and social-interactive clusters the most affected [5]. In a similar manner, growth restricted rabbit pups in this model showed weakened motor activity and olfactory function, which is their principal way of social interactions [117]. These findings reinforce previous evidence suggesting the capability of this animal model to reproduce features of human IUGR [47, 116]. Previous studies suggested the ability of the rabbit model to illustrate the neonatal effects of acute severe prenatal conditions. Thus, hypoxic-ischemic injury and endotoxin exposure produce hypertonic motor deficits [54, 74], reduced limb movement [75] and olfactory deficits [76] in this model. The present study demonstrates that selective ligation of uteroplacental vessels is suitable to reflect the neurodevelopmental impact of mild and sustained reduction of placental blood flow occurring in IUGR. These results illustrate a more general concept that lower animal species are also susceptible of developing brain reorganization *in utero*,

and therefore they are suitable models to assess the chronic effects of adverse intrauterine environment on brain development.

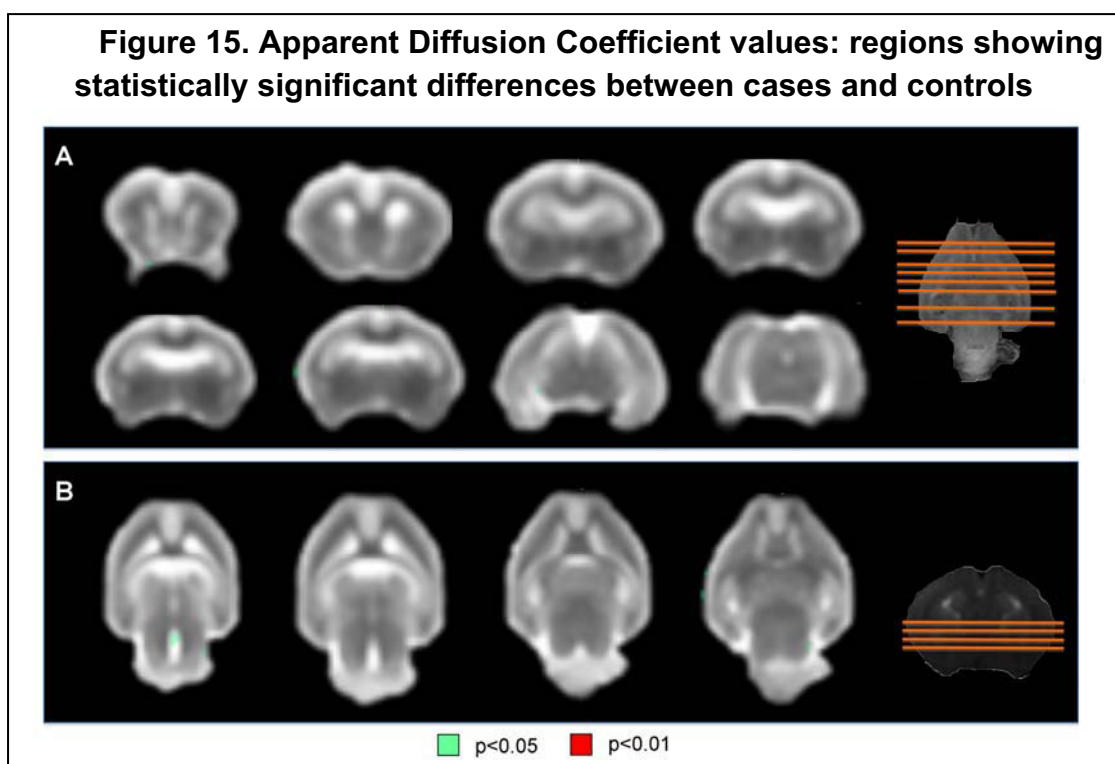
Diffusion MRI analysis

Changes in brain diffusivity and anisotropy have previously been reported after acute severe hypoxic experimental conditions in adults [68] and developing brain [118]. However, placental insufficiency results in mild and sustained injury, which may challenge the ability to find obvious differences between groups. With the purpose of detecting subtle changes we used high-resolution MRI acquisition in fixed whole brain preparations. This approach allows revealing submillimetric tissue structure differences, particularly in the GM, which are difficult to detect *in vivo* [72]. Regional analysis of diffusivity parameters may provide information of the anatomical pattern of brain microstructural changes in IUGR. Manual brain segmentation is a standard approach to find differences between brain regions. However, as shown in previous studies, this approach has limitations in small structures, due to the difficulty in obtaining accurate delineations [119] and to the partial volume effects [120]. Since these limitations were known, a VBA strategy was applied. VBA approach performs the analysis of the whole brain voxel-wise avoiding the need of a *a priori* hypothesis or previous delineation [121], and allowed to localize regional differences between cases and controls distribution of diffusion parameters.

a) Apparent Diffusion Coefficient

ADC is directly related with the overall magnitude of water diffusion, typically decreasing as brain maturation occurs [66]. After perinatal acute

hypoxic-ischemic event, it shows a dynamic process with a quickly decrease followed by a pseudo-normalization to finally increase to higher values than normal [118]. In humans, ADC values have been demonstrated to be increased in multiple brain regions after chronic fetal conditions including IUGR [71] and fetal cardiac defects [70]. Interestingly, these changes in ADC persist after birth in neonates with cardiac anomalies [122, 123]. In animal models, increased ADC values have been reported after prenatal acute hypoxic-ischemic injury in hypertonic rabbits [55]. In our study, global diffusivity analysis revealed a non-significant trend for increased ADC in the IUGR group, and when VBA was applied, it also did not reveal regional differences between cases and controls (Figure 15). The lack of remarkable differences in ADC is possibly a reflection of the abovementioned notion that IUGR results in delayed brain maturation and reorganization rather than in significant brain injury [33, 124]. However, we could not rule out that due to our sample size, our study was underpowered to detect such differences.



b) Fractional anisotropy

In growth restricted pups, global decreased FA values were demonstrated in both whole brain and WM mask analyses. These findings are similar to those observed in acute hypoxic-ischemic injury models [55] and perinatal asphyxia in humans [66] demonstrating decreased values in FA particularly in WM areas. Aside from acute models, preliminary evidence in neonates with cyanotic congenital heart defects suggests also the presence of brain FA changes [122, 123]. FA indicates the degree of anisotropic diffusion and typically increases in WM areas during brain maturation, being closely related with myelination processes [66]. After acute hypoxic-ischemic injury in rat pups, decreased values of FA have been related with decreased myelin content in WM areas [125]. Consistently with decreased FA, our findings demonstrated that IUGR had a significant decrease in linearity and a significant increase in sphericity, changes that have been related to reduced organization of WM tracts [79]. Therefore, the results of the study are consistent with the presence of decreased WM myelination and brain reorganization after exposure to IUGR in the rabbit model.

Regional analysis of FA distribution revealed that cortical and subcortical GM areas were the most altered regions. Cortical changes are a feature of IUGR, as suggested by decreased cortical volume [13] and discordant patterns of gyrification due to pronounced reduction in cortical expansion in neonates [20] and differences in GM brain structure in infants [21] suffering this condition. Our results support the notion that these changes are based on microstructural differences. In line with this contention, microstructural changes in cortical regions have previously been demonstrated in a sheep model of IUGR, including

cortical astrogliosis, fragmentation of fibers and thinner subcortical myelin sheaths [49]. Importantly, these histological features have been shown to correlate with decreased FA in cortex [69] and subcortical WM [126].

Regional analysis also revealed changes in multiple WM structures. The most pronounced differences were found in the internal capsule, anterior commissure and fimbria of hippocampus. Changes in WM structures have also been reported in human fetuses, with increased ADC in pyramidal tract in IUGR [71] and increased ADC in multiple WM in areas in fetuses [70] and newborns [122, 123] with congenital cardiac defects. Consistently with our results, prenatal chronic hypoxia models have demonstrated inflammatory microgliosis, mild astrogliosis [127], and a delay in the maturation of oligodendrocytes leading to a transient delay in myelination [124]. These changes result in global reduction in axonal myelination in absence of overt WM damage [128] which in turn is reflected by decreased values of FA [126] as observed in this study.

The evidence of a significant decrease in global and regional analyses of FA together with lack of marked changes in ADC could seem inconsistent. However, previous evidence indicates that both parameters are actually independent [66]. It is known that the FA increase takes place before the histologic appearance of myelin [129-131]. The increases in FA in the “premyelinating state” could be due to an increase in the number of microtubule-associated proteins in axons, a change in axon calibre, and a significant increase in the number of oligodendrocytes [131]. In rabbits, a rapid increase in immature oligodendrocyte density occurs from 29 days of pregnancy to postnatal day +5, followed by beginning of myelination around postnatal day +3 [74]. On the other

hand, the ADC decrease during brain maturation has been postulated to be due to the concomitant decrease in overall water content [130]. Thus, we hypothesize that the pattern of changes described in our model with significant decreased FA and lack of marked changes in ADC could be explained by two mechanisms. First, histological changes in brain organization due to “premyelinating state” have already appeared in rabbit pups suffering IUGR. Consequently, delayed or reduced brain organization occurring in IUGR leads to the decrease in FA values. Secondly, as myelin has not appeared in postnatal day+ 1 (in cases nor in controls), water content and the restriction to its movement which conditions ADC values remains similar in both groups. We acknowledge however that the results in ADC could have also been influenced by fixation processes used in this study, which decrease water content in a non-homogeneous, and therefore non-predictable, manner [132].

Functional-structural correlates

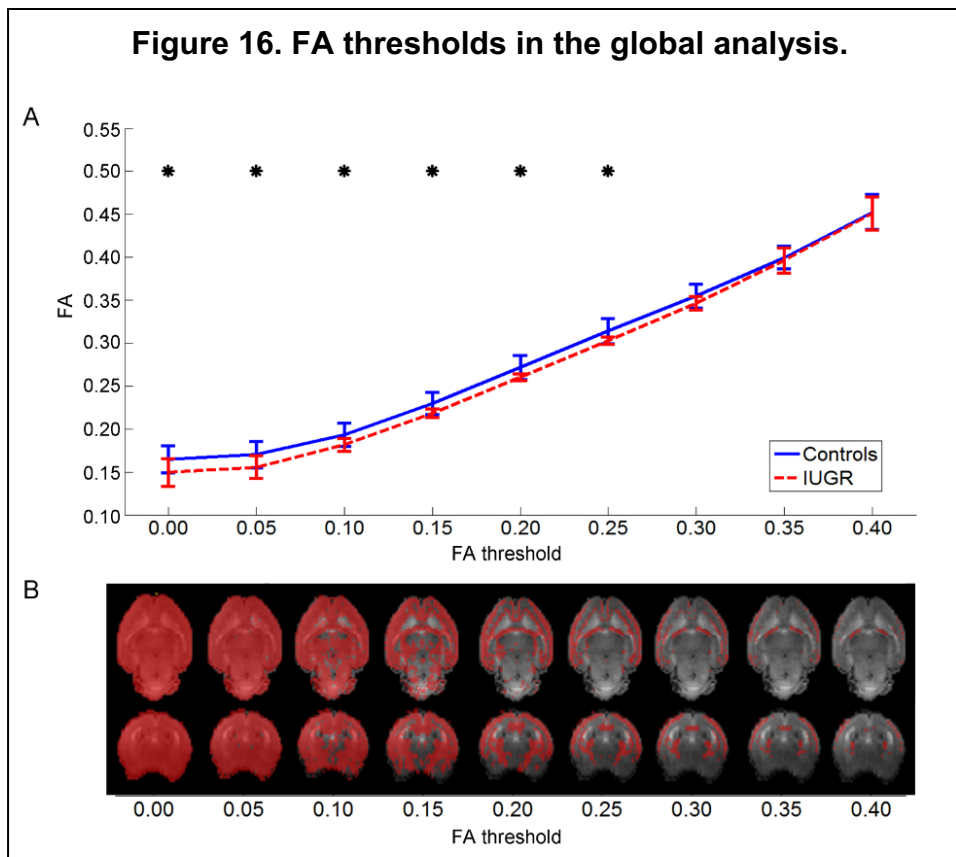
Correlation between FA distribution and neurobehavioral function reveals different patterns in WM and GM areas. Reductions in FA values in cortical and subcortical GM areas showed high correlations with functional impairment. Among GM affected regions, the hippocampus showed the highest number of correlations with neurobehavioral domains. The hippocampus is known for its crucial role in cognitive function such as memory and learning. In human IUGR neonates, a reduction in neonatal hippocampal volume was associated with poor neurofunctional outcomes in neonatal period including autonomic motor state, attention-interaction, self-regulation and examiner facilitation [19]. Additionally, previous experimental data have demonstrated reduced number of neurons in

hippocampus [133] and alterations in the dendritic morphology of pyramidal neurons [134] after IUGR. These findings support that impaired neurocognition in IUGR is mediated by microstructural changes in cortical and subcortical areas detectable with diffusion MRI, with hippocampus playing an important role. Concerning WM regions, internal capsule, anterior commissure and fimbria of hippocampus showed significant correlations with locomotion parameters and posture. Interestingly, anterior commissure and fimbria of hippocampus, WM structures with significant differences in FA distribution demonstrated by VBA, were the WM structures correlated with more altered neurobehavioral items, especially locomotion parameters and posture. Of note, these two WM tracks connect GM structures that also presented significantly decreased FA demonstrated by VBA. Anterior commissure contains axonal tracts connecting temporal lobes and fimbria of hippocampus contains efferent fibers from hippocampus. Finally, changes in olfactory tract and lateral lemniscus WM tracts, which are closely related with olfaction, were significantly correlated with smelling test results. This finding is consistent with previous data demonstrating that neurons of the olfactory epithelium in rabbit are sensitive to global acute hypoxia-ischemia [76]. In summary, this study characterized regional alterations in WM diffusion parameters, findings which were in line with GM data and further suggest the presence of microstructural regional changes underlying brain reorganization in IUGR.

Strengths and limitations

Firstly, the absolute values of ADC obtained in this study were lower than those previously reported in the neonatal rabbit brain [55, 135]. As

abovementioned, that could be explained by the fact that brain fixation decreases water content in the brain reducing ADC values [132]. However, in order to preserve diffusion contrast we used high b-values as previously suggested [136]. In addition, all the brains followed the same fixation process and, theoretically, must be affected in a similar way. Secondly, in the global analysis, a FA thresholding approach was used to identify the voxels belonging to the WM. Although this thresholding has usually been described in order to segment the WM in human brains [137], to the best of our knowledge, it has not been defined for perinatal rabbit brain. Therefore, different thresholds were analyzed, showing that the differences between controls and IUGR are preserved for a wide range of values of the FA threshold (Figure 16).



Thirdly, regional analysis of the images has been performed by means of VBA technique in order to overcome manual delineation limitations. However, the use

of VBA implies weaker statistical power due to the large number of voxels tested [138], increasing type I error rate even after smoothing diffusion related measures volumetric maps. Another issue concerning VBA is that the method requires registration of all the subjects in the dataset to a template volume, and therefore the arbitrary choice of this template could bias the results [138]. To avoid such a bias, the VBA procedure was repeated taking all subjects as template. Similar results were obtained with each template, and there was a high consistency among repeated tests for the regional changes identified. Finally, this work is based on diffusion related parameters, which measure either the amount of diffusivity or the anisotropy of the diffusion, but do not provide information about diffusion direction and therefore, about the fiber bundles trajectories. Further connectivity studies, where WM tracts connecting different areas are identified, will permit a better understanding of the consequences of IUGR in the brain development.

Conclusions

In conclusion, we developed a fetal rabbit model reproducing neurobehavioral and neurostructural consequences of IUGR. The results illustrate that sustained intrauterine restriction of oxygen and nutrient induces a complex pattern of maturational changes, in both GM and WM areas, expressed in diffusivity changes. The findings of the study reveal in detail the pattern of brain microstructural disruptions and their functional correlates in early neonatal life. The model here described allowed to characterize the most significantly affected regions. These anatomical findings will be of help in future multi-scale studies designed to provide a more complete picture of the adaptive processes

6. DISCUSSION

associated with IUGR. Therefore this study contributes to current and future research to improve the understanding of the mechanisms underlying abnormal neurodevelopment of prenatal origin.

7. CONCLUSIONS

1. Selective ligation of uteroplacental vessels in the pregnant rabbit reproduces more closely the features of human intrauterine growth restriction -including mortality and the cardiovascular adaptative changes- than models based on maternal undernutrition.
2. The gestational age and the proportion of vessels ligated produces gradual changes in mortality and biometrical restriction. Likewise, early and late growth restriction insults result in different patterns of histological changes in the fetal rabbit brain.
3. Intrauterine growth restriction results in a complex regional pattern of neurostructural differences as demonstrated by high-resolution MRI global and regional diffusion related parameters. Regional changes are present already at birth and correlate with specific neurobehavioral changes in neonatal life.

8. REFERENCES

1. Kady S and Gardosi J. Perinatal mortality and fetal growth restriction. *Best Pract Res Clin Obstet Gynaecol.* 2004; **18**(3): 397-410.
2. Jarvis S, Glinianaia SV, Torrioli MG, Platt MJ, Miceli M, Jouk PS, et al. Cerebral palsy and intrauterine growth in single births: European collaborative study. *Lancet.* 2003; **362**(9390): 1106-11.
3. Walker DM and Marlow N. Neurocognitive outcome following fetal growth restriction. *Arch Dis Child Fetal Neonatal Ed.* 2008; **93**(4): F322-5.
4. Bassan H, Stolar O, Geva R, Eshel R, Fattal-Valevski A, Leitner Y, et al. Intrauterine growth-restricted neonates born at term or preterm: how different? *Pediatr Neurol.* 2011; **44**(2): 122-30.
5. Figueras F, Oros D, Cruz-Martinez R, Padilla N, Hernandez-Andrade E, Botet F, et al. Neurobehavior in term, small-for-gestational age infants with normal placental function. *Pediatrics.* 2009; **124**(5): e934-41.
6. Eixarch E, Meler E, Iraola A, Illa M, Crispi F, Hernandez-Andrade E, et al. Neurodevelopmental outcome in 2-year-old infants who were small-for-gestational age term fetuses with cerebral blood flow redistribution. *Ultrasound Obstet Gynecol.* 2008; **32**(7): 894-9.
7. Feldman R and Eidelman AI. Neonatal state organization, neuromaturation, mother-infant interaction, and cognitive development in small-for-gestational-age premature infants. *Pediatrics.* 2006; **118**(3): e869-78.
8. Geva R, Eshel R, Leitner Y, Fattal-Valevski A, and Harel S. Memory functions of children born with asymmetric intrauterine growth restriction. *Brain Res.* 2006; **1117**(1): 186-94.

8. REFERENCES

9. Geva R, Eshel R, Leitner Y, Valevski AF, and Harel S. Neuropsychological outcome of children with intrauterine growth restriction: a 9-year prospective study. *Pediatrics*. 2006; **118**(1): 91-100.
10. Leitner Y, Fattal-Valevski A, Geva R, Eshel R, Toledano-Alhadeef H, Rotstein M, et al. Neurodevelopmental outcome of children with intrauterine growth retardation: a longitudinal, 10-year prospective study. *J Child Neurol*. 2007; **22**(5): 580-7.
11. McCarton CM, Wallace IF, Divon M, and Vaughan HG, Jr. Cognitive and neurologic development of the premature, small for gestational age infant through age 6: comparison by birth weight and gestational age. *Pediatrics*. 1996; **98**(6 Pt 1): 1167-78.
12. Scherjon S, Briet J, Oosting H, and Kok J. The discrepancy between maturation of visual-evoked potentials and cognitive outcome at five years in very preterm infants with and without hemodynamic signs of fetal brain-sparing. *Pediatrics*. 2000; **105**(2): 385-91.
13. Tolsa CB, Zimine S, Warfield SK, Freschi M, Sancho Rossignol A, Lazeyras F, et al. Early alteration of structural and functional brain development in premature infants born with intrauterine growth restriction. *Pediatr Res*. 2004; **56**(1): 132-8.
14. Schothorst PF and van Engeland H. Long-term behavioral sequelae of prematurity. *J Am Acad Child Adolesc Psychiatry*. 1996; **35**(2): 175-83.
15. Scherjon SA, Smolders-DeHaas H, Kok JH, and Zondervan HA. The "brain-sparing" effect: antenatal cerebral Doppler findings in relation to neurologic outcome in very preterm infants. *Am J Obstet Gynecol*. 1993; **169**(1): 169-75.

16. Larroque B, Bertrais S, Czernichow P, and Leger J. School difficulties in 20-year-olds who were born small for gestational age at term in a regional cohort study. *Pediatrics*. 2001; **108**(1): 111-5.
17. O'Keeffe MJ, O'Callaghan M, Williams GM, Najman JM, and Bor W. Learning, cognitive, and attentional problems in adolescents born small for gestational age. *Pediatrics*. 2003; **112**(2): 301-7.
18. Heinonen K, Raikkonen K, Pesonen AK, Andersson S, Kajantie E, Eriksson JG, et al. Behavioural symptoms of attention deficit/hyperactivity disorder in preterm and term children born small and appropriate for gestational age: a longitudinal study. *BMC Pediatr*. 2010; **10**: 91.
19. Lodygensky GA, Seghier ML, Warfield SK, Tolsa CB, Sizonenko S, Lazeyras F, et al. Intrauterine growth restriction affects the preterm infant's hippocampus. *Pediatr Res*. 2008; **63**(4): 438-43.
20. Dubois J, Benders M, Borradori-Tolsa C, Cachia a, Lazeyras F, {Ha-Vinh Leuchter} R, et al. Primary cortical folding in the human newborn: an early marker of later functional development. *Brain*. 2008; **131**: 2028-41.
21. Padilla N, Falcón C, Sanz-Cortés M, Figueras F, Bargallo N, Crispi F, et al. Differential effects of intrauterine growth restriction on brain structure and development in preterm infants: A magnetic resonance imaging study. *Brain research*. 2011; **1382**(25): 98-108.
22. Esteban F, Padilla N, Sanz-Cortés M, and de Miras J. Fractal-dimension analysis detects cerebral changes in preterm infants with and without intrauterine growth restriction. *NeuroImage*. 2010; **53**(4): 1225-32.
23. Baschat AA. Pathophysiology of fetal growth restriction: implications for diagnosis and surveillance. *Obstet Gynecol Surv*. 2004; **59**(8): 617-27.

8. REFERENCES

24. Rees S, Harding R, and Walker D. An adverse intrauterine environment: implications for injury and altered development of the brain. *Int J Dev Neurosci.* 2007; **26**(1): 3-11.
25. Sebire NJ. Umbilical artery Doppler revisited: pathophysiology of changes in intrauterine growth restriction revealed. *Ultrasound Obstet Gynecol.* 2003; **21**(5): 419-22.
26. Hernandez-Andrade E, Figueroa-Diesel H, Jansson T, Rangel-Nava H, and Gratacos E. Changes in regional fetal cerebral blood flow perfusion in relation to hemodynamic deterioration in severely growth-restricted fetuses. *Ultrasound Obstet Gynecol.* 2008; **32**(1): 71-6.
27. Hershkovitz R, Kingdom JC, Geary M, and Rodeck CH. Fetal cerebral blood flow redistribution in late gestation: identification of compromise in small fetuses with normal umbilical artery Doppler. *Ultrasound Obstet Gynecol.* 2000; **15**(3): 209-12.
28. Oros D, Figueras F, Cruz-Martinez R, Padilla N, Meler E, Hernandez-Andrade E, et al. Middle versus anterior cerebral artery Doppler for the prediction of perinatal outcome and neonatal neurobehavior in term small-for-gestational-age fetuses with normal umbilical artery Doppler. *Ultrasound Obstet Gynecol.* 2010; **35**(4): 456-61.
29. Oros D, Figueras F, Cruz-Martinez R, Padilla N, Meler E, Hernandez-Andrade E, et al. Middle versus anterior cerebral artery Doppler for the prediction of perinatal outcome and neonatal neurobehavior in term small-for-gestational-age fetuses with normal umbilical artery Doppler. *Ultrasound Obstet Gynecol.* **35**(4): 456-61.

30. Rees S, Breen S, Loeliger M, McCrabb G, and Harding R. Hypoxemia near mid-gestation has long-term effects on fetal brain development. *J Neuropathol Exp Neurol.* 1999; **58**(9): 932-45.
31. Loeliger M, Louey S, Cock ML, Harding R, and Rees SM. Chronic placental insufficiency and foetal growth restriction lead to long-term effects on postnatal retinal structure. *Clin Experiment Ophthalmol.* 2003; **31**(3): 250-3.
32. Back SA, Gan X, Li Y, Rosenberg PA, and Volpe JJ. Maturation-dependent vulnerability of oligodendrocytes to oxidative stress-induced death caused by glutathione depletion. *J Neurosci.* 1998; **18**(16): 6241-53.
33. Rees S, Harding R, and Walker D. The biological basis of injury and neuroprotection in the fetal and neonatal brain. *Int J Dev Neurosci.* 2011: in press.
34. Toft PB. Prenatal and perinatal striatal injury: a hypothetical cause of attention-deficit-hyperactivity disorder? *Pediatr Neurol.* 1999; **21**(3): 602-10.
35. Hecher K. From the fetus at risk to intelligence, educational attainment and psychological distress in the young adult. *Ultrasound Obstet Gynecol.* 2007; **29**(6): 612-3.
36. Schroder HJ. Models of fetal growth restriction. *Eur J Obstet Gynecol Reprod Biol.* 2003; **110 Suppl 1**: S29-39.
37. Vuguin PM. Animal models for small for gestational age and fetal programming of adult disease. *Horm Res.* 2007; **68**(3): 113-23.

8. REFERENCES

38. Gagnon R, Johnston L, and Murotsuki J. Fetal placental embolization in the late-gestation ovine fetus: alterations in umbilical blood flow and fetal heart rate patterns. *Am J Obstet Gynecol.* 1996; **175**(1): 63-72.
39. Duncan JR, Cock ML, Loeliger M, Louey S, Harding R, and Rees SM. Effects of exposure to chronic placental insufficiency on the postnatal brain and retina in sheep. *J Neuropathol Exp Neurol.* 2004; **63**(11): 1131-43.
40. Wigglesworth JS. Experimental Growth Retardation in the Foetal Rat. *J Pathol Bacteriol.* 1964; **88**: 1-13.
41. Lang U, Baker RS, Braems G, Zygmunt M, Kunzel W, and Clark KE. Uterine blood flow--a determinant of fetal growth. *Eur J Obstet Gynecol Reprod Biol.* 2003; **110 Suppl 1**: S55-61.
42. Neitzke U, Harder T, Schellong K, Melchior K, Ziska T, Rodekamp E, et al. Intrauterine growth restriction in a rodent model and developmental programming of the metabolic syndrome: a critical appraisal of the experimental evidence. *Placenta.* 2008; **29**(3): 246-54.
43. Bassan H, Kidron D, Bassan M, Rotstein M, Kariv N, Giladi E, et al. The effects of vascular intrauterine growth retardation on cortical astrocytes. *J Matern Fetal Neonatal Med.* 2009: 1-6.
44. Bassan H, Trejo LL, Kariv N, Bassan M, Berger E, Fattal A, et al. Experimental intrauterine growth retardation alters renal development. *Pediatr Nephrol.* 2000; **15**(3-4): 192-5.
45. Turner AJ and Trudinger BJ. A modification of the uterine artery restriction technique in the guinea pig fetus produces asymmetrical ultrasound growth. *Placenta.* 2009; **30**(3): 236-40.

46. Camprubi M, Ortega A, Balaguer A, Iglesias I, Girabent M, Callejo J, et al. Cauterization of meso-ovarian vessels, a new model of intrauterine growth restriction in rats. *Placenta*. 2009; **30**(9): 761-6.
47. Eixarch E, Figueras F, Hernandez-Andrade E, Crispi F, Nadal A, Torre I, et al. An experimental model of fetal growth restriction based on selective ligation of uteroplacental vessels in the pregnant rabbit. *Fetal Diagn Ther*. 2009; **26**(4): 203-11.
48. Ballesteros MC, Hansen PE, and Soila K. MR imaging of the developing human brain. Part 2. Postnatal development. *Radiographics*. 1993; **13**(3): 611-22.
49. Mallard E, Rees S, Stringer M, ML C, and Harding R. Effects of chronic placental insufficiency on brain development in fetal sheep. *Pediatr Res*. 1998; **43**(2): 262-270.
50. Carter AM. Animal models of human placentation--a review. *Placenta*. 2007; **28 Suppl A**: S41-7.
51. Tan S, Drobyshevsky A, Jilling T, Ji X, Ullman LM, Englof I, et al. Model of cerebral palsy in the perinatal rabbit. *J Child Neurol*. 2005; **20**(12): 972-9.
52. Rees S and Inder T. Fetal and neonatal origins of altered brain development. *Early Hum Dev*. 2005; **81**(9): 753-61.
53. Hildebrand C, Remahl S, Persson H, and Bjartmar C. Myelinated nerve fibres in the CNS. *Prog Neurobiol*. 1993; **40**(3): 319-84.
54. Derrick M, Luo NL, Bregman JC, Jilling T, Ji X, Fisher K, et al. Preterm fetal hypoxia-ischemia causes hypertonia and motor deficits in the neonatal rabbit: a model for human cerebral palsy? *J Neurosci*. 2004; **24**(1): 24-34.

8. REFERENCES

55. Drobyshevsky A, Derrick M, Wyrwicz AM, Ji X, Englof I, Ullman LM, et al. White matter injury correlates with hypertonia in an animal model of cerebral palsy. *J Cereb Blood Flow Metab.* 2007; **27**(2): 270-81.
56. Heizmann CW. Ca²⁺-binding S100 proteins in the central nervous system. *Neurochem Res.* 1999; **24**(9): 1097-100.
57. Gerlach R, Demel G, König HG, Gross U, Prehn J, Raabe A, et al. Active secretion of S100B from astrocytes during metabolic stress. *Neuroscience.* 2006; **141**: 1697-1701.
58. Korfiatis S, Stranjalis G, Papadimitriou A, Psachoulia C, Daskalakis G, Antsaklis A, et al. Serum S-100B protein as a biochemical marker of brain injury: a review of current concepts. *Curr Med Chem.* 2006; **13**(30): 3719-31.
59. Gazzolo D, Marinoni E, Di Iorio R, Bruschetti M, Kornacka M, Lituania M, et al. Urinary S100B protein measurements: A tool for the early identification of hypoxic-ischemic encephalopathy in asphyxiated full-term infants. *Crit Care Med.* 2004; **32**(1): 131-6.
60. Gazzolo D, Marinoni E, di Iorio R, Lituania M, Bruschetti PL, and Michetti F. Circulating S100beta protein is increased in intrauterine growth-retarded fetuses. *Pediatr Res.* 2002; **51**(2): 215-9.
61. Mollgard K and Schumacher U. Immunohistochemical assessment of cellular proliferation in the developing human CNS using formalin-fixed paraffin-embedded material. *J Neurosci Methods.* 1993; **46**(3): 191-6.
62. Zaidi AU, Bessert DA, Ong JE, Xu H, Barks JD, Silverstein FS, et al. New oligodendrocytes are generated after neonatal hypoxic-ischemic brain injury in rodents. *Glia.* 2004; **46**(4): 380-90.

-
63. Ong J, Plane JM, Parent JM, and Silverstein FS. Hypoxic-ischemic injury stimulates subventricular zone proliferation and neurogenesis in the neonatal rat. *Pediatr Res*. 2005; **58**(3): 600-6.
 64. Fagel DM, Ganat Y, Silbereis J, Ebbitt T, Stewart W, Zhang H, et al. Cortical neurogenesis enhanced by chronic perinatal hypoxia. *Exp Neurol*. 2006; **199**(1): 77-91.
 65. Basser PJ and Pierpaoli C. Microstructural and physiological features of tissues elucidated by quantitative-diffusion-tensor MRI. *J Magn Reson B*. 1996; **111**(3): 209-19.
 66. Neil J, Miller J, Mukherjee P, and Huppi PS. Diffusion tensor imaging of normal and injured developing human brain - a technical review. *NMR Biomed*. 2002; **15**(7-8): 543-52.
 67. Merino JG and Warach S. Imaging of acute stroke. *Nat Rev Neurol*. 2010; **6**(10): 560-71.
 68. Rivers CS and Wardlaw JM. What has diffusion imaging in animals told us about diffusion imaging in patients with ischaemic stroke? *Cerebrovasc Dis*. 2005; **19**(5): 328-36.
 69. Sizonenko SV, Camm EJ, Garbow JR, Maier SE, Inder TE, Williams CE, et al. Developmental changes and injury induced disruption of the radial organization of the cortex in the immature rat brain revealed by in vivo diffusion tensor MRI. *Cereb Cortex*. 2007; **17**(11): 2609-17.
 70. Berman JI, Hamrick SE, McQuillen PS, Studholme C, Xu D, Henry RG, et al. Diffusion-weighted imaging in fetuses with severe congenital heart defects. *AJNR Am J Neuroradiol*. 2011; **32**(2): E21-2.

8. REFERENCES

71. Sanz-Cortes M, Figueras F, Bargallo N, Padilla N, Amat-Roldan I, and Gratacos E. Abnormal brain microstructure and metabolism in small-for-gestational-age term fetuses with normal umbilical artery Doppler. *Ultrasound Obstet Gynecol.* 2010; **36**(2): 159-65.
72. D'Arceuil H, Liu C, Levitt P, Thompson B, Kosofsky B, and de Crespigny A. Three-dimensional high-resolution diffusion tensor imaging and tractography of the developing rabbit brain. *Dev Neurosci.* 2008; **30**(4): 262-75.
73. Hudson R, Cruz Y, Lucio A, Ninomiya J, and Martinez-Gomez M. Temporal and behavioral patterning of parturition in rabbits and rats. *Physiol Behav.* 1999; **66**(4): 599-604.
74. Saadani-Makki F, Kannan S, Lu X, Janisse J, Dawe E, Edwin S, et al. Intrauterine administration of endotoxin leads to motor deficits in a rabbit model: a link between prenatal infection and cerebral palsy. *Am J Obstet Gynecol.* 2008; **199**(6): 651 e1-7.
75. Derrick M, Drobyshevsky A, Ji X, Chen L, Yang Y, Ji H, et al. Hypoxia-ischemia causes persistent movement deficits in a perinatal rabbit model of cerebral palsy: assessed by a new swim test. *Int J Dev Neurosci.* 2009; **27**(6): 549-57.
76. Drobyshevsky A, Robinson AM, Derrick M, Wyrwicz AM, Ji X, Englof I, et al. Sensory deficits and olfactory system injury detected by novel application of MEMRI in newborn rabbit after antenatal hypoxia-ischemia. *Neuroimage.* 2006; **32**(3): 1106-12.

-
77. Tyszka JM, Readhead C, Bearer EL, Pautler RG, and Jacobs RE. Statistical diffusion tensor histology reveals regional dysmyelination effects in the shiverer mouse mutant. *Neuroimage*. 2006; **29**(4): 1058-65.
 78. Toussaint N, Souplet J-C, and Fillard P, *MedINRIA: Medical Image Navigation and Research Tool by INRIA*, in *Proc. of MICCAI'07 Workshop on Interaction in medical image analysis and visualization*. 2007: Brisbane, Australia.
 79. Westin CF, Maier SE, Mamata H, Nabavi A, Jolesz FA, and Kikinis R. Processing and visualization for diffusion tensor MRI. *Med Image Anal*. 2002; **6**(2): 93-108.
 80. Jones DK, Griffin LD, Alexander DC, Catani M, Horsfield MA, Howard R, et al. Spatial normalization and averaging of diffusion tensor MRI data sets. *Neuroimage*. 2002; **17**(2): 592-617.
 81. Martin-Ancel A, Garcia-Alix A, Pascual-Salcedo D, Cabanas F, Valcarce M, and Quero J. Interleukin-6 in the cerebrospinal fluid after perinatal asphyxia is related to early and late neurological manifestations. *Pediatrics*. 1997; **100**(5): 789-94.
 82. Giles WB, Trudinger BJ, and Baird PJ. Fetal umbilical artery flow velocity waveforms and placental resistance: pathological correlation. *Br J Obstet Gynaecol*. 1985; **92**(1): 31-8.
 83. Galan HL, Anthony RV, Rigano S, Parker TA, de Vrijer B, Ferrazzi E, et al. Fetal hypertension and abnormal Doppler velocimetry in an ovine model of intrauterine growth restriction. *Am J Obstet Gynecol*. 2005; **192**(1): 272-9.

8. REFERENCES

84. Morrow RJ, Adamson SL, Bull SB, and Ritchie JW. Effect of placental embolization on the umbilical arterial velocity waveform in fetal sheep. *Am J Obstet Gynecol.* 1989; **161**(4): 1055-60.
85. Polisca A, Scotti L, Orlandi R, Brecchia G, and Boiti C. Doppler evaluation of maternal and fetal vessels during normal gestation in rabbits. *Theriogenology.* 2010; **73**(3): 358-66.
86. Kiserud T, Jauniaux E, West D, Ozturk O, and Hanson MA. Circulatory responses to maternal hyperoxaemia and hypoxaemia assessed non-invasively in fetal sheep at 0.3-0.5 gestation in acute experiments. *BJOG.* 2001; **108**(4): 359-64.
87. Tchirikov M, Schroder HJ, and Hecher K. Ductus venosus shunting in the fetal venous circulation: regulatory mechanisms, diagnostic methods and medical importance. *Ultrasound Obstet Gynecol.* 2006; **27**(4): 452-61.
88. Bensley BA, *Practical anatomy of the rabbit: An elementary laboratory text-book in mammalian anatomy.* 8th ed. The Blakistoh Company. 1948, Philadelphia.
89. Harman CR and Baschat AA. Arterial and venous Dopplers in IUGR. *Clin Obstet Gynecol.* 2003; **46**(4): 931-46.
90. Dagdelen S, Eren N, Karabulut H, and Caglar N. Importance of the index of myocardial performance in evaluation of left ventricular function. *Echocardiography.* 2002; **19**(4): 273-8.
91. Crispi F, Hernandez-Andrade E, Pelsers MM, Plasencia W, Benavides-Serralde JA, Eixarch E, et al. Cardiac dysfunction and cell damage across clinical stages of severity in growth-restricted fetuses. *Am J Obstet Gynecol.* 2008; **199**(3): 254 e1-8.

92. Comas M, Crispi F, Cruz-Martinez R, Figueras F, and Gratacos E. Tissue Doppler echocardiographic markers of cardiac dysfunction in small-for-gestational age fetuses. *Am J Obstet Gynecol.* 2011.
93. Comas M, Crispi F, Cruz-Martinez R, Martinez JM, Figueras F, and Gratacos E. Usefulness of myocardial tissue Doppler vs conventional echocardiography in the evaluation of cardiac dysfunction in early-onset intrauterine growth restriction. *Am J Obstet Gynecol.* 2010; **203**(1): 45 e1-7.
94. Battista MC, Calvo E, Chorvatova A, Comte B, Corbeil J, and Brochu M. Intra-uterine growth restriction and the programming of left ventricular remodelling in female rats. *J Physiol.* 2005; **565**(Pt 1): 197-205.
95. Battista MC, Oligny LL, St-Louis J, and Brochu M. Intrauterine growth restriction in rats is associated with hypertension and renal dysfunction in adulthood. *Am J Physiol Endocrinol Metab.* 2002; **283**(1): E124-31.
96. Battista MC, Otis M, Cote M, Laforest A, Peter M, Lalli E, et al. Extracellular matrix and hormones modulate DAX-1 localization in the human fetal adrenal gland. *J Clin Endocrinol Metab.* 2005; **90**(9): 5426-31.
97. Corstius HB, Zimanyi MA, Maka N, Herath T, Thomas W, van der Laarse A, et al. Effect of intrauterine growth restriction on the number of cardiomyocytes in rat hearts. *Pediatr Res.* 2005; **57**(6): 796-800.
98. Fouron JC. The unrecognized physiological and clinical significance of the fetal aortic isthmus. *Ultrasound Obstet Gynecol.* 2003; **22**(5): 441-7.
99. Figueras F, Benavides A, Del Rio M, Crispi F, Eixarch E, Martinez JM, et al. Monitoring of fetuses with intrauterine growth restriction: longitudinal

8. REFERENCES

- changes in ductus venosus and aortic isthmus flow. *Ultrasound Obstet Gynecol.* 2009; **33**(1): 39-43.
100. Fouron JC, Gosselin J, Amiel-Tison C, Infante-Rivard C, Fouron C, Skoll A, et al. Correlation between prenatal velocity waveforms in the aortic isthmus and neurodevelopmental outcome between the ages of 2 and 4 years. *Am J Obstet Gynecol.* 2001; **184**(4): 630-6.
101. Fouron JC, Gosselin J, Raboisson MJ, Lamoureux J, Tison CA, Fouron C, et al. The relationship between an aortic isthmus blood flow velocity index and the postnatal neurodevelopmental status of fetuses with placental circulatory insufficiency. *Am J Obstet Gynecol.* 2005; **192**(2): 497-503.
102. Nagase K, Iida H, and Dohi S. Effects of ketamine on isoflurane- and sevoflurane-induced cerebral vasodilation in rabbits. *J Neurosurg Anesthesiol.* 2003; **15**(2): 98-103.
103. Flake AW, Villa RL, Adzick NS, and Harrison MR. Transamniotic fetal feeding. II. A model of intrauterine growth retardation using the relationship of "natural runting" to uterine position. *J Pediatr Surg.* 1987; **22**(9): 816-9.
104. Thakur A, Sase M, Lee JJ, Thakur V, and Buchmiller TL. Ontogeny of insulin-like growth factor 1 in a rabbit model of growth retardation. *J Surg Res.* 2000; **91**(2): 135-40.
105. Thakur A, Sase M, Lee JJ, Thakur V, and Buchmiller TL. Effect of dexamethasone on insulin-like growth factor-1 expression in a rabbit model of growth retardation. *J Pediatr Surg.* 2000; **35**(6): 898-904; discussion 904-5.

106. Buchmiller-Crair TL, Gregg JP, Rivera FA, Jr., Choi RS, Diamond JM, and Fonkalsrud EW. Delayed disaccharidase development in a rabbit model of intrauterine growth retardation. *Pediatr Res.* 2001; **50**(4): 520-4.
107. Skarsgard ED, Amii LA, Dimmitt RA, Sakamoto G, Brindle ME, and Moss RL. Fetal therapy with rhIGF-1 in a rabbit model of intrauterine growth retardation. *J Surg Res.* 2001; **99**(1): 142-6.
108. Cellini C, Xu J, Arriaga A, and Buchmiller-Crair TL. Effect of epidermal growth factor infusion on fetal rabbit intrauterine growth retardation and small intestinal development. *J Pediatr Surg.* 2004; **39**(6): 891-7; discussion 891-7.
109. Cellini C, Xu J, and Buchmiller-Crair T. Effect of epidermal growth factor on small intestinal sodium/glucose cotransporter-1 expression in a rabbit model of intrauterine growth retardation. *J Pediatr Surg.* 2005; **40**(12): 1892-7.
110. Persson L, Hardemark HG, Gustafsson J, Rundstrom G, Mendel-Hartvig I, Esscher T, et al. S-100 protein and neuron-specific enolase in cerebrospinal fluid and serum: markers of cell damage in human central nervous system. *Stroke.* 1987; **18**(5): 911-8.
111. Nagdyman N, Komen W, Ko HK, Muller C, and Obladen M. Early biochemical indicators of hypoxic-ischemic encephalopathy after birth asphyxia. *Pediatr Res.* 2001; **49**(4): 502-6.
112. Thorngren-Jerneck K, Alling C, Herbst A, Amer-Wahlin I, and Marsal K. S100 protein in serum as a prognostic marker for cerebral injury in term newborn infants with hypoxic ischemic encephalopathy. *Pediatr Res.* 2004; **55**(3): 406-12.

8. REFERENCES

113. Raponi E, Agenes F, Delphin C, Assard N, Baudier J, Legraverend C, et al. S100B expression defines a state in which GFAP-expressing cells lose their neural stem cell potential and acquire a more mature developmental stage. *Glia*. 2007; **55**(2): 165-77.
114. Barrett RD, Bennet L, Davidson J, Dean JM, George S, Emerald BS, et al. Destruction and reconstruction: hypoxia and the developing brain. *Birth Defects Res C Embryo Today*. 2007; **81**(3): 163-76.
115. Hermans B, Lewi L, Jani J, De Buck F, Deprest J, and Puers R. Feasibility of in utero telemetric fetal ECG monitoring in a lamb model. *Fetal Diagn Ther*. 2008; **24**(2): 81-5.
116. Eixarch E, Hernandez-Andrade E, Crispi F, Illa M, Torre I, Figueras F, et al. Impact on fetal mortality and cardiovascular Doppler of selective ligation of uteroplacental vessels compared with undernutrition in a rabbit model of intrauterine growth restriction. *Placenta*. 2011; **32**(4): 304-9.
117. Val-Laillet D and Nowak R. Early discrimination of the mother by rabbit pups. *Applied Animal Behaviour Science*. 2008; **111**: 173-182.
118. Lodygensky GA, Inder TE, and Neil JJ. Application of magnetic resonance imaging in animal models of perinatal hypoxic-ischemic cerebral injury. *Int J Dev Neurosci*. 2008; **26**(1): 13-25.
119. Abe O, Takao H, Gono W, Sasaki H, Murakami M, Kabasawa H, et al. Voxel-based analysis of the diffusion tensor. *Neuroradiology*. 2010; **52**(8): 699-710.
120. Van Camp N, Blockx I, Verhoye M, Casteels C, Coun F, Leemans A, et al. Diffusion tensor imaging in a rat model of Parkinson's disease after lesioning of the nigrostriatal tract. *NMR Biomed*. 2009; **22**(7): 697-706.

121. Snook L, Plewes C, and Beaulieu C. Voxel based versus region of interest analysis in diffusion tensor imaging of neurodevelopment. *Neuroimage*. 2007; **34**(1): 243-52.
122. Miller SP, McQuillen PS, Hamrick S, Xu D, Glidden DV, Charlton N, et al. Abnormal Brain Development in Newborns with Congenital Heart Disease. *New England Journal of Medicine*. 2007; **357**(19): 1928-1938.
123. Shedeed S and Elfaytouri E. Brain Maturity and Brain Injury in Newborns With Cyanotic Congenital Heart Disease. *Pediatric Cardiology*. 2011; **32**(1): 47-54.
124. Tolcos M, Bateman E, O'Dowd R, Markwick R, Vrijssen K, Rehn A, et al. Intrauterine growth restriction affects the maturation of myelin. *Experimental Neurology*. 2011; **In Press, Uncorrected Proof**.
125. Wang S, Wu EX, Tam CN, Lau HF, Cheung PT, and Khong PL. Characterization of white matter injury in a hypoxic-ischemic neonatal rat model by diffusion tensor MRI. *Stroke*. 2008; **39**(8): 2348-53.
126. Kochunov P, Williamson DE, Lancaster J, Fox P, Cornell J, Blangero J, et al. Fractional anisotropy of water diffusion in cerebral white matter across the lifespan. *Neurobiology of Aging*. 2010; **In Press**.
127. Olivier P, Baud O, Bousslama M, Evrard P, Gressens P, and Verney C. Moderate growth restriction: deleterious and protective effects on white matter damage. *Neurobiol Dis*. 2007; **26**(1): 253-63.
128. Nitsos I and Rees S. The effects of intrauterine growth retardation on the development of neuroglia in fetal guinea pigs. An immunohistochemical and an ultrastructural study. *Int J Dev Neurosci*. 1990; **8**(3): 233-44.

8. REFERENCES

129. Huppi PS, Maier SE, Peled S, Zientara GP, Barnes PD, Jolesz FA, et al. Microstructural development of human newborn cerebral white matter assessed in vivo by diffusion tensor magnetic resonance imaging. *Pediatr Res.* 1998; **44**(4): 584-90.
130. Neil JJ, Shiran SI, McKinstry RC, Schefft GL, Snyder AZ, Almlí CR, et al. Normal brain in human newborns: apparent diffusion coefficient and diffusion anisotropy measured by using diffusion tensor MR imaging. *Radiology.* 1998; **209**(1): 57-66.
131. Wimberger DM, Roberts TP, Barkovich AJ, Prayer LM, Moseley ME, and Kucharczyk J. Identification of "premyelination" by diffusion-weighted MRI. *J Comput Assist Tomogr.* 1995; **19**(1): 28-33.
132. Sun SW, Neil JJ, and Song SK. Relative indices of water diffusion anisotropy are equivalent in live and formalin-fixed mouse brains. *Magn Reson Med.* 2003; **50**(4): 743-8.
133. Mallard C, Loeliger M, Copolov D, and Rees S. Reduced number of neurons in the hippocampus and the cerebellum in the postnatal guinea-pig following intrauterine growth-restriction. *Neuroscience.* 2000; **100**(2): 327-33.
134. Dieni S and Rees S. Dendritic morphology is altered in hippocampal neurons following prenatal compromise. *J Neurobiol.* 2003; **55**(1): 41-52.
135. Saadani-Makki F, Kannan S, Makki M, Muzik O, Janisse J, Romero R, et al. Intrauterine endotoxin administration leads to white matter diffusivity changes in newborn rabbits. *J Child Neurol.* 2009; **24**(9): 1179-89.

136. Miller KL, Stagg CJ, Douaud G, Jbabdi S, Smith SM, Behrens TE, et al. Diffusion imaging of whole, post-mortem human brains on a clinical MRI scanner. *Neuroimage*. 2011; **57**(1): 167-81.
137. Mori S and Zhang J. Principles of diffusion tensor imaging and its applications to basic neuroscience research. *Neuron*. 2006; **51**(5): 527-39.
138. Lee JE, Chung MK, Lazar M, DuBray MB, Kim J, Bigler ED, et al. A study of diffusion tensor imaging by tissue-specific, smoothing-compensated voxel-based analysis. *Neuroimage*. 2009; **44**(3): 870-83.

9. ACKNOWLEDGMENTS

I would like to express my gratitude to my thesis directors who have always encouraged me to continue with research and have been the best example for improving myself day by day.

To all coauthors of the attached papers, who have been indispensable in order to achieve this thesis and from whom I could learn.

Acknowledgements for financial support:

Elisenda Eixarch is supported by a Emili Letang fellowship by Hospital Clinic (Barcelona, Spain) and Rio Hortega grant (CM08/00105) from the Carlos III Institute of Health (Spain).

The Fetal and Perinatal Medicine Research Group (IDIBAPS) is founded by the Centro de Investigación Biomédica en Red de Enfermedades Raras (CIBERER,ISCIII, Spain), and supported by grants from the Fondo the Investigación Sanitaria (PI/060347) (Spain), Cerebra Foundation for the Brain Injured Child (Carmarthen, Wales, UK), Thrasher Research Fund (Salt Lake City, USA) and the European Commission and Obra Social La Caixa (Barcelona, Spain)

El meu més sincer agraïment al meus dos directors de tesi. A l'Eduard per haver dipositat la seva confiança en mi, per deixar-me formar part del seu apassionant projecte i per ensenyar-me tantes coses en els darrers anys. Al Francesc per haver-me introduït en el món de la recerca, per la seva dedicació, per tots els coneixements transmesos i per haver tingut cura de mi i de la meva carrera professional.

El meu agraïment a tots els co-autors dels articles inclosos en aquest projecte. En especial a l'Edgar que em va introduir en el món de l'experimentació animal i que malgrat la distància sempre m'ha donat el seu suport, a la Fàtima que sempre em contagia amb el seu entusiasme, a la Míriam que va acceptar el repte de l'experimentació animal i l'ha superat amb escreixos i al Dafnis que sempre m'ajuda amb la seva especial visió de les coses.

A tots els companys del grup de recerca i de l'hospital, gràcies per tots els bons moments que hem compartit junts. En especial als companys de l'oficina d'enginyers, gràcies per escoltar i per les vostres rialles.

Finalment, voldria fer una menció especial a la meva família. A la meva mare que em va ensenyar a valorar les coses que són realment importants, al meu pare i la meva germana que sempre m'han donant el seu suport i m'han encoratjat a continuar inclús en els pitjors moments i finalment al Víctor, per la seva paciència i suport, sense ell aquesta tesi no hauria estat mai possible

10. ANNEXES

10.1. Project 1: Ethic committee approval



REGISTRE	
C.E.E.A.	
Comitè Ètic d'Experimentació Animal	
Data:	16 GEN. 2008
Entrada:	
Sortida:	286/08

COMITÈ ÈTIC D'EXPERIMENTACIÓ ANIMAL (CEEA)**Formulari d'acceptació de procediments****DADES PROCEDIMENT**

Títol: Impacte del moment i severitat de l'insult en la distribució regional del dany neurològic fetal en model animal d'hiponutrició en conilla gestant

Investigador Responsable: **Elisenda Eixarch Roca**

Un cop examinada la documentació presentada, en compliment del Decret 214/97 de la Generalitat de Catalunya, el CEEA de la UB ha resolt **ACCEPTAR** el procediment sol.licitat

Three handwritten signatures in black ink, representing the members of the CEEA who approved the procedure. The signatures are written in a cursive style.

Signat pels membres del CEEA que han prè l'acord

Barcelona, 26 d'octubre de 2007

NOTA: El CEEA delega en el/la responsable en benestar animal de la Unitat d'Experimentació Animal on s'allotjaran els animals, el seguiment de la realització del procediment d'acord amb el que està establert a la memòria aprovada per aquest comitè.

10.2. Project 2: Ethic committee approval



CEEA
(Comitè Ètic d'Experimentació Animal)

Parc Científic de Barcelona - Edifici Modular
Josep Samitier, 1-5
08028 Barcelona
Tel./Fax 93 403 72 58



INFORME DEL COMITÈ ÈTIC D'EXPERIMENTACIÓ ANIMAL


El sotassignat, Dr. Jordi Guinea Mejias, Secretari del Comitè Ètic d'Experimentació Animal de la Universitat de Barcelona, **FA CONSTAR:**

Que el Comitè Ètic d'Experimentació Animal ha analitzat els procediments del projecte d'investigació titulat **"Impacte del moment i severitat de l'insult en la distribució regional del dany neurològic fetal en un model animal d'hipòxia crònica"** del qual l'investigador principal és la **Dra. Elisenda Eixarch**.

Aquest Comitè entén que l'esmentat procediment s'ajusta a les normes ètiques essencials i a la legislació vigent i, per tant, ha decidit la seva aprovació.

La qual cosa signo als efectes oportuns a Barcelona, set d'abril de dos mil sis.

10.3. Project 3: Ethic committee approval

 U UNIVERSITAT DE BARCELONA B	C.E.E.A. (Comitè Ètic d'Experimentació Animal) Parc Científic de Barcelona Baldri i reixac 10-12 08028 Barcelona Tel. 93.403.72.58 ccea@sct.ub.es	REGISTRE C.E.E.A. Comitè Ètic d'Experimentació Animal
		11 MAIG 2010 Entrada: Sortida: 206/10 Med

COPIA **COMITÈ ÈTIC D'EXPERIMENTACIÓ ANIMAL (CEEA)**
Formulari d'acceptació de procediments

DADES PROCEDIMENT	
Títol:	Evaluación de la disfunción cardíaca y de la lesión neurológica en el periodo postnatal en un modelo animal de restricción de crecimiento intrauterino por hipoxia crónica en coneja gestante
Investigador Responsable:	Elisenda Eixarch Roca

Un cop examinada la documentació presentada, en compliment del Decret 214/97 de la Generalitat de Catalunya, el CEEA de la UB ha resolt **ACCEPTAR** el procediment sol·licitat








Signat pels membres del CEEA que han pres l'acord

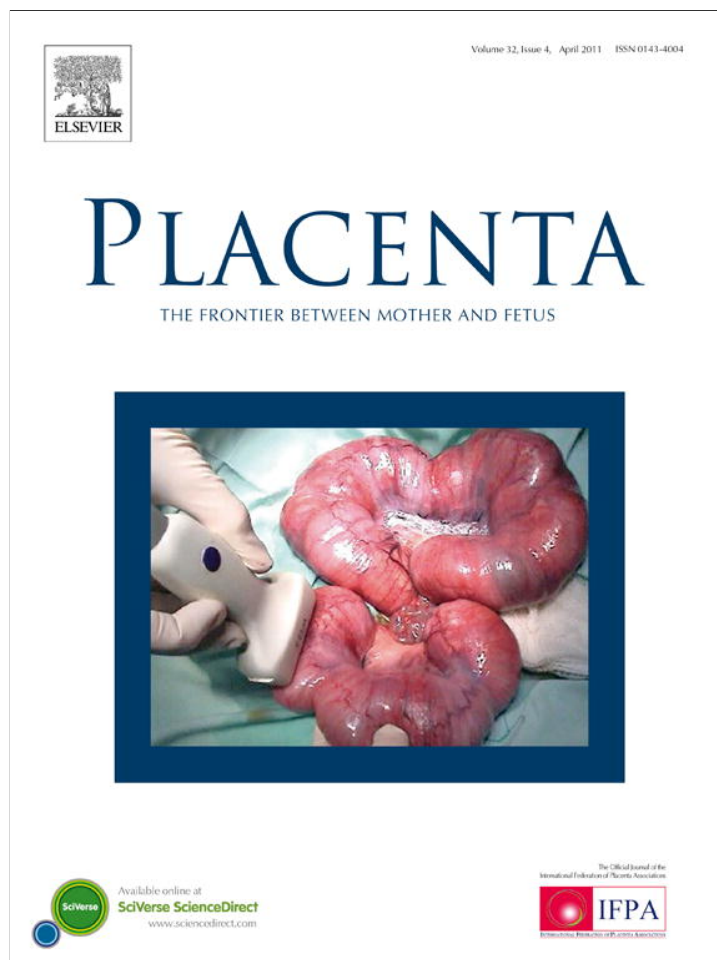
Barcelona, 23 de març de 2010

11. PAPERS

PROJECT 1:

Impact on fetal mortality and cardiovascular Doppler of selective ligation of uteroplacental vessels compared with undernutrition in a rabbit model of intrauterine growth restriction.

Provided for non-commercial research and education use.
Not for reproduction, distribution or commercial use.



This article appeared in a journal published by Elsevier. The attached copy is furnished to the author for internal non-commercial research and education use, including for instruction at the authors institution and sharing with colleagues.

Other uses, including reproduction and distribution, or selling or licensing copies, or posting to personal, institutional or third party websites are prohibited.

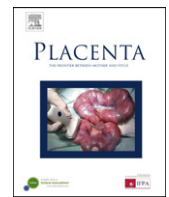
In most cases authors are permitted to post their version of the article (e.g. in Word or Tex form) to their personal website or institutional repository. Authors requiring further information regarding Elsevier's archiving and manuscript policies are encouraged to visit:

<http://www.elsevier.com/copyright>



Contents lists available at ScienceDirect

Placenta

journal homepage: www.elsevier.com/locate/placenta

Impact on fetal mortality and cardiovascular Doppler of selective ligation of uteroplacental vessels compared with undernutrition in a rabbit model of intrauterine growth restriction

E. Eixarch^{a,b}, E. Hernandez-Andrade^{a,b}, F. Crispi^{a,b}, M. Illa^{a,b}, I. Torre^{a,b}, F. Figueras^{a,b}, E. Gratacos^{a,b,*}

^a Department of Maternal-Fetal Medicine, Institut Clinic de Ginecologia, Obstetricia i Neonatologia (ICGON), Hospital Clinic and Institut d'Investigacions Biomèdiques August Pi i Sunyer (IDIBAPS), University of Barcelona, Sabino de Arana 1, 08028 Barcelona, Spain

^b Centro de Investigación Biomédica en Red de Enfermedades Raras (CIBERER), Barcelona, Spain

ARTICLE INFO

Article history:

Accepted 17 January 2011

Keywords:

Intrauterine growth restriction
Animal model
Rabbit
Selective ligation
Undernutrition
Doppler

ABSTRACT

Objectives: To compare the impact on birth weight, mortality and fetal haemodynamic changes of selective ligation of uteroplacental vessels vs maternal undernutrition as experimental models of intrauterine growth restriction in the pregnant rabbit.

Methods: Three groups of NewZealand rabbit fetuses were compared: controls ($n = 60$), selective ligation of 40–50% of uteroplacental vessels ($n = 38$) and 70% diet restriction ($n = 19$), both starting at 25 days of gestation. Cardiovascular Doppler evaluation was performed before delivery in a subgroup of fetuses (15 controls and cases from surgical model and 10 fetuses from the undernutrition model) before delivery including: umbilical artery pulsatility index (UAPI), middle cerebral artery pulsatility index (MCAPI), ductus venosus pulsatility index (DVPI), aortic isthmus pulsatility index (AoIPI), isovolumetric contraction time, ejection time, isovolumetric relaxation time (IRT), and myocardial performance index. Fetuses were delivered at 30 days of gestation by caesarean section and biometric measurements were recorded.

Results: The mortality rate was significantly higher in the surgical group (54.2%) than in the undernutrition (5%) and control (14.3%) groups ($p < 0.001$). Changes of biometrical measurements increased across experimental groups, being more pronounced in the surgical model. Ultrasound evaluation demonstrated linear trend for increased values in DVPI ($p = 0.003$) and AoIPI ($p = 0.029$), and IRT ($p = 0.003$) across study groups, but statistically significant changes were only observed in the surgical model. No significant differences were observed in the UAPI or MCAPI.

Conclusions: While animal models fail to perfectly reproduce the human condition, selective ligation of uteroplacental vessels reproduces more closely cardiovascular features observed in human fetuses with intrauterine growth restriction when compared with undernutrition.

© 2011 Elsevier Ltd. All rights reserved.

1. Introduction

Intrauterine growth restriction (IUGR) due to placental insufficiency occurs in 7–10% of all gestations [1] and is associated with an increased risk of stillbirth, perinatal morbidity and neonatal mortality [2]. The use of animal models is essential to advance in the pathophysiological understanding of intrauterine growth

restriction, but reproducing the features of the human condition in an experimental model is challenging.

Animal models described in the literature have preferentially been based on maternal food restriction or in surgical reduction of placental mass and/or blood supply [3,4]. Undernutrition models are easier to implement, but they disregard the role of the placenta and fail to reproduce the restriction of oxygen supply [5], which is considered to be among the critical factors in the pathogenesis of brain injury in IUGR [6]. As an alternative, methods based on ligation of uteroplacental vessels [7,8,9,10,11] are proposed as more appropriate models to achieve a combined restriction of nutrients and oxygen, and to better assess the impact of IUGR on fetal and neonatal brain [7]. The ability of any of the above models to reproduce the haemodynamic changes observed in human fetuses

* Corresponding author. Department of Maternal-Fetal Medicine, Institut Clinic de Ginecologia, Obstetricia i Neonatologia (ICGON), Hospital Clinic and Institut d'Investigacions Biomèdiques August Pi i Sunyer (IDIBAPS), University of Barcelona, Sabino de Arana 1, 08028 Barcelona, Spain. Tel.: +34 932279946/06; fax: +34 932275605.

E-mail address: gratacos@clinic.ub.es (E. Gratacos).

has been poorly documented. In a previous study on guinea pigs, vascular ligation failed to induce clear changes in the pulsatility index of the umbilical artery [10], but the presence of differences in other fetal vessels was not investigated.

In this study, we tested the hypothesis that surgical ligation of uteroplacental vessels could better reproduce the cardiovascular Doppler changes described in human fetuses with IUGR than a model based on undernutrition. We compared the impact of these two experimental models on mortality, biometric measurements and haemodynamic Doppler changes in rabbit fetuses.

2. Material and methods

2.1. Animals

Eighteen white New Zealand pregnant rabbits provided by a certified breeder were included in the study. Dams were housed for 1 week before surgery in separate cages on a reversed 12/12 h light cycle, with free access to water and standard rabbit chow containing 17.7% protein, 3.3% fat and 16% crude fiber (2030 Teklad Global Rabbit Diet; Harlan Laboratories, USA). Animal handling and all procedures were performed in accordance with applicable regulations and guidelines and with the approval of the Animal Experimental Ethics Committee of the University of Barcelona.

2.2. Surgical model

In order to create the surgical model of fetal growth restriction, 16 dams were included at 25 days of gestation (term at 31 days). At that time, we performed ligation of 40–50% of uteroplacental vessels following a previously described technique [7]. Briefly, prior to surgery tocolysis and antibiotic prophylaxis were administered. Ketamine 35 mg/kg and xylazine 5 mg/kg were given intramuscularly for anesthetic induction. Inhaled anesthesia was maintained with a mixture of 1–5% isoflurane and 1–1.5 L/min oxygen. An abdominal midline laparotomy was performed and the gestational sacs of both horns were counted and numbered. At random, one horn was assigned as the case horn and the other horn was considered as the control horn (no procedure was performed). In case horn, 40–50% of the uteroplacental vessels of all gestational sacs were ligated. Ligatures were performed with silk sutures (4/0). During the procedure only the manipulated sac was exteriorized and the remainder was kept inside the abdomen. The exteriorized sac was continuously rinsed with warm ringer lactate solution. After the procedure the abdomen was closed in two layers with a single suture of silk (3/0). Postoperative analgesia was administered and animals were again housed and well-being was controlled each day. After surgery, animals were allowed free access to water and standard chow for 5 days until delivery.

2.3. Undernutrition model

In order to create the undernutrition model, 2 dams were included. At 25 days of gestation, a sham-surgery following the surgical protocol previously described was performed. Briefly, after the abdominal midline laparotomy, the gestational sacs of both horns were counted and numbered. Then, both uterine horns were placed back into the abdominal cavity and abdomen was closed in two layers with a single silk suture (3/0). Postoperative analgesia was administered and animals were again housed and well-being was controlled each day. After surgery, severe undernutrition was induced by restricting 70% of the normal diet (45 g/day of standard chow) for 5 days until delivery.

2.4. Ultrasound evaluation

Ultrasound evaluation (US) was performed in one case fetus and in one control fetus of each dam of the surgical model and in 5 fetuses of each dam of the undernutrition model, using a Siemens Sonoline Antares (Siemens Medical Systems, Malvern, PA, USA) with a 14–10 MHz linear probe. For technical reasons, data from one malnourished fetus was not available. The US examination was performed under the same anesthetic procedure placing the probe directly on the uterine wall before fetal extraction at the time of the caesarean section (Fig. 1). The angle of insonation was $<30^\circ$ in all measurements and a 70 Hz high pass filter was used to avoid slow flow noise. Fig. 2 shows the parameters included in the US evaluation: (i) the abdominal perimeter measured in a transverse view of the fetal abdomen at the level of the intrahepatic umbilical vein; (ii) the umbilical artery pulsatility index (UAPI) was calculated in a free-floating portion of the umbilical cord; (iii) the middle cerebral artery pulsatility index (MCAPI) was measured in a transverse view of the fetal skull at the level of the circle of Willis; (iv) the ductus venosus pulsatility index (DVPI) was obtained in a midsagittal or transverse section of the fetal abdomen positioning the Doppler gate at its isthmus portion; (v) the aortic isthmus pulsatility index (AoIPI) was also obtained in a sagittal view of the fetal thorax with a clear view of the aortic arch, placing the sample volume between the origin of the last vessel of

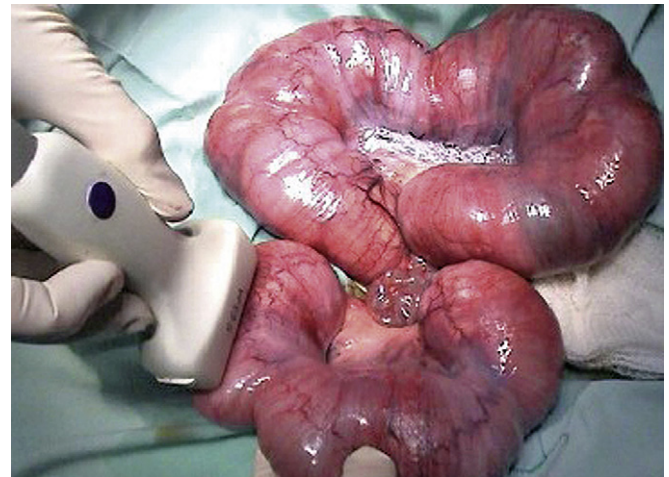


Fig. 1. Ultrasound evaluation at the time of caesarean section. The uterine horn is fixed and the linear probe is placed directly on the uterine wall.

the aortic arch and the aortic joint of the ductus arteriosus; and, (vi) the myocardial performance index (MPI) was evaluated in the left fetal cardiac ventricle, as previously described [12]. Briefly, Doppler sample volume was placed on the lateral wall of the ascending aorta in an apical 4-chamber view. The time-periods were then estimated as follows: isovolumetric contraction time (ICT) from the closure of the mitral valve to the opening of the aortic valve, ejection time (ET) from the opening to the closure of the aortic valve, and isovolumetric relaxation time (IRT) from the closure of the aortic valve to the opening of the mitral valve (Fig. 2). The final MPI was calculated as: $(ICT + IRT)/ET$.

2.5. Sample collection and processing

Following US examination, caesarean section was performed at 30 days of gestation. Living and stillborn fetuses were identified. After delivery, all living newborns and their placentas were weighed. Crown-rump length, anterior-posterior cranial diameter and transverse cranial diameter were also measured in living fetuses. Cephalic perimeter was calculated as: $((\text{anterior-posterior diameter} + \text{transverse diameter})/2) \times 3.14$. Newborns were sacrificed by decapitation and dams by pentobarbital 200 mg/kg injection. The brains of all case newborns (surgical and undernutrition models) and one control newborn of each dam of the surgical model selected at random were collected and weighed.

2.6. Statistical analysis

Nominal variables were analyzed by the Pearson χ^2 test. For quantitative variables, normality was assessed by the Shapiro-Francia W' test [13]. Normal-distributed quantitative variables were analyzed by one-way ANOVA. Additionally, a linear polynomial contrast was used to analyze linear trends across the experimental groups, where the weighted p value was considered. Non-normal-distributed variables were analyzed with the non-parametric Kruskal–Wallis test. The software SPSS 15.0 (SPSS Inc., Chicago, IL, USA) was used for the statistical analysis.

3. Results

There were no surgical or postoperative complications in the 18 dams included. A total of 153 fetuses were obtained (70 controls and 83 ligated fetuses) in the surgical group, 98 of which were alive at delivery (60 controls and 38 ligated fetuses) while a total of 20 fetuses were obtained in the undernutrition group, 19 being alive at delivery.

Table 1 depicts the mortality and biometric outcome of the study groups. Overall, the fetal mortality rate in controls was 14.3% ($n = 10/70$), with no significant differences when compared with the undernutrition group which showed a mortality rate of 5% ($n = 1/20$). On the contrary, the ligature group showed a significantly higher mortality rate (54.2% ($n = 45/83$)) than the control ($p < 0.001$) and the undernutrition ($p < 0.001$) groups. Neonatal weight and length, cephalic perimeter and brain weight decreased significantly across the experimental groups (control, undernutrition and

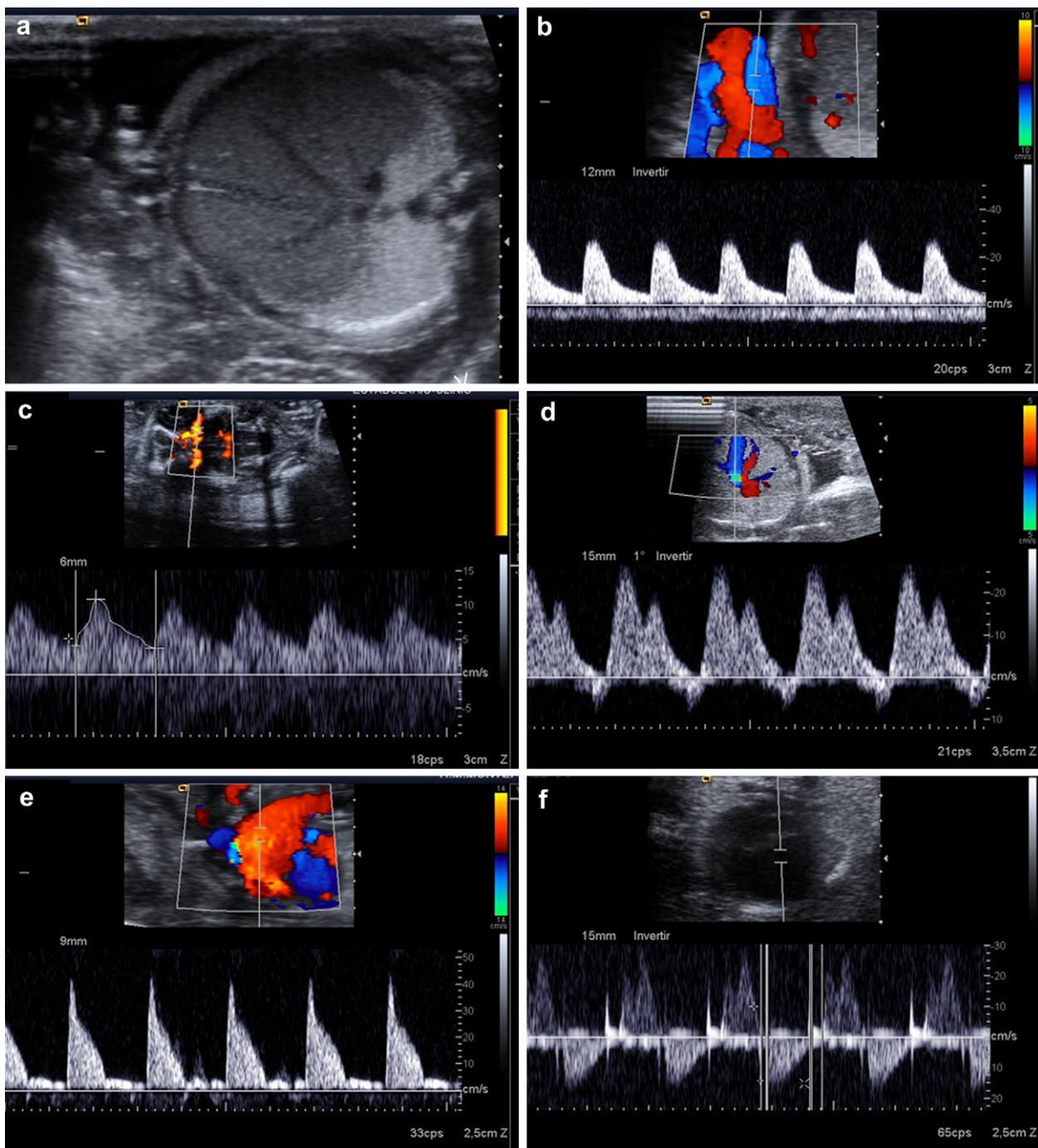


Fig. 2. Biometric and Doppler measurements. (a) abdominal perimeter measured in a transverse view of the fetal abdomen, (b) UAPI obtained in a free-floating portion of the umbilical cord, (c) MCAPI obtained in a transverse view of the fetal skull at the level of the circle of Willis; (d) DVPI acquired in a midsagittal section of the fetal abdomen (e) AoLPI obtained in a sagittal view of the fetal thorax; (f) MPI evaluated in an apical 4-chamber view.

Table 1
Mortality and biometric measurements in experimental groups.

Parameter	Control (n = 60)	Undernutrition (n = 19)	Ligature (n = 38)	Linear trend	Control vs under	Control vs ligature
Mortality rate	14.3 (10/70)	5.0 (1/20)	54.2 (45/83)	<0.001	n.s.	<0.001
Neonatal weight (g)	45.9 (8.5)	37.9 (9.7)	33.2 (9.5)	<0.001	0.003	0.000
Placental weight (g)	6.8 (1.8)	5.3 (1.1)	6.1 (1.8)	n.s.	0.006	n.s.
Crown-rump length (mm)	9.52 (0.99)	9.16 (0.87)	8.84 (1.16)	0.002	n.s.	0.006
Cephalic perimeter (mm)	8.08 (0.57)	7.75 (0.84)	7.43 (0.65)	<0.001	n.s.	0.000
Brain weight (g)	1.45 (0.14)	1.38 (0.16)	1.28 (0.15)	0.002	n.s.	0.001
Brain/neonatal weight ratio	0.020 (0.004)	0.038 (0.008)	0.037 (0.006)	0.004	0.001	0.001

Values are mean and standard deviation (mean (sd)) or rate (%(n/total)). g: grams; mm: millimetres.

ligature). Placental weight was significantly different in the undernutrition model and did not show a linear decrease among experimental groups.

Table 2 and Fig. 3 depict the ultrasound and Doppler parameters obtained in the experimental groups. DVPI and IRT were significantly different and changed across the experimental groups. However, only ligature group showed significant changes when compared with control ($p = 0.009$ and $p = 0.008$, respectively). Similarly, AoIPI showed a significant increase through the study groups ($p = 0.029$). However, neither the undernutrition nor the ligature group significantly differed from the control group. In the same way, UAPI and MCAPI did not show significant differences between groups.

4. Discussion

The results of this study show that both surgical and undernutrition models in the pregnant rabbit result in a reduction of biometric parameters, although only selective ligature of uteroplacental vessels was associated with an increase in fetal mortality. In agreement with the hypothesis of the study, surgical ligation was associated with remarkably more pronounced changes in cardiovascular Doppler parameters. Interestingly, subjects exposed to undernutrition displayed trends for abnormal cardiovascular parameters, which are further discussed later in this section.

Selective ligature of uteroplacental vessels has previously been used in rabbits [7,8,9], guinea pigs [10] and rats [11]. In rabbits, this model results in a reduction in fetal weight, increased mortality and astrocytic changes in the brain [7,8]. Undernutrition has mainly been reported in rodents by means of either caloric restriction or low-protein diet leading to a decrease in birth weight [4]. We found that both experimental models resulted in a significant reduction in fetal weight, with lower values in the surgical model. In keeping with previously reported data [4], maternal food restriction did not increase fetal mortality. This finding supports the notion that hypoxia is an essential mechanism in the cascade of events leading to the increased risk of fetal death in IUGR [14].

In this study both of the two evaluated experimental models failed to induce changes in umbilical artery (UA) Doppler. This observation is in line with a previous study in Guinea pigs [10]. In humans, increased pulsatility index in the UA is thought to result from profound changes in placental vasculature, including a reduction of over 30% of the placental mass [15] and severe vasoconstriction phenomena in the fetal-sided tertiary stemvilli [16]. Since models based on uteroplacental vessel occlusion do not alter placental micro-anatomy, the absence of changes in the UA is not surprising. Indeed, previous experiments in sheep have shown that only direct embolization of placental tissue from the fetal side is capable of inducing changes in UA Doppler [17,18,19].

In contrast with the observations in the UA, experimental growth restriction was associated with changes in fetal cardiovascular

function parameters, particularly in the ductus venosus. This venous vessel has a central role in regulating the distribution of oxygen and nutrients in fetal life [20] and has been anatomically demonstrated in several species [21] including rabbits [22]. In IUGR, ductus venosus flow velocity during atrial contraction is progressively reduced as hypoxemia and acidemia progress, with a consequent increase in pulsatility index [23]. In addition, there was a remarkable increase in isovolumetric relaxation time (IRT), with increasing values in the study groups. IRT is used in the calculation of the myocardial performance index (MPI) in fetuses and is an early marker of fetal cardiac dysfunction [24]. Concerning MPI, which has been reported to be increased in IUGR fetuses [7], we could only demonstrate a non-significant trend for increased values. We hypothesize that the lack of significance may have been due to sample size restrictions. Overall, changes in cardiovascular Doppler were substantially more pronounced and statistically significant in the surgical ligation group. However, the undernutrition model was associated with a trend for increased values in IRT. This observation should be confirmed in a large sample size, although the findings are in line with previous data demonstrating postnatal changes in cardiac structure and hypertension in the offspring of rats exposed to undernutrition during pregnancy [25,26,27]. In conclusion, while we cannot exclude a modest effect of undernutrition on cardiac function parameters, uteroplacental vessel ligation induced pronounced cardiovascular Doppler changes supporting the suitability of this experimental model for future research on cardiac dysfunction in IUGR.

Increased values of the aortic isthmus pulsatility index across the study groups were demonstrated in this study, with more pronounced differences being observed in the surgical model. The aortic isthmus plays an important role in redistributing blood flow to the brain under hypoxic conditions [28]. The aortic isthmus pulsatility index has been demonstrated to increase as placental insufficiency progresses in growth restricted fetuses [29] and this has been correlated with abnormal postnatal neurodevelopment [30,31]. Our findings are consistent with previous data reporting changes in maturation of cortical astrocytes [8] and in S100 β expression [7] in rabbit models of fetal growth restriction. However, neither model was associated with Doppler changes in the middle cerebral artery (MCA). Interestingly, both undernutrition and ligature models resulted in an increased brain/neonatal weight ratio, that could be related with redistribution of blood flow to maintain the development of the brain. In human fetuses with IUGR, the key sign to identify cerebral blood flow redistribution is a reduction in the pulsatility index in the MCA and this sign has been found to be associated with impaired cognitive function at 5 years of age [32]. The lack of changes in fetal rabbits could be due to fundamental differences with human fetuses. However, since ultrasound examinations were done under anesthetic drugs, which are associated with brain vasodilatation [33], we cannot exclude a systematic bias induced by the experimental setting.

Table 2
Ultrasound parameters in experimental groups.

Parameter	Control (n = 15)	Undernutrition (n = 9)	Ligature (n = 15)	Linear trend	Control vs under	Control vs ligature
Abdominal perimeter (mm)	79.0 (5.5)	70.4 (5.5)	68.3 (8.8)	0.004	0.031	0.006
Umbilical artery pulsatility index	1.9 (0.5)	1.8 (0.5)	1.9 (0.4)	n.s.	ns	ns
Middle cerebral artery pulsatility index	1.1 (0.3)	1.2 (0.4)	1.0 (0.2)	n.s.	ns	ns
Ductus venosus pulsatility index	0.8 (0.3)	0.9 (0.1)	1.3 (0.7)	0.003	ns	0.009
Aortic isthmus pulsatility index	3.0 (0.5)	3.5 (1.3)	3.8 (1.2)	0.029	ns	ns
Isovolumetric contraction time (ms)	25.5 (9.5)	29.1 (6.3)	25.5 (8.1)	n.s.	ns	ns
Isovolumetric relaxation time (ms)	38.1 (7.7)	42.0 (8.5)	50.1 (12.4)	0.003	ns	0.008
Ejection time (ms)	149.2 (220.6)	150.6 (11.6)	155.9 (21.8)	n.s.	ns	ns
Myocardial performance index	0.44 (0.10)	0.48 (0.07)	0.49 (0.08)	n.s.	ns	ns

Values are mean and standard deviation (mean (sd)). mm: millimetres; ms: milliseconds.

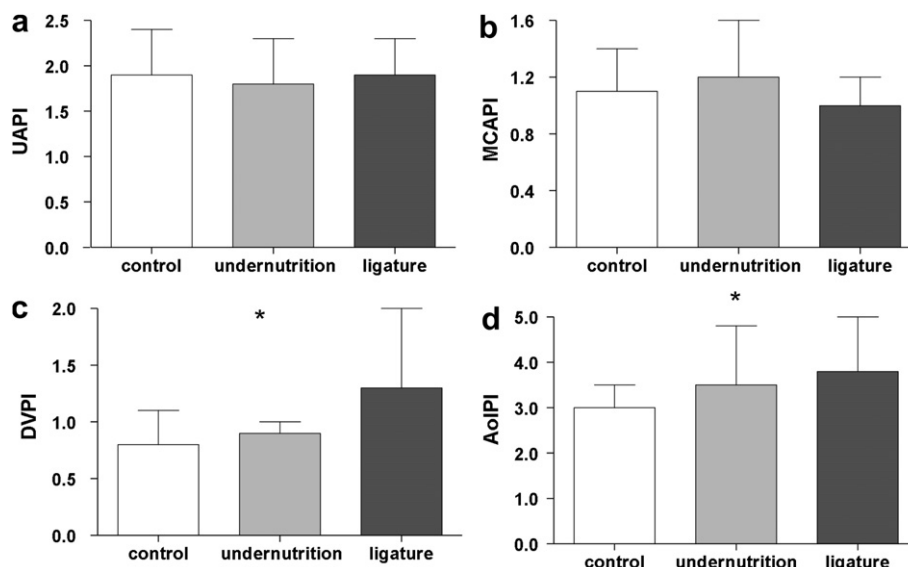


Fig. 3. Mean and standard deviation for the pulsatility index of ultrasound parameters in each experimental group. (a) umbilical artery; (b) middle cerebral artery; (c) ductus venosus; (d) aortic isthmus. * Linear trend < 0.05 .

This study has some limitations and technical considerations. The high mortality rate in the ligature group may have biased our results, since biometric and ultrasound evaluations could only be performed in the surviving fetuses. However, it is likely to be a conservative bias as only the less affected fetuses would have been analyzed, attenuating the differences between groups. As discussed above, all ultrasound examinations were done under anesthetic conditions that produce haemodynamic changes in rabbit brain [33], and we cannot exclude that this may have prevented the observation of differences in fetal Doppler brain parameters. In this study we used pregnant rabbits, which have been proposed as suitable models to study intrauterine growth restriction [9]. The rabbit presents characteristics that confer some advantages when compared with other models: the placenta is discoid, villous, and hemodichorial [34] and the fetal size may facilitate obtaining fetal biological samples *in vivo* [35] and ultrasound biometric [36] and Doppler investigations [37]. As a trade-off, the pregnant rabbit model is limited with respect to rodent models regarding to the availability of commercial kits for molecular or genomic studies which might constitute a limitation for certain types of studies.

5. Conclusion

Selective ligation of uteroplacental vessels in the pregnant rabbit partially reproduces the haemodynamic features of IUGR of human fetuses, particularly with regards to changes in cardiovascular function. In this respect, this model seems to be a better approach to mimic the human condition than undernutrition models.

Acknowledgements

This study was supported by grants from the Fondo the Investigación Sanitaria (PI/060347) (Spain). E.E. was supported by an Emili Letang fellowship by Hospital Clinic and a Rio Hortega grant from the Carlos III Institute of Health (Spain) (CM08/00105). E.H.A. was supported by a Juan de la Cierva post-doctoral fellowship. F.C. was supported by a Rio Hortega grant from the Carlos III Institute of Health (Spain) (CM07/00076). M.I. was supported by an Emili

Letang fellowship by Hospital Clinic. I.T. was supported by a Sara Borrell post-doctoral fellowship (CD08/00176).

References

- [1] Marsal K. Intrauterine growth restriction. *Curr Opin Obstet Gynecol* 2002;14(2):127–35.
- [2] Kady S, Gardosi J. Perinatal mortality and fetal growth restriction. *Best Pract Res Clin Obstet Gynaecol* 2004;18(3):397–410.
- [3] Schroder HJ. Models of fetal growth restriction. *Eur J Obstet Gynecol Reprod Biol* 2003;110(Suppl. 1):S29–39.
- [4] Vuguin PM. Animal models for small for gestational age and fetal programming of adult disease. *Horm Res* 2007;68(3):113–23.
- [5] Huizinga CT, Engelbregt MJ, Rekers-Mombarg LT, Vaessen SF, Deleamarre-van de Waal HA, Fodor M. Ligation of the uterine artery and early postnatal food restriction – animal models for growth retardation. *Horm Res* 2004;62(5):233–40.
- [6] Rees S, Harding R, Walker D. An adverse intrauterine environment: implications for injury and altered development of the brain. *Int J Dev Neurosci*; 2007.
- [7] Eixarch E, Figueras F, Hernandez-Andrade E, Crispi F, Nadal A, Torre I, et al. An experimental model of fetal growth restriction based on selective ligation of uteroplacental vessels in the pregnant rabbit. *Fetal Diagn Ther* 2009;26(4):203–11.
- [8] Bassan H, Kidron D, Bassan M, Rotstein M, Kariv N, Giladi E, et al. The effects of vascular intrauterine growth retardation on cortical astrocytes. *J Matern Fetal Neonatal Med*; 2009:1–6.
- [9] Bassan H, Trejo LL, Kariv N, Bassan M, Berger E, Fattal A, et al. Experimental intrauterine growth retardation alters renal development. *Pediatr Nephrol* 2000;15(3–4):192–5.
- [10] Turner AJ, Trudinger BJ. A modification of the uterine artery restriction technique in the guinea pig fetus produces asymmetrical ultrasound growth. *Placenta* 2009;30(3):236–40.
- [11] Camprubi M, Ortega A, Balaguer A, Iglesias I, Girabent M, Callejo J, et al. Cauterization of meso-ovarian vessels, a new model of intrauterine growth restriction in rats. *Placenta* 2009;30(9):761–6.
- [12] Hernandez-Andrade E, Lopez-Tenorio J, Figueroa-Diesel H, Sanin-Blair J, Carreras E, Cabero L, et al. A modified myocardial performance (Tei) index based on the use of valve clicks improves reproducibility of fetal left cardiac function assessment. *Ultrasound Obstet Gynecol* 2005;26(3):227–32.
- [13] Royston P. A pocket-calculator algorithm for the Shapiro-Francia test for non-normality: an application to medicine. *Stat Med* 1993;12(2):181–4.
- [14] Martin-Ancel A, Garcia-Alix A, Pascual-Salcedo D, Cabanas F, Valcarce M, Quero J. Interleukin-6 in the cerebrospinal fluid after perinatal asphyxia is related to early and late neurological manifestations. *Pediatrics* 1997;100(5):789–94.
- [15] Giles WB, Trudinger BJ, Baird PJ. Fetal umbilical artery flow velocity waveforms and placental resistance: pathological correlation. *Br J Obstet Gynaecol* 1985;92(1):31–8.
- [16] Sebire NJ. Umbilical artery Doppler revisited: pathophysiology of changes in intrauterine growth restriction revealed. *Ultrasound Obstet Gynecol* 2003;21(5):419–22.

- [17] Gagnon R, Johnston L, Murotsuki J. Fetal placental embolization in the late-gestation ovine fetus: alterations in umbilical blood flow and fetal heart rate patterns. *Am J Obstet Gynecol* 1996;175(1):63–72.
- [18] Galan HL, Anthony RV, Rigano S, Parker TA, de Vrijer B, Ferrazzi E, et al. Fetal hypertension and abnormal Doppler velocimetry in an ovine model of intrauterine growth restriction. *Am J Obstet Gynecol* 2005;192(1):272–9.
- [19] Morrow RJ, Adamson SL, Bull SB, Ritchie JW. Effect of placental embolization on the umbilical arterial velocity waveform in fetal sheep. *Am J Obstet Gynecol* 1989;161(4):1055–60.
- [20] Kiserud T, Jauniaux E, West D, Ozturk O, Hanson MA. Circulatory responses to maternal hyperoxaemia and hypoxaemia assessed non-invasively in fetal sheep at 0.3–0.5 gestation in acute experiments. *BJOG* 2001;108(4):359–64.
- [21] Tchirikov M, Schroder HJ, Hecher K. Ductus venosus shunting in the fetal venous circulation: regulatory mechanisms, diagnostic methods and medical importance. *Ultrasound Obstet Gynecol* 2006;27(4):452–61.
- [22] Bensley BA. *Practical anatomy of the rabbit: an elementary laboratory textbook in mammalian anatomy*. 8th ed. Philadelphia: The Blakistoh Company; 1948.
- [23] Harman CR, Baschat AA. Arterial and venous Dopplers in IUGR. *Clin Obstet Gynecol* 2003;46(4):931–46.
- [24] Dagdelen S, Eren N, Karabulut H, Caglar N. Importance of the index of myocardial performance in evaluation of left ventricular function. *Echocardiography* 2002;19(4):273–8.
- [25] Corstius HB, Zimanyi MA, Maka N, Herath T, Thomas W, van der Laarse A, et al. Effect of intrauterine growth restriction on the number of cardiomyocytes in rat hearts. *Pediatr Res* 2005;57(6):796–800.
- [26] Battista MC, Calvo E, Chorvatova A, Comte B, Corbeil J, Brochu M. Intra-uterine growth restriction and the programming of left ventricular remodelling in female rats. *J Physiol* 2005;565(Pt 1):197–205.
- [27] Battista MC, Oligny LL, St-Louis J, Brochu M. Intrauterine growth restriction in rats is associated with hypertension and renal dysfunction in adulthood. *Am J Physiol Endocrinol Metab* 2002;283(1):E124–31.
- [28] Fouron JC. The unrecognized physiological and clinical significance of the fetal aortic isthmus. *Ultrasound Obstet Gynecol* 2003;22(5):441–7.
- [29] Figueras F, Benavides A, Del Rio M, Crispi F, Eixarch E, Martinez JM, et al. Monitoring of fetuses with intrauterine growth restriction: longitudinal changes in ductus venosus and aortic isthmus flow. *Ultrasound Obstet Gynecol* 2009;33(1):39–43.
- [30] Fouron JC, Gosselin J, Amiel-Tison C, Infante-Rivard C, Fouron C, Skoll A, et al. Correlation between prenatal velocity waveforms in the aortic isthmus and neurodevelopmental outcome between the ages of 2 and 4 years. *Am J Obstet Gynecol* 2001;184(4):630–6.
- [31] Fouron JC, Gosselin J, Raboisson MJ, Lamoureux J, Tison CA, Fouron C, et al. The relationship between an aortic isthmus blood flow velocity index and the postnatal neurodevelopmental status of fetuses with placental circulatory insufficiency. *Am J Obstet Gynecol* 2005;192(2):497–503.
- [32] Scherjon S, Briet J, Oosting H, Kok J. The discrepancy between maturation of visual-evoked potentials and cognitive outcome at five years in very preterm infants with and without hemodynamic signs of fetal brain-sparing. *Pediatrics* 2000;105(2):385–91.
- [33] Nagase K, Iida H, Dohi S. Effects of ketamine on isoflurane- and sevoflurane-induced cerebral vasodilation in rabbits. *J Neurosurg Anesthesiol* 2003;15(2):98–103.
- [34] Carter AM. Animal models of human placentation—a review. *Placenta* 2007;28 (Suppl. A):S41–7.
- [35] Moise Jr KJ, Saade G, Knudsen L, Valdez-Torres A, Belfort MA, Hsu H, et al. Ultrasound-guided cardiac blood sampling of the rabbit fetus. *Fetal Diagn Ther* 1994;9(5):331–6.
- [36] Chavatte-Palmer P, Laigre P, Simonoff E, Chesne P, Challah-Jacques M, Renard JP. In utero characterisation of fetal growth by ultrasound scanning in the rabbit. *Theriogenology* 2008;69(7):859–69.
- [37] Eixarch E, Hernandez-Andrade E, Figueras F, Gratacos E. Selective ligation of uteroplacental vessels in the pregnant rabbit: a novel experimental model of intrauterine growth restriction. *Ultrasound Obstet Gynecol* 2007;30(4):442–3.

PROJECT 2:

**An Experimental Model of Fetal Growth
Restriction Based on Selective Ligature of
Uteroplacental Vessels in the Pregnant Rabbit.**

An Experimental Model of Fetal Growth Restriction Based on Selective Ligature of Uteroplacental Vessels in the Pregnant Rabbit

E. Eixarch^a F. Figueras^a E. Hernández-Andrade^a F. Crispí^a A. Nadal^b I. Torre^a
S. Oliveira^a E. Gratacós^a

^aDepartment of Maternal-Fetal Medicine, Institut Clínic de Ginecologia, Obstetrícia i Neonatologia, and Centro de Investigación Biomédica en Red de Enfermedades Raras, ^bDepartment of Pathology, Hospital Clínic and Institut d'Investigacions Biomèdiques August Pi i Sunyer, University of Barcelona, Barcelona, Spain

Key Words

Growth restriction • Animal model • Pregnant rabbit • Selective ligature • Brain injury

Abstract

Introduction: To describe an animal model of growth restriction based on selective ligature of uteroplacental vessels in the pregnant rabbit. **Material and Methods:** Two experimental protocols (+21 and +25 days of gestation) with three groups were defined: controls, mild (20–30%) and severe (40–50%) uteroplacental vessel ligature. Fetuses were delivered 120 h after the procedure by cesarean section. Biometrical measurements were carried out. Brains were obtained and glial response and cell proliferation were studied by S100 β and Ki-67 immunohistochemistry. **Results:** Mortality rate and biometrical restriction increased across experimental groups according to the time and severity of the procedure. S100 β expression was significantly higher in the severe reduction group at 25 days. Ki-67 expression was significantly higher in the mild reduction group at 21 days and in the severe reduction group at 25 days. **Discussion:** Selec-

tive ligature of uteroplacental vessels in the pregnant rabbit results in a gradual model of growth restriction in terms of mortality, biometrical restriction and histological brain changes.

Copyright © 2009 S. Karger AG, Basel

Introduction

Intrauterine growth restriction (IUGR) due to placental insufficiency is associated with an increased prevalence of mortality and neurological injury [1–3]. The pathophysiological pathways leading to these adverse outcomes remain poorly understood. Although reproducing the features of the human condition in an experimental model is challenging, the use of animal models is essential to improve our understanding of the mechanism of key events.

The rabbit model has previously been used to study IUGR [4] and acute perinatal brain damage [5–7]. It is an inexpensive and readily available animal model which presents features that may have some advantages when

compared to other models used to investigate fetal growth restriction, such as rats or sheep. Similar to humans, the placenta of the rabbit is discoid, villous, and hemocho-rial [8]. Furthermore, rabbits resemble humans more closely than other species in terms of the timing of peri-natal brain white matter maturation [5]. As in humans, brain maturation begins in the intrauterine period and continues during the first years of life [9].

Several induction methods have been previously re-ported in the literature. The rabbit provides a natural model of IUGR based on fetal position within the uterus, but with an uncontrollable and mild effect on birth weight [10–16]. Food restriction models do not decrease fetal oxygen supply, which may be a critical factor in the pathogenesis of brain injury [17]. Uteroplacental embolization [18, 19] and bilateral uterine artery ligation [20] result in massive, nonpredictable reductions of placental blood supply [21]. A systematic review of the latter technique concludes that it lacks efficacy in reproducing the growth restriction in the offspring [22]. Selective ligation of the uteroplacental vessels has been used to produce growth restriction in guinea pigs and rabbits [4, 23]. However, the effects on the key events of IUGR, that are mortality and brain injury, of different timings of intervention and proportions of vessels ligated are unknown.

Some markers of brain injury secondary to chronic hypoxia are available for animal experimentation. S100 β is a calcium-binding protein which is mainly present in the cytosol of glial cells of the central and peripheral nervous system [24]. In vitro studies have demonstrated that S100 β is actively secreted by astrocytes under hypoxic conditions [25], and serum levels of this protein are increased in several forms of brain injury. Thus this parameter has been suggested as a biochemical marker of brain damage [26]. Ki-67 is a nuclear protein that is expressed by proliferating cells [27]. Changes in cell proliferation in the central nervous system (CNS) have been previously described in response to either acute [28, 29] or chronic hypoxic damage [30].

The aim of this study was to develop a gradable model of fetal growth restriction based on selective ligation of uteroplacental vessels in the pregnant rabbit. We compared the effects of different timings of intervention and proportions of vessels ligated in terms of fetal mortality, biometrical restriction and histological markers of brain injury.

Material and Methods

Animals

Thirty-three pregnant New Zealand White pregnant rabbits were provided by a certified breeder. Before surgery, dams were housed for 1 week in separate cages on a reversed 12/12 h light cycle, with free access to water and standard chow. Animal handling and all procedures were performed in accordance with applicable regulations and guidelines, and with the approval of the Animal Experimental Ethics Committee of the University of Barcelona.

Two experimental protocols were defined according to the gestational age at the time of the surgical procedure (21 days (21D) or 25 days of gestation (25D)), designating the day of mating as day 0 of pregnancy. These 2 days match with the different stages of CNS development in rabbit [31]. Additionally, complete organogenesis has been achieved at 19.5 days of gestation [32]. Within each experimental protocol (21D and 25D), two experimental groups were created: ligation of 20–30% of uteroplacental vessels (mild reduction) and ligation of 40–50% of uteroplacental vessels (severe reduction). For each dam, all gestational sacs of one uterine horn were treated, and all fetuses from the other horn were used as sham controls. Thus, a total of six study groups resulted for comparisons, 21D (controls, mild and severe reduction) and 25D (controls, mild and severe reduction). Allocation of dams to the different protocols and experimental groups was performed at random, using the SPSS 14.0 statistical package (SPSS, Inc., Chicago, Ill., USA).

Surgical Procedure

Prior to surgery, progesterone 0.9 mg/kg was administered intramuscularly for tocolysis. A peripheral ear venous catheter was placed, and antibiotic prophylaxis (penicillin G, 300,000 IU) was administered. Ketamine 35 mg/kg and xylazine 5 mg/kg were given intramuscularly for anesthetic induction. Inhaled anesthesia was maintained with a mixture of 1–5% isoflurane and 1–1.5 l/min oxygen. Maternal heart rate, oxygen saturation, central temperature and blood pressure were monitored during the procedure (Pluto Veterinary Medical Monitor; Bionics Corp.). An abdominal midline laparotomy was performed and both uterine horns were exteriorized. Gestational sacs of both horns were counted and numbered and each fetus was identified taking into account the fetal position within the bicornuate uterus. The fetus at the ovarian end was considered to be the first fetus. At random, one horn was assigned as the case horn and the other horn was considered as the control horn (no procedure was performed). In the case horn, part of the uteroplacental vessels of all gestational sacs were ligated in a proportion of 20–30 or 40–50%, according to the experimental group previously allocated. Ligatures were performed with silk sutures (4/0) (fig. 1). The exteriorized sacs were continuously rinsed with warm Ringer lactate solution. After the procedure the abdomen was closed in two layers with a single suture of silk (3/0). Animals were kept under a warming blanket until they awoke and became active, and received intramuscular meloxicam 0.4 mg/kg/24 h for 48 h, as postoperative analgesia. The animals were again housed and their well-being was controlled daily.

Sample Collection and Processing

A cesarean section following the anesthetic protocol previously described was performed to obtain and identify all fetuses. In

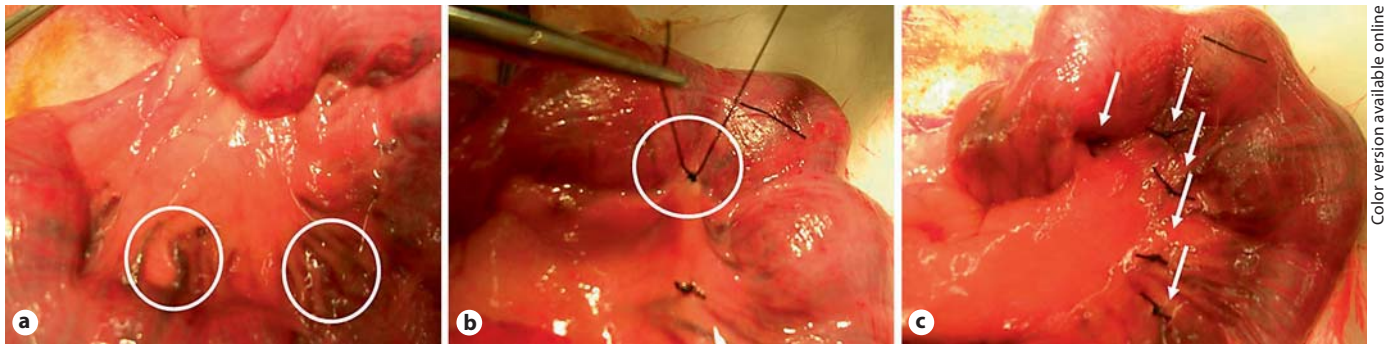


Fig. 1. Description of surgical procedure. Identification of uteroplacental vessels of each placenta (a) and selective ligation of vessels with 4/0 silk suture (b). Final appearance of uterine horn with vessel occlusion done (c).

Color version available online

previous procedures, it was attempted to perform cesarean section at term in the 21D group, but none of the procedures were successful in both mild and severe groups with a mortality rate of 100% in case fetuses (data not shown). Therefore, a 120-hour period of injury was defined for both the 21D and 25D group and cesarean section was performed on day +26 or +30 in relation to the group.

A cesarean section was performed under the same anesthetic procedure 120 h after surgery, on day +26 in the 21D protocol or on day +30 in the 25D protocol. Living and stillborn fetuses were identified. After delivery, all living newborns and their placentas were weighed. Crown-rump length, anterior-posterior cranial diameter and transverse cranial diameter were measured. Newborns were sacrificed by decapitation and dams by a pentobarbital 200 mg/kg injection. Within each dam, the brains of all case newborns and 1 control newborn selected at random were collected, weighed and fixed with 4% paraformaldehyde phosphate-buffered saline (PBS), for 24 h at 4°C. Brain coronal blocks (2 mm) were embedded in paraffin and sectioned in 3- to 5- μ m coronal slides containing the following regions of interest: cortex and basal ganglia (temporal level) and brainstem (at the level of colliculus inferior). S100 β protein expression was analyzed immunohistochemically upon formaldehyde-fixed, paraffin-embedded samples. Briefly, 3- μ m sections were obtained, dewaxed and rehydrated. Antigen retrieval consisted of incubation in 4 g/l of pepsin (Sigma-Aldrich P7012) in 0.01 N HCl at 37°C for 8 min. Sections were incubated with the primary antibody (Sigma-Aldrich SH-B1) at 1/500 1 h at room temperature. Reaction was detected with Envision (Dako Cytomation) and developed with 3,3'-diaminobenzidine. Sections were lightly counterstained with hematoxylin. For each case, a section of rabbit tongue was equally processed as a positive control, and for the negative control the incubation with the primary antibody was replaced with PBS. Ki-67 expression was analyzed immunohistochemically upon formaldehyde-fixed, paraffin-embedded samples. Paraffin tissue sections were incubated with 0.3% H₂O₂ in methanol in order to quench the endogenous peroxidase activity. Unspecific binding of the antibody was blocked by incubating the tissue sections with 10% sheep serum in TBS. Then, tissue sections were incubated with the primary antibody that detects the Ki-67 antigen, monoclonal mouse anti-human Ki-67 (clone MIB-1; Dako Cytomation; 1.6

μ g/ml). Primary antibody was detected with the secondary antibody biotinylated horse anti-mouse IgG (H+L) (Vector Laboratories; 5 μ g/ml). Sections were lightly counterstained with hematoxylin. In the negative control the incubation with the primary antibody was replaced with PBS.

Images were captured and analyzed with ARIOL (automated scanning microscope and image analysis system). At least four circular areas corresponding to 40 \times were selected in the medial area of three brain regions: cortex (including all gray matter layers, white matter under the cortex and part of the subventricular zone), basal ganglia (including thalamus) and brainstem (including nucleus pontis and nucleus raphis). Automatic counting of positive and negative cells was performed with Multi-Stain High-Resolution assay. Finally, the ratios of S100 β - and Ki-67-positive cells over the total number of cells in the regions of interest were calculated.

Statistical Analysis

Qualitative variables were analyzed by Pearson's χ^2 test. For quantitative variables, normality was assessed by the Shapiro-Francia W' test [33]. Normal-distributed quantitative variables were analyzed by means of one-way ANOVA. Additionally, a linear polynomial contrast was used to analyze linear trends across the experimental groups, where the weighed p value was considered. Non-normal distributed variables were analyzed by the non-parametric Kruskal-Wallis test. SPSS 14.0 software (SPSS, Inc.) was used for the statistical analysis.

Results

Of the 33 dams, 7 were excluded for different reasons (1 preterm delivery, 1 evisceration, 1 intestinal obstruction and 4 unexplained deaths), leaving 26 for analysis (fig. 2). In the 21D protocol a total of 101 fetuses were obtained (36 controls, and 29 and 36 in the mild and severe reduction groups, respectively). Of these 101 fetuses, 62 were alive at delivery (32 controls, 19 mild reduction and 11 severe reduction). In the 25D protocol a total of 145

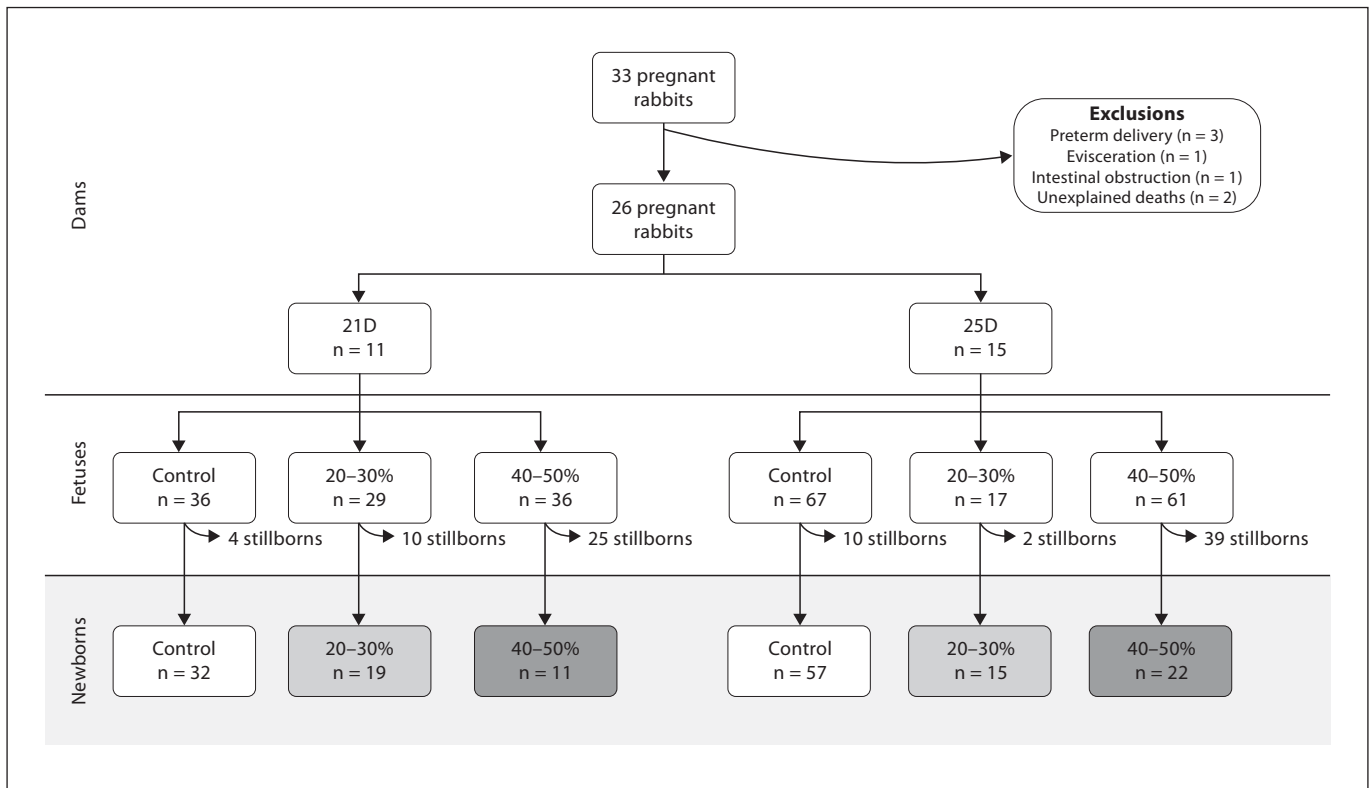


Fig. 2. Distribution of rabbits in the experimental groups.

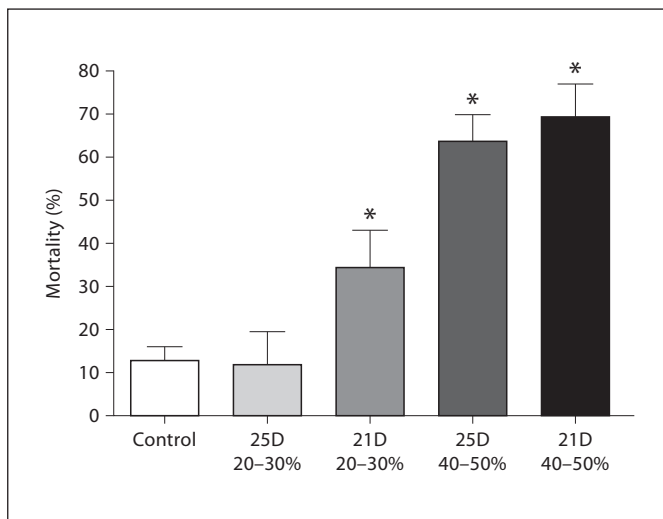


Fig. 3. Mortality rates (percentage and standard error) across the study groups. * $p < 0.05$ when compared with control group.

fetuses were obtained (67 controls, 17 mild reduction and 61 severe reduction). Of these 145 fetuses, 94 were alive at delivery (57 controls, and 15 and 22 in the mild and severe reduction groups, respectively). Figure 2 shows the flow of cases in the study.

Overall, fetal mortality rate in sham controls was 12.7% ($n = 14/110$). All experimental groups showed significantly higher mortality rates than sham controls except for the 25D mild reduction group. There was a linear increase in mortality rates across the experimental groups when ordered by gestational age and severity (linear-by-linear $p < 0.001$) (fig. 3).

Table 1 details the biometrical outcome in the study groups. Fetal weight, fetal length and brain weight decreased significantly across the experimental groups (control, mild and severe reduction) both at 21D and 25D. Additionally, brain/birth weight ratio increased throughout the study groups in both 21D and 25D protocols. Placental weight showed no significant differences among experimental groups in either protocol.

Satisfactory samples for CNS immunohistochemistry were retrieved in 16 controls (61.5%) and 54 cases (80.5%).

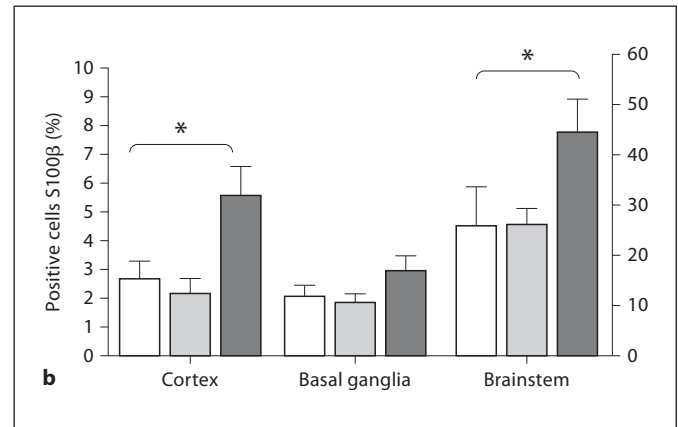
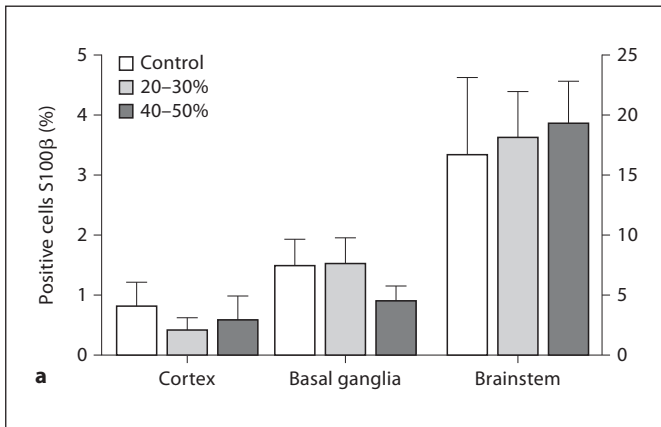


Fig. 4. S100 β expression in fetal brain regions in the study groups. Data mean \pm SE. Percentage of S100 β -positive cells in the 21D group (**a**; control n = 8, 20-30% n = 18 and 40-50% n = 9) and 5D group (**b**; control n = 8, 20-30% n = 15 and 40-50% n = 12). * p < 0.05.

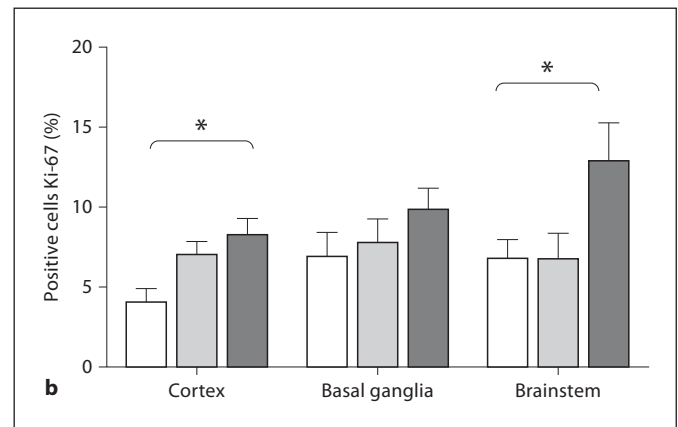
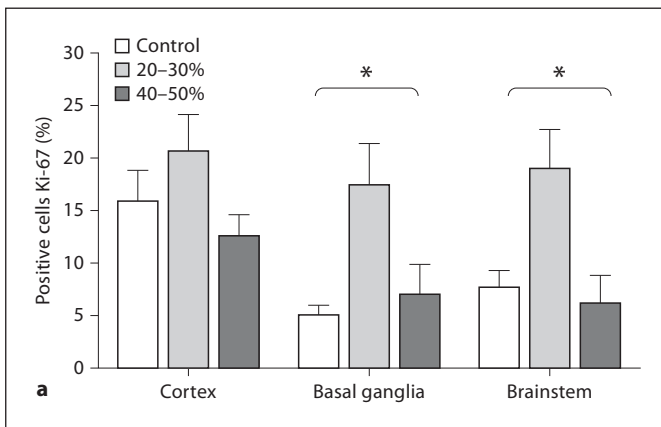


Fig. 5. Ki-67 expression in fetal brain regions in the study groups. Data are mean \pm SE. Percentage of Ki-67-positive cells in the 21D group (**a**; control n = 8, 20-30% n = 18 and 40-50% n = 9) and 25D group (**b**; control n = 8, 20-30% n = 15 and 40-50% n = 12). * p < 0.05.

The main reasons for considering samples unsatisfactory were tearing during extraction or inadequacy of immunohistochemical staining. Figure 4 displays the results of the S100 β expression for each anatomical region. No significant differences among study groups were observed in the 21D protocol. In the 25D protocol, the expression was significantly higher in the severe reduction group in cortical and brainstem regions. Figure 5 shows the results of the Ki-67 expression for each anatomical region. In the 21D protocol, Ki-67 expression was significantly higher in the cortex and brainstem regions of the mild reduction group. In contrast, in the 25D proto-

col, Ki-67 expression was significantly higher in the cortex and brainstem regions of the severe reduction group (fig. 6).

Discussion

Our results show that selective ligation of uteroplacental vessels in the pregnant rabbit induces different degrees of fetal growth restriction associated with progressive increases in mortality and biometrical restriction and differences in brain histological response to hypoxia.

Fig. 6. S100 β immunohistochemistry. Representative images of S100 β expression in the brainstem of a case 25D 40–50% the (a) and control 25D (b). In both pictures, brown cells are those expressing S100 β (black arrowheads) and blue cells (white arrowheads) are negative cells. In figure 6a there is also an increase in S100 β presence in extracellular space. Orig. magnif. 20 \times .

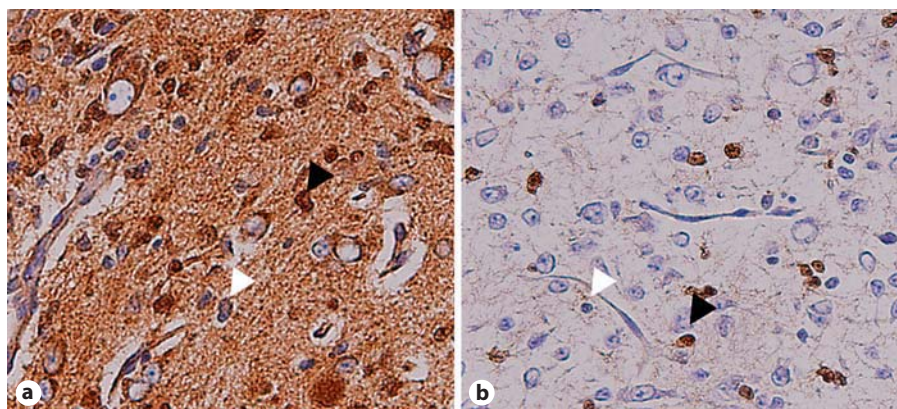


Table 1. Biometric measurements of fetuses obtained from the different experimental groups

21D	Control (n = 32)	20–30% (n = 19)	40–50% (n = 11)	p	Linear trend
Birth weight, g*	23.1 ± 4.2	21.5 ± 3.7	18.2 ± 5.6	0.008	0.002
Placental weight, g ⁺	5.3 ± 1.7	4.4 ± 1.7	4.6 ± 2.2	0.261	
Crown-rump length, mm*	7.7 ± 0.5	7.3 ± 0.5	7.1 ± 0.6	0.002	0.002
Cephalic perimeter, mm*	6.3 ± 0.4	6.2 ± 0.4	6.1 ± 0.6	0.190	0.074
Brain weight, g*	0.8 ± 0.07 [!]	0.8 ± 0.08	0.7 ± 0.06	0.005	0.007
Brain/birth weight ratio*	0.032 ± 0.003 [!]	0.038 ± 0.006	0.044 ± 0.012	0.004	0.001
25D	(n = 57)	20–30% (n = 15)	40–50% (n = 22)	p	Linear trend
Birth weight, g*	45.5 ± 8.5	36.4 ± 8.9	35.4 ± 8.6	0.000	0.000
Placental weight, g ⁺	6.5 ± 2.2	5.5 ± 2.3	5.9 ± 2.6	0.108	
Crown-rump length, mm*	9.5 ± 1	9.4 ± 1.4	8.8 ± 0.8	0.014	0.004
Cephalic perimeter, mm ⁺	8 ± 0.8	7.6 ± 1.1	7.4 ± 0.6	0.009	
Brain weight, g*	1.4 ± 0.1 [!]	1.2 ± 0.1	1.3 ± 0.1	0.005	0.072
Brain/birth weight ratio*	0.028 ± 0.003 [!]	0.035 ± 0.007	0.038 ± 0.005	0.002	0.001

* Values are mean ± SD, ANOVA test.

⁺ Values are median ± interquartile range, Kruskal-Wallis test.

[!] Data were available in only 10 fetuses.

This may provide a guide for next studies to choose the model according to the degree of injury intended.

This model has previously been used by Bassan et al. [4] in an experimental study to assess the impact of fetal growth restriction on renal development. The authors used a 20–30% ligature at 25 days of gestation and demonstrated a decrease in biometrical measurements and a deleterious effect on kidney development. Partial occlusion of uteroplacental vessels has also been used in guinea pigs, which produced a decrease in body weight and a

mild increase in umbilical artery resistance, with no differences when compared with uterine artery ligation, but with lower mortality rate [23]. In the present study we have further developed this experimental approach and evaluated the capability of the model to induce different degrees of growth restriction by modulating the timing and the proportion of vessels ligated. Firstly, we obtained a linear decrease in mortality rate across experimental groups, suggesting that gestational age and severity of blood flow reduction have a key role in fetal survival. Sec-

only, linear changes in biometric measurements and in brain/birth weight ratio were obtained in both protocols, 21D and 25D, in a similar proportion to those obtained in previous studies [4, 23]. Thus, these results support our hypothesis that it is possible to induce a progressive model of fetal growth restriction. It could be argued that fetal position in the uterine horn, which is a 'natural model' of fetal growth restriction [10–16], could influence these results. However, we have found that in our model, mortality rate and biometrics of growth-restricted fetuses is not influenced by uterine position (results not shown).

The rabbit model described may have several advantages compared to previously used models of IUGR. Firstly, the model mimics human pregnancy, since it is based on a reduction of placental supply, inducing a combined restriction of oxygen and nutrients. IUGR models based on food restriction do not reproduce these conditions as the role of the placenta is not considered [34]. In line with this reasoning, hyponutrition models do not result in consistent increases in fetal mortality [35–37], which in humans is a key event in the natural history of growth restriction. Secondly, the model allows adjusting the timing and the severity of fetal growth restriction. As illustrated by the progression in biometrical reduction and mortality rates observed in our study, different degrees of reduction in the uteroplacental blood flow may be achieved with a technically feasible and reproducible surgical procedure, which allows establishing comparisons among different severity groups. Thirdly, although the fetal size in the rabbit does not allow us to place vascular catheters or sensors as in sheep models [38], it still may allow us to perform certain manipulations more easily and reproducibly than in rodents, for example obtaining *in vivo* fetal biological samples or performing Doppler investigations [39]. Finally, the rabbit model may present some advantages with respect to other models to evaluate the impact of IUGR in basic aspects of brain development and maturation. Like humans, rabbits show an important progression in the maturation of white matter during pregnancy that continues postnatally [5], while in lambs and rodents such maturation occurs predominantly in fetal or postnatal life, respectively [40].

We assessed histological markers of brain injury and proliferation to demonstrate that different timings of intervention and degrees of severity achieved demonstrable histological brain changes. Brain damage was evaluated by means of S100 β expression that has been suggested as a biochemical marker of brain damage [26, 41–43]. We demonstrated an increase of S100 β expression in the 25D severe reduction group in cortex and brainstem, while at

21 days no differences were observed. This could be speculatively explained by the fact that this protein is a marker of astrocyte maturation during development [44]. It could then be argued that the CNS at an earlier gestational age has less capability to increase S100 β expression in the presence of an injury. Another explanation could be that placental insufficiency at 21 days of gestation induces a transient increase in S100 β expression that is later inhibited. Indeed, *in vitro* studies have demonstrated that chronic hypoxia induces a transient increase in S100 β mRNA expression, followed by rapid downregulation with a sustained reduction of protein release [25]. Additionally, no changes were found in the 25D mild reduction group. It could be argued that at 25 days of gestation only severe chronic hypoxia could trigger astrocyte response or that mild chronic hypoxia produces a transient increase of S100 β that later normalizes.

Regional changes in proliferation by means of Ki-67 expression were found in our model: while at 21D only the mild occlusion group showed signs of increased proliferation in basal ganglia and brainstem, at 25 days this phenomenon was only observed in the severe occlusion group in cortex and brainstem. The data support the notion that the impact of chronic hypoxia on brain proliferation may differ depending on gestational age and severity of the insult [17]. Preterm birth is associated with white matter injury and neuronal damage in cortical and subcortical areas [45]. We could hypothesize that, at 21 days of gestation, mild chronic hypoxia enhances proliferation in order to protect subcortical areas, while severe hypoxia inhibits this proliferation. On the other hand, cortical neurons are predominantly injured after hypoxic insult in term neonates [17]. Actually, when we analyzed the stained tissue, we discovered that in most cases proliferating cells were found in the subventricular zone as reported before [28–30]. Thus, these differences observed in brain histological changes at different gestational ages illustrate the potential usefulness of the model to explore the neurological impact of growth restriction at different gestational ages.

Our study has some limitations. Firstly, the high mortality rate in the more severe occlusion groups reduces the number of fetuses available for analysis. This high mortality may have biased our results, since biometrical and immunohistochemical measurements could only be performed in the surviving fetuses. However, it is likely to be a conservative bias as only the less affected fetuses would have been analyzed, attenuating the differences between cases and controls. Secondly, although S100 β has been described as a serological marker of brain damage, it is

unclear whether and how chronic hypoxia could modulate S100 β expression. Brain histological markers in this study were used to demonstrate that the progressive experimental model described here resulted in different histological brain changes, but the study was not designed to draw any pathophysiological conclusion on the impact of IUGR on brain injury. Thirdly, although the availability of commercial kits for molecular or genomic studies in rabbits is increasing steadily, we acknowledge that the number is still relatively low as compared with other models widely used in experimental research such as the rat or the mouse, and this might constitute a limitation for certain type of studies.

In conclusion, selective ligation of uteroplacental vessels in the pregnant rabbit may be used to create a model of fetal growth restriction that reproduces in a progressive manner different clinical manifestations of the hu-

man condition, such as fetal mortality and biometrical restriction, and results in histological changes in fetal brain.

Acknowledgements

The Fetal and Perinatal Medicine Research Group is supported by the Centro de Investigación Biomédica en Red de Enfermedades Raras (CIBERER), ISCIII, Spain. This study was supported by grants from the Fondo the Investigación Sanitaria (PI/060347) (Spain). E.E. was supported by an Emili Letang Fellowship by the Hospital Clinic and a grant from the Carlos III Institute of Health (Spain) (CM08/00105), F.C. was supported by a grant from the Carlos III Institute of Health (Spain) (CM07/00076), E.H.A. by a Juan de la Cierva post-doctoral fellowship, I.T. by a Sara Borrell post-doctoral fellowship (CD08/00176), and S.O. was supported by a Marie Curie Host Fellowship for Early Stage Researchers, FETAL-MED-019707-2.

References

- Marsal K: Intrauterine growth restriction. *Curr Opin Obstet Gynecol* 2002;14:127–135.
- Kady S, Gardosi J: Perinatal mortality and fetal growth restriction. *Best Pract Res Clin Obstet Gynaecol* 2004;18:397–410.
- Jarvis S, Glinianaia SV, Torrioli MG, Platt MJ, Miceli M, Jouk PS, Johnson A, Hutton J, Hemming K, Hagberg G, Dolk H, Chalmers J: Cerebral palsy and intrauterine growth in single births: European collaborative study. *Lancet* 2003;362:1106–1111.
- Bassan H, Trejo LL, Kariv N, Bassan M, Berger E, Fattal A, Gozes I, Harel S: Experimental intrauterine growth retardation alters renal development. *Pediatr Nephrol* 2000;15:192–195.
- Derrick M, Luo NL, Bregman JC, Jilling T, Ji X, Fisher K, Gladson CL, Beardsley DJ, Murdoch G, Back SA, Tan S: Preterm fetal hypoxia-ischemia causes hypertonia and motor deficits in the neonatal rabbit: a model for human cerebral palsy? *J Neurosci* 2004;24:24–34.
- Drobyshevsky A, Derrick M, Wyrwicz AM, Ji X, Englof I, Ullman LM, Zelaya ME, Northington FJ, Tan S: White matter injury correlates with hypertonia in an animal model of cerebral palsy. *J Cereb Blood Flow Metab* 2007;27:270–281.
- Tan S, Drobyshevsky A, Jilling T, Ji X, Ullman LM, Englof I, Derrick M: Model of cerebral palsy in the perinatal rabbit. *J Child Neurol* 2005;20:972–979.
- Carter AM: Animal models of human placentation – a review. *Placenta* 2007;28:S41–S47.
- Ballesteros MC, Hansen PE, Soila K: MR imaging of the developing human brain. Part 2. Postnatal development. *Radiographics* 1993;13:611–622.
- Flake AW, Villa RL, Adzick NS, Harrison MR: Transamniotic fetal feeding. II. A model of intrauterine growth retardation using the relationship of ‘natural runting’ to uterine position. *J Pediatr Surg* 1987;22:816–819.
- Thakur A, Sase M, Lee JJ, Thakur V, Buchmiller TL: Ontogeny of insulin-like growth factor 1 in a rabbit model of growth retardation. *J Surg Res* 2000;91:135–140.
- Thakur A, Sase M, Lee JJ, Thakur V, Buchmiller TL: Effect of dexamethasone on insulin-like growth factor-1 expression in a rabbit model of growth retardation. *J Pediatr Surg* 2000;35:898–905.
- Buchmiller-Crair TL, Gregg JP, Rivera FA Jr, Choi RS, Diamond JM, Fonkalsrud EW: Delayed disaccharidase development in a rabbit model of intrauterine growth retardation. *Pediatr Res* 2001;50:520–524.
- Skarsgard ED, Amii LA, Dimmitt RA, Sakamoto G, Brindle ME, Moss RL: Fetal therapy with rhIGF-1 in a rabbit model of intrauterine growth retardation. *J Surg Res* 2001;99:142–146.
- Cellini C, Xu J, Arriaga A, Buchmiller-Crair TL: Effect of epidermal growth factor infusion on fetal rabbit intrauterine growth retardation and small intestinal development. *J Pediatr Surg* 2004;39:891–897.
- Cellini C, Xu J, Buchmiller-Crair T: Effect of epidermal growth factor on small intestinal sodium/glucose co-transporter-1 expression in a rabbit model of intrauterine growth retardation. *J Pediatr Surg* 2005;40:1892–1897.
- Rees S, Harding R, Walker D: An adverse intrauterine environment: implications for injury and altered development of the brain. *Int J Dev Neurosci* 2008;26:3–11.
- Gagnon R, Johnston L, Murotsuki J: Fetal placental embolization in the late-gestation ovine fetus: alterations in umbilical blood flow and fetal heart rate patterns. *Am J Obstet Gynecol* 1996;175:63–72.
- Duncan JR, Cock ML, Loeliger M, Louey S, Harding R, Rees SM: Effects of exposure to chronic placental insufficiency on the postnatal brain and retina in sheep. *J Neuro-pathol Exp Neurol* 2004;63:1131–1143.
- Wigglesworth JS: Experimental growth retardation in the foetal rat. *J Pathol Bacteriol* 1964;88:1–13.
- Lang U, Baker RS, Braems G, Zygmunt M, Kunzel W, Clark KE: Uterine blood flow – a determinant of fetal growth. *Eur J Obstet Gynecol Reprod Biol* 2003;110(suppl 1):S55–S61.
- Neitzke U, Harder T, Schellong K, Melchior K, Ziska T, Rodekamp E, Dudenhausen JW, Plagemann A: Intrauterine growth restriction in a rodent model and developmental programming of the metabolic syndrome: a critical appraisal of the experimental evidence. *Placenta* 2008;29:246–254.

- 23 Turner AJ, Trudinger BJ: A modification of the uterine artery restriction technique in the guinea pig fetus produces asymmetrical ultrasound growth. *Placenta* 2009;30:236–240.
- 24 Heizmann CW: Ca²⁺-binding S100 proteins in the central nervous system. *Neurochem Res* 1999;24:1097–1100.
- 25 Gerlach R, Demel G, König HG, Gross U, Prehn J, Raabe A, Seifert V, Kögel D: Active secretion of S100 β from astrocytes during metabolic stress. *Neuroscience* 2006;141:1697–1701.
- 26 Korfiatis S, Stranjalis G, Papadimitriou A, Psachoulia C, Daskalakis G, Antsaklis A, Sakas DE: Serum S100 β protein as a biochemical marker of brain injury: a review of current concepts. *Curr Med Chem* 2006;13:3719–3731.
- 27 Mollgard K, Schumacher U: Immunohistochemical assessment of cellular proliferation in the developing human CNS using formalin-fixed paraffin-embedded material. *J Neurosci Methods* 1993;46:191–196.
- 28 Zaidi AU, Bessert DA, Ong JE, Xu H, Barks JD, Silverstein FS, Skoff RP: New oligodendrocytes are generated after neonatal hypoxic-ischemic brain injury in rodents. *Glia* 2004;46:380–390.
- 29 Ong J, Plane JM, Parent JM, Silverstein FS: Hypoxic-ischemic injury stimulates subventricular zone proliferation and neurogenesis in the neonatal rat. *Pediatr Res* 2005;58:600–606.
- 30 Fagel DM, Ganat Y, Silbereis J, Ebbitt T, Stewart W, Zhang H, Ment LR, Vaccarino FM: Cortical neurogenesis enhanced by chronic perinatal hypoxia. *Exp Neurol* 2006;199:77–91.
- 31 Clancy B, Darlington RB, Finlay BL: Translating developmental time across mammalian species. *Neuroscience* 2001;105:7–17.
- 32 Beaudoin S, Barbet P, Bary F: Developmental stages in the rabbit embryo: guidelines to choose an appropriate experimental model. *Fetal Diagn Ther* 2003;8:422–427.
- 33 Royston P: A pocket-calculator algorithm for the Shapiro-Francia test for non-normality: an application to medicine. *Stat Med* 1993;12:181–184.
- 34 Huizinga CT, Engelbregt MJ, Rekers-Mombarg LT, Vaessen SF, Delemarre-van de Waal HA, Fodor M: Ligation of the uterine artery and early postnatal food restriction – animal models for growth retardation. *Horm Res* 2004;62:233–240.
- 35 Cappon GD, Fleeman TL, Chapin RE, Hurtt ME: Effects of feed restriction during organogenesis on embryo-fetal development in rabbit. *Birth Defects Res B Dev Reprod Toxicol* 2005;74:424–430.
- 36 Ergaz Z, Avgil M, Ornoy A: Intrauterine growth restriction – etiology and consequences: what do we know about the human situation and experimental animal models? *Reprod Toxicol* 2005;20:301–322.
- 37 Vuguin PM: Animal models for small for gestational age and fetal programming of adult disease. *Horm Res* 2007;68:113–123.
- 38 Hermans B, Lewi L, Jani J, De Buck F, Deprest J, Puers R: Feasibility of in utero telemetric fetal ECG monitoring in a lamb model. *Fetal Diagn Ther* 2008;24:81–85.
- 39 Eixarch EH-AE, Figueras F, Gratacos G: Selective ligation of uteroplacental vessels in the pregnant rabbit: a novel experimental model of intrauterine growth restriction. *Ultrasound Obstet Gynecol* 2007;30:442–443.
- 40 Rees S, Inder T: Fetal and neonatal origins of altered brain development. *Early Hum Dev* 2005;81:753–761.
- 41 Persson L, Hardemark HG, Gustafsson J, Rundstrom G, Mendel-Hartvig I, Esscher T, Pahlman S: S-100 protein and neuron-specific enolase in cerebrospinal fluid and serum: markers of cell damage in human central nervous system. *Stroke* 1987;8:911–918.
- 42 Nagdyman N, Komen W, Ko HK, Muller C, Obladen M: Early biochemical indicators of hypoxic-ischemic encephalopathy after birth asphyxia. *Pediatr Res* 2001;49:502–506.
- 43 Thorngren-Jerneck K, Alling C, Herbst A, Amer-Wahlin I, Marsal K: S100 protein in serum as a prognostic marker for cerebral injury in term newborn infants with hypoxic ischemic encephalopathy. *Pediatr Res* 2004;55:406–412.
- 44 Raponi E, Agenes F, Delphin C, Assard N, Baudier J, Legraverend C, Deloulme JC: S100 β expression defines a state in which GFAP-expressing cells lose their neural stem cell potential and acquire a more mature developmental stage. *Glia* 2007;55:165–177.
- 45 Barrett RD, Bennet L, Davidson J, Dean JM, George S, Emerald BS, Gunn AJ: Destruction and reconstruction: hypoxia and the developing brain. *Birth Defects Res C Embryo Today*, 2007;81:163–176.

PROJECT 3:

Neonatal neurobehavior and diffusion MRI changes in brain reorganization due to intrauterine growth restriction in a rabbit model.

Neonatal Neurobehavior and Diffusion MRI Changes in Brain Reorganization Due to Intrauterine Growth Restriction in a Rabbit Model
--Manuscript Draft--

Manuscript Number:	
Article Type:	Research Article
Full Title:	Neonatal Neurobehavior and Diffusion MRI Changes in Brain Reorganization Due to Intrauterine Growth Restriction in a Rabbit Model
Short Title:	Neurobehavior and Diffusion MRI Correlates in IUGR
Corresponding Author:	Eduard Gratacos, MD PhD Hospital Clinic, University of Barcelona Barcelona, Barcelona SPAIN
Keywords:	brain reorganization; intrauterine growth restriction (IUGR); animal model; selective ligature; diffusion MRI; neurobehavior; diffusion tensor imaging (DTI); voxel based analysis (VBA)
Abstract:	<p>BACKGROUND: Intrauterine growth restriction (IUGR) affects 5-10% of all newborns and is associated with a high risk of abnormal neurodevelopment. The timing and patterns of brain reorganization underlying IUGR are poorly documented. We developed a rabbit model allowing neonatal neurobehavioral assessment and high resolution brain diffusion magnetic resonance imaging (MRI). The aim of the study was to describe the pattern and functional correlates of fetal brain reorganization induced by IUGR.</p> <p>METHODOLOGY/PRINCIPAL FINDINGS: IUGR was induced in 10 New Zealand fetal rabbits by ligation of 40-50% of uteroplacental vessels in one horn at 25 days of gestation. Ten contralateral horn fetuses were used as controls. Cesarean section was performed at 30 days (term 31 days). At postnatal day +1, neonates were assessed by validated neurobehavioral tests including evaluation of tone, spontaneous locomotion, reflex motor activity, motor responses to olfactory stimuli, and coordination of suck and swallow. Subsequently, brains were collected and fixed and MRI was performed using a high resolution acquisition scheme. Global and regional (manual delineation and voxel based analysis) diffusion tensor imaging parameters were analyzed. IUGR was associated with significantly poorer neurobehavioural performance in most domains. Voxel based analysis revealed fractional anisotropy (FA) differences in multiple brain regions of gray and white matter, including frontal, insular, occipital and temporal cortex, hippocampus, putamen, thalamus, claustrum, medial septal nucleus, anterior commissure, internal capsule, fimbria of hippocampus, medial lemniscus and olfactory tract. Regional FA changes were correlated with poorer outcome in neurobehavioral tests.</p> <p>CONCLUSIONS: IUGR is associated with a complex pattern of brain reorganization already at birth, which may open opportunities for early intervention. Diffusion MRI can offer suitable imaging biomarkers to characterize and monitor brain reorganization due to fetal diseases.</p>
All Authors:	<p>Elisenda Eixarch</p> <p>Dafnis Batalle</p> <p>Miriam Illa</p> <p>Emma Muñoz-Moreno</p> <p>Ariadna Arbat</p> <p>Ivan Amat-Roldan</p> <p>Francesc Figueras</p> <p>Eduard Gratacos, MD PhD</p>
Suggested Reviewers:	Sandra Rees Department of Anatomy and Cell Biology, University of Melbourne, Vic. 3010, Australia

	<p>s.rees@unimelb.edu.au She is an expert in the effects of intrauterine hypoxia on the fetal brain development</p>
	<p>Gregory A Lodyginsky Division of Pediatric and Neonatal Intensive Care, University Hospital of Geneva, Geneva, Switzerland. gregory.lodyginsky@unige.ch He is an expert in neurodevelopment, brain damage due to prenatal conditions and MRI applications in animal models</p>
Opposed Reviewers:	

31 st August 2011

To PLoS ONE,

Enclosed please find our manuscript entitled "Neonatal neurobehavior and diffusion MRI changes in brain reorganization due to intrauterine growth restriction in a rabbit model" which you might want to consider for publication in the Journal. Each author has made substantial contributions to the study and has approved the final version of the manuscript.

The study describes the pattern and functional correlates of fetal brain reorganization induced by intrauterine growth restriction (IUGR) in a rabbit model. IUGR affects 5-10% of all newborns worldwide and it is a well recognized cause of abnormal neurodevelopmental outcome during childhood. There is limited understanding of brain organization processes occurring under chronic restriction of oxygen and nutrients during intrauterine life.

The study entailed development of a complex experimental setting which combined neurobehavioral tests and high resolution diffusion MRI in whole brain preparations. The findings demonstrate that IUGR results in a complex pattern of maturational changes in grey and white matter areas, as illustrated by voxel based analysis of regional changes in diffusion MRI. The results provide new information as to the functional and structural correlates occurring in IUGR which will be useful to the understanding of brain reorganization under chronic prenatal conditions. In addition, the study provides a new experimental setting to develop future studies to test the impact of interventions aimed at improving neurodevelopmental outcomes. Finally, the results support the use of diffusion MRI for the development of imaging biomarkers of brain reorganization and injury in IUGR and other prenatal conditions.

The information included in the manuscript is of interest for scientists working in neurobiology and brain development, and in particular to healthcare professionals involved in neurodevelopmental aspects and care of fetal and child diseases, including maternal-fetal specialists, pediatricians, neurologists, neuropsychologists, and neuroradiologists.

Finally, we would like to suggest Dr. Olivier Baud as Academic Editor, since he is an expert in neurodevelopment.

Thank you for considering our manuscript.

Yours sincerely,



Eduard Gratacos, MD PhD
Head and Professor
Maternal-Fetal Medicine Department and Research Centre
Hospital Clinic - Universitat de Barcelona
Sabino de Arana 1, 08028 Barcelona, Spain
Phone: +34 93 227 9946 / +34 93 227 9931
Fax: +34 93 227 5612
Email: egratacos@clinic.ub.es

1 **Neonatal neurobehavior and diffusion MRI changes in brain reorganization due to**
22 **intrauterine growth restriction in a rabbit model**

4 **Authors:**

8
95 Elisenda Eixarch ^a eixarch@clinic.ub.es

116 Dafnis Batalle ^a dbatalle@clinic.ub.es

137 Miriam Illa ^a miriamil@clinic.ub.es

168 Emma Muñoz-Moreno ^a emunozm@clinic.ub.es

189 Ariadna Arbat ^a arbat@clinic.ub.es

210 Ivan Amat-Roldan ^a iamat@clinic.ub.es

221 Francesc Figueras ^a ffiguera@clinic.ub.es

242 Eduard Gratacos (corresponding author) ^a egratacos@clinic.ub.es

28 ^a Department of Maternal-Fetal Medicine, Institut Clinic de Ginecologia, Obstetricia i Neonatologia
30 (ICGON), Hospital Clinic; Institut d'Investigacions Biomèdiques August Pi i Sunyer (IDIBAPS),
31 University of Barcelona; and Centro de Investigación Biomédica en Red de Enfermedades Raras
32 (CIBERER), Barcelona, Spain.

39
40 **Corresponding Author:**

42 Eduard Gratacos

44 Head and Professor

46 Maternal-Fetal Medicine Department and Research Centre

48 Hospital Clinic - Universitat de Barcelona

50 Sabino de Arana 1, 08028 Barcelona, Spain

52 Phone: +34 93 227 9946 / +34 93 227 9931

54 Fax: +34 93 227 5612

56 Email: egratacos@clinic.ub.es

1 **ABSTRACT (<300 words)**

2
3
4
5
6
7
8
9
10
11
12
13
14
15
16
17
18
19
20
21
22
23
24
25
26
27
28
29
30
31
32
33
34
35
36
37
38
39
40
41
42
43
44
45
46
47
48
49
50
51
52
53
54
55
56
57
58
59
60
61
62
63
64
65

BACKGROUND: Intrauterine growth restriction (IUGR) affects 5-10% of all newborns and is associated with a high risk of abnormal neurodevelopment. The timing and patterns of brain reorganization underlying IUGR are poorly documented. We developed a rabbit model allowing neonatal neurobehavioral assessment and high resolution brain diffusion magnetic resonance imaging (MRI). The aim of the study was to describe the pattern and functional correlates of fetal brain reorganization induced by IUGR.

METHODOLOGY/PRINCIPAL FINDINGS: IUGR was induced in 10 New Zealand fetal rabbits by ligation of 40-50% of uteroplacental vessels in one horn at 25 days of gestation. Ten contralateral horn fetuses were used as controls. Cesarean section was performed at 30 days (term 31 days). At postnatal day +1, neonates were assessed by validated neurobehavioral tests including evaluation of tone, spontaneous locomotion, reflex motor activity, motor responses to olfactory stimuli, and coordination of suck and swallow. Subsequently, brains were collected and fixed and MRI was performed using a high resolution acquisition scheme. Global and regional (manual delineation and voxel based analysis) diffusion tensor imaging parameters were analyzed. IUGR was associated with significantly poorer neurobehavioral performance in most domains. Voxel based analysis revealed fractional anisotropy (FA) differences in multiple brain regions of gray and white matter, including frontal, insular, occipital and temporal cortex, hippocampus, putamen, thalamus, claustrum, medial septal nucleus, anterior commissure, internal capsule, fimbria of hippocampus, medial lemniscus and olfactory tract. Regional FA changes were correlated with poorer outcome in neurobehavioral tests.

CONCLUSIONS: IUGR is associated with a complex pattern of brain reorganization already at birth, which may open opportunities for early intervention. Diffusion MRI can offer suitable imaging biomarkers to characterize and monitor brain reorganization due to fetal diseases.

Keywords: brain reorganization; intrauterine growth restriction; animal model; selective ligation; diffusion MRI; neurobehavior, diffusion tensor imaging (DTI)

1-INTRODUCTION

Intrauterine growth restriction (IUGR) due to placental insufficiency affects 5-10% of all pregnancies and induces cognitive disorders in a substantial proportion of children [1]. Reduction of placental blood flow results in chronic exposure to hypoxemia and undernutrition [2] and this has consequences on the developing brain [3]. The association between IUGR and short [4,5] and long-term [4,6-12] neurodevelopmental and cognitive dysfunctions has been extensively described. Additionally, magnetic resonance imaging (MRI) studies have consistently demonstrated brain structural changes on IUGR [13-17]. Decreased volume in gray matter (GM) [13] and hippocampus [14], and major delays in cortical development [15] have been reported in neonates, as well as reduced GM volumes [16] and decreased fractal dimension of both GM and white matter (WM) [17] in infants.

The development of imaging biomarkers for early diagnosis and monitoring of brain changes associated with IUGR is among the challenges to improve management and outcomes of these children. There is a need to improve MRI characterization of the anatomical patterns of brain reorganization associated with IUGR and to develop specific imaging biomarkers. In spite of previous studies the timing and pattern of brain abnormalities associated with IUGR is still ill-defined. The acquisition of high resolution MRI images is limited in fetuses and neonates due to size and motion artefact issues [18,19]. In addition, there is some variability among MRI postnatal studies, which may be influenced by variations in the case definition used and the postnatal morbidity associated with IUGR [20]. Notwithstanding their obvious shortcomings, animal models may overcome some limitations of human studies. Aside from the reproducibility of experimental conditions, such settings permit performing MRI on isolated whole brain preparations, which allows increasing substantially the duration of acquisition time and hence, the use of high resolution acquisition approaches [21].

Contrary to acute perinatal events, IUGR is a chronic condition that induces brain reorganization and abnormal maturation rather than gross tissue destruction [22]. Consequently, it requires the use of MRI modalities allowing to identify subtle changes in brain structure. Among these, diffusion MRI offers a promising approach to assess abnormalities in brain maturation and

1 develop biomarkers for clinical use [23]. Diffusion MRI measures the diffusion of water molecules in
2 tissues and obtains information about brain microstructure and the disposition of fiber tracts [24].
3
4 Diffusion MRI has been consistently shown to be highly sensitive to changes after acute hypoxia in
5
6 adults [25,26] and developing brain [23,27]. Aside from reflecting acute injury, diffusion MRI
7
8 parameters seem to correlate well with brain maturation and organization in fetal and early postnatal
9
10 life [23,28]. In addition, preliminary clinical results suggests that diffusion MRI could also be suitable
11
12 to detect maturational changes occurring in chronic fetal conditions, including fetal cardiac defects
13
14 [29] and IUGR [30].
15

16
17
18 In this study we developed a rabbit model allowing to perform neurobehavioral tests and high
19
20 resolution diffusion MRI. The fetal rabbit was selected for several reasons. Firstly, selective ligation
21
22 of uteroplacental vessels in this model has been demonstrated to reproduce growth impairment and
23
24 hemodynamic adaptation as occurring in human IUGR [31-33]. Secondly, the rabbit presents a
25
26 human-like timing of perinatal brain WM maturation [34]. Finally, validated tests for the objective
27
28 evaluation of neonatal neurobehavior are available [35]. In addition, we developed a protocol to
29
30 perform diffusion MRI with long acquisition periods in fixed whole brain preparations. This approach
31
32 allowed high resolution images which can reveal submillimetric structures. Such high quality would
33
34 be difficult to achieve *in vivo* due to motion artifacts and limited acquisition times. Moreover, the use
35
36 of high angular resolution schemes provides more accurate diffusion related parameters even using
37
38 diffusion tensor imaging (DTI) approaches [36]. Since segmentation of anatomic regions in small
39
40 developing brains presents substantial challenges [37], we explored a voxel based analysis (VBA)
41
42 approach in order to overcome the limitations described for manual delineation. VBA approach
43
44 performs the analysis of the whole brain voxel-wise and identifies anatomical areas presenting
45
46 differences avoiding the need of *a priori* hypothesis or previous delineation [38]. The aims of the
47
48 study were to describe the anatomical pattern of fetal brain maturation changes as assessed by
49
50 MRI, and to establish functional-structural correlates of fetal brain reorganization induced by IUGR.
51
52
53
54
55
56
57
58
59
60
61
62
63
64
65

2-MATERIAL AND METHODS

The methodology of the study is shown in Figure 1. Each of the steps of the procedure is detailed in this section.

2.1-STUDY PROTOCOL AND PROCEDURES

a) Animals and study protocol

Animal experimentation of this study was approved by the Animal Experimental Ethics Committee of the University of Barcelona (permit number: 206/10-5440). Animal handling and all the procedures were performed following all applicable regulations and guidelines of the Animal Experimental Ethics Committee of the University of Barcelona. The study groups were composed by 10 cases with induced IUGR and 10 sham controls obtained from New Zealand pregnant rabbits provided by a certified breeder. Dams were housed for 1 week before surgery in separate cages on a reversed 12/12h light cycle, with free access to water and standard chow.

At 25 days of gestation (term at 31 days), we performed ligation of 40-50% of uteroplacental vessels following a previously described technique [32]. Cesarean section was performed at 30 days of gestation and living and stillborn fetuses were obtained. At postnatal day +1, neurobehavioral evaluation was performed and afterwards neonates were sacrificed. Then, brains were collected and fixed with 4% paraformaldehyde phosphate-buffered saline (PBS).

b) Surgical model

Induction of IUGR was performed at 25 days of gestation as previously described [32]. Briefly, prior to surgery tocolysis and antibiotic prophylaxis were administered. Ketamine 35 mg/kg and xylazine 5 mg/kg were given intramuscularly for anaesthetic induction. Inhaled anaesthesia was maintained with a mixture of 1-5% isoflurane and 1-1.5 L/min oxygen. An abdominal midline laparotomy was performed and the gestational sacs of both horns were counted and numbered. In one uterine horn, 40-50% of the uteroplacental vessels of all gestational sacs were ligated. Ligatures were performed with silk sutures (4/0). During the procedure only the manipulated sac was exteriorized and the remainder was kept inside the abdomen. The exteriorized sac was continuously rinsed with warm ringer lactate solution. After the procedure the abdomen was closed

1 in two layers with a single suture of silk (3/0). Postoperative analgesia was administered and
2 animals were again housed and well-being was controlled each day. After surgery, animals were
3
4 allowed free access to water and standard chow for 5 days until delivery.
5

6
7
8
9
10
11
12
13
14
15
16
17
18
19
20
21
22
23
24
25
26
27
28
29
30
31
32
33
34
35
36
37
38
39
40
41
42
43
44
45
46
47
48
49
50
51
52
53
54
55
56
57
58
59
60
61
62
63
64
65

Cesarean section was performed at 30 days of gestation and living and stillborn fetuses were obtained. Dams were sacrificed by pentobarbital 200 mg/kg injection. After delivery, all living newborns were weighed and identified by ear punching.

c) Neurobehavioral test

Neurobehavioral evaluation was performed at postnatal day +1 following methodology previous described by Derrick et al. [35]. For each animal, the testing was videotaped and scored on a scale of 0–3 (0, worst; 3, best) by a blinded observer. Locomotion on a flat surface was assessed by grading the amount of spontaneous movement of the head, trunk, and limbs. Tone was assessed by active flexion and extension of the forelimbs and hindlimbs (0: No increase in tone, 1: Slight increase in tone when limb is moved, 2: Marked increase in tone but limb is easily flexed, 3: Increase in tone, passive movement difficult, 4: Limb rigid in flexion or extension). The righting reflex was assessed when the pups were placed on their backs and the number of times turned prone from supine position in 10 tries was registered. Suck and swallow were assessed by introduction of formula (Lactadiet with omega 3; Royal Animal, S.C.P.) into the pup's mouth with a plastic pipette. Olfaction was tested by recording time to aversive response to a cotton swab soaked with pure ethanol. After neurobehavioral evaluation, neonates were sacrificed by decapitation after administration of Ketamine 35 mg/kg given intramuscularly. Brains were collected and fixed with 4% paraformaldehyde phosphate-buffered saline (PBS), for 24 hours at 4 °C.

d) Magnetic resonance acquisition

MRI was performed on fixed brains using a 7T animal MRI scanner (Bruker BioSpin MRI GMBH). High-resolution three-dimensional T1 weighted images were obtained by a Modified Driven Equilibrium Fourier Transform (MDEFT) 3D sequence with the following parameters: Time of Echo (TE) = 3.5 ms, Time of Repetition (TR) = 4000 ms, 0.25-mm slice thickness with no interslice gap, 84 coronal slices, in-plane acquisition matrix of 128 x 128 and Field of View (FoV) of 32 x 32 mm²,

1 which resulted in a voxel dimension of $0.25 \times 0.25 \times 0.25 \text{ mm}^3$. Diffusion weighted images (DWI)
2 were acquired by using a standard diffusion sequence covering 126 gradient directions with a b-
3 value of 3000 s/mm^2 together with a reference ($b=0$) image. Other experimental parameters were:
4 TR = 26 ms, TE = 250 ms, slice thickness = 0.35 mm with no interslice gap, 60 coronal slices, in-
5 plane acquisition matrix of 46×46 , FoV of $16 \times 16 \text{ mm}^2$, which resulted in a voxel dimension of 0.35
6 $\times 0.35 \times 0.35 \text{ mm}^3$. Total scan time for both acquisitions was 14h20m04s.

14 2.2-MRI PROCESSING AND ANALYSIS

16 a) Processing of diffusion MRI

17 As a first step, the brain was segmented from the background. The 126 DWI images were
18 averaged to generate a high SNR isotropic diffusion weighted image (iDWI) that was used to create
19 a binary mask to segment the brain from the background, in a similar way as previously described
20 [39]. In brief, iDWI of each subject was min-max normalized, and non-brain tissue values were
21 estimated to have values below 5% of the maximum of the iDWI normalized volume. After applying
22 the threshold, internal holes in the mask were filled by 3D morphological closing and isolated islands
23 were removed by 3D morphological opening. This mask was used to estimate brain volume and
24 constrain the area where the diffusion related measures were analyzed.

25 Tensor model of diffusion MRI was constructed by using MedINRIA 1.9.4 [40] (available at
26 www-sop.inria.fr/asclepios/software/MedINRIA/). Once the tensors were estimated at each voxel
27 inside the brain mask, a set of measures describing the diffusion was computed: apparent diffusion
28 coefficient (ADC), fractional anisotropy (FA), axial and radial diffusivity and the coefficients of
29 linearity, planarity and sphericity [24,41]. They are all based on the three eigenvalues of each voxel
30 tensor ($\lambda_1, \lambda_2, \lambda_3$). ADC measures the global amount of diffusion at each voxel, whereas axial
31 diffusivity measures the diffusion along the axial direction, that is, along the fiber direction. On the
32 other hand, radial diffusivity provides information of the amount of diffusion orthogonal to the fiber
33 direction. The other parameters are related to the shape and anisotropy of the diffusion. FA
34 describes the anisotropy of the diffusion, since diffusion in fibers is highly anisotropic its value is
35 higher in areas where fiber bundles are [24]. Linearity, planarity and sphericity coefficients describe

1 the shape of the diffusion; higher values of the linear coefficient indicates that diffusion occurs
2
3
4
5
6
7
8
9
10
11
12
13
14
15
16
17
18
19
20
21
22
23
24
25
26
27
28
29
30
31
32
33
34
35
36
37
38
39
40
41
42
43
44
45
46
47
48
49
50
51
52
53
54
55
56
57
58
59
60
61
62
63
64
65

the shape of the diffusion; higher values of the linear coefficient indicates that diffusion occurs mainly in one direction; higher planarity involves that diffusion is performed mostly in one plane, and higher values of sphericity are related to isotropic diffusion [41].

b) Global analysis

The parameters described in the previous section were computed at each voxel belonging to the brain mask, and their value was averaged in the whole brain, in order to perform a global analysis of the differences between controls and IUGR.

In addition, so as to avoid potential confounding values produced by GM and cerebrospinal fluid (CSF), a second mask was applied to analyse the changes in the WM. It is known that WM is related to higher values of FA, and therefore a FA threshold can be defined to identify this kind of tissue. Thus, masks were built by a set of thresholds ranging from 0.05 to 0.40, and the diffusion parameters inside these masks were computed. The consistency of the results achieved using the set of masks was analyzed (Figure 2A). By visual inspection, it was estimated that a threshold of FA=0.20 allowed to best discriminate the structures of WM in the brains (Figure 2B), and thus, this threshold was used in further analyses.

c) Regional analysis

Manual delineation

Manual delineation of GM regions of interest (ROIs) was performed in T1 weighted images including thalamus, putamen and caudate nucleus, prefrontal cortex, cerebellar hemispheres and vermis structures of each hemisphere. WM ROIs (corpus callosum, fimbria of hippocampus, internal capsule and corona radiata) were delineated directly in FA map.

GM ROIs were co-registered to DWI by applying a previously calculated affine transformation of the T1 weighted images to DWI space. Mean diffusion related measures were obtained including ADC, axial and radial diffusivities, FA, linearity, planarity and sphericity coefficients.

Voxel based analysis

1 All rabbit brains were registered to a reference brain using their FA volumes [42] by means
2 of an affine registration that maximized mutual information of volume [43] followed by an elastic
3 warping based on diffeomorphic demons [44] both available in MedINRIA 1.9.4 software. Registered
4 volumes were smoothed with a Gaussian kernel of 3 x 3 x 3 voxels (1.05 x 1.05 x 1.05 mm³) in
5 order to compensate for possible misregistrations, reduce noise and signal variations and reduce
6 the effective number of multiple comparisons in the statistical testing thus improving statistical
7 power [45].

8 Once the images are aligned to the reference, it can be assumed that the voxels in the same
9 location in all the registered images belong to the same structure, and therefore, they can be
10 compared. Voxel-wise t-test was performed, obtaining the voxels with a statistically significant
11 different distribution of diffusion related parameters between controls and IUGR. Moreover, in this
12 study, the Pearson correlation between the diffusion parameters and the neurobehavior test
13 outcome at each voxel was also computed, to identify which regions were related to the observed
14 changes in neurobehavioral tests. In order to increase the reliability of the results obtained, the
15 procedure was repeated using all the subjects as the reference in the elastic warping, allowing to
16 discard variability produced by the arbitrary choice of the reference template.

17 **2.3-STATISTICAL ANALYSIS**

18 Given the absence of preliminary data and the difficulty in estimating the magnitude of
19 differences, sample size was arbitrarily established at 10 subjects and 10 controls. For quantitative
20 variables, normality was assessed by the Shapiro-Francia W' test [46]. Normal-distributed
21 quantitative variables were analysed by t-test. Non-normal distributed variables were analysed with
22 the non-parametric Mann–Whitney U test. Correlation between different variables was assessed by
23 means of Pearson correlation. In VBA approach, registered and smoothed volumes of FA and ADC
24 were used to obtain volumetric maps of t-statistics, showing the voxels that presented a significant
25 difference between groups (uncorrected $p < 0.01$ and $p < 0.05$). In addition, a correlation volume (ρ)
26 was also calculated for each neurofunctional item, expressing positive and negative Pearson
27 correlations between FA and neurofunctional outcome. Image analysis and processing was

1 performed by means of in-house software implemented in Matlab 2011a (The Mathworks Inc,
2
3 Natick, MA, USA). SPSS 15.0 (SPSS Inc., Chicago, IL, USA) was used for statistical analysis.
4
5
6
7
8
9
10
11
12
13
14
15
16
17
18
19
20
21
22
23
24
25
26
27
28
29
30
31
32
33
34
35
36
37
38
39
40
41
42
43
44
45
46
47
48
49
50
51
52
53
54
55
56
57
58
59
60
61
62
63
64
65

3- RESULTS

3.1-Perinatal data and neonatal neurobehavior

Birth weight was significantly lower in cases than in controls (30.4 ± 12.2 g. vs. 47.0 ± 9.3 g., $p=0.007$). Regarding neurobehavioral test, growth restricted pups showed poorer results in all parameters, reaching significance in righting reflex, tone of the limbs, locomotion, lineal movement, forepaw distance, head turn during feeding and smelling response (Table 1 and Video S1).

3.2-Brain MRI analysis

MRI analysis revealed significant lower brain volume in growth restricted group (1345 ± 110 mm³ vs. 1211 ± 152 mm³, $p=0.037$). When brain volume was adjusted by means of the brain/birth-weight ratio, case group showed significantly higher values (29.2 ± 7.9 vs. 39.9 ± 6.5 , $p= 0.033$).

a) Global analysis

Table 2 depicts the results of global analysis of diffusion related parameters. Whole brain analysis revealed non-significantly higher ADC values and significantly lower FA and linearity values in the growth restricted group. When the WM mask was applied, FA significantly differed between cases and controls (Figure 2). Regarding the correlation between neurobehavioral and diffusion parameters, head turn during feeding was significantly positively correlated with global FA ($r=0.545$, $p=0.016$), maintained when the WM mask was applied ($r=0.566$, $p=0.012$) (Table 3).

b) Regional analysis

Manual delineation

ROIs analysis of diffusion parameters only found differences in right fimbria of hippocampus, showing decreased values of FA in IUGR ($p=0.048$) (Table S1).

Voxel based analysis

When VBA analysis was applied, statistically significant differences were found in FA distribution between cases and controls in multiple structures such as different cortical regions (frontal, insular, occipital and temporal), hippocampus, putamen, thalamus, claustrum, medial septal nucleus, anterior commissure, internal capsule, fimbria of hippocampus, medial lemniscus and olfactory tract (Figure 3). Non consistent significant changes were found in ADC (Figure S1).

3.3-Correlation between MRI diffusion and neurobehavioral outcome

1 FA map showed multiple areas correlated with most of neurobehavioral domains, being
2 posture, locomotion, circular motion, intensity, fore-hindpaw distance and head turn the domains
3 showing more statistically significant correlated areas (Figure 4 and Table 4). Subcortical GM areas
4 were mainly significantly correlated with posture, locomotion and head turn and WM structures
5 essentially with posture and locomotion parameters. Interestingly, hippocampus is the GM structure
6 that presented more correlations with neurobehavioral domains (locomotion, circular motion, lineal
7 movement, fore-hindpaw distance and head turn). Within WM structures, both anterior commissure
8 and fimbria of hippocampus were the areas correlated with a bigger amount of neurobehavioral
9 items. To be highlighted, olfactory items correlate with very specific areas, including prefrontal and
10 temporal cortex, caudate nucleus, olfactory tract and lateral lemniscus.

4-DISCUSSION

In this study we developed a rabbit model to evaluate functional and structural impact of IUGR, providing high-resolution MRI description of the anatomical patterns of brain maturational changes occurring *in utero*. We demonstrated that IUGR was associated with different patterns of brain diffusivity in multiple brain regions, which were significantly correlated with the neurobehavioral impairments observed. The model developed may be a powerful tool to correlate functional and structural brain information with histological, molecular and other imaging techniques. In addition, it allows detailed regional assessment of the impact of interventions in the complex patterns of brain reorganization induced by adverse prenatal environment.

Neonatal neurobehavior

It is known that IUGR in humans is associated with neonatal neurodevelopmental dysfunctions [4,5], being attention, habituation, regulation of state, motor and social-interactive clusters the most affected [5]. In a similar manner, growth restricted rabbit pups in this model showed weakened motor activity and olfactory function, which is their principal way of social interactions [47]. The findings reinforce previous evidence suggesting the capability of this animal model to reproduce features of human IUGR [32,33]. Previous studies suggested the ability of the rabbit model to illustrate the neonatal effects of acute severe prenatal conditions. Thus, hypoxic-ischemic injury and endotoxin exposure produce hypertonic motor deficits [35,48], reduced limb movement [49] and olfactory deficits [50] in this model. The present study demonstrates that selective ligation of uteroplacental vessels is suitable to reflect the neurodevelopmental impact of mild and sustained reduction of placental blood flow occurring in IUGR. These results illustrate a more general concept that lower animal species are also susceptible of developing brain reorganization *in utero*, and therefore they are suitable models to assess the chronic effects of adverse intrauterine environment on brain development.

MRI global analysis

Changes in brain diffusivity and anisotropy have previously been reported after acute severe hypoxic experimental conditions in adults [26] and developing brain [27]. Placental insufficiency results in mild and sustained injury, which may challenge the ability to find obvious differences

1 between groups. With the purpose of detecting subtle changes we used high-resolution MRI
2 acquisition in fixed whole brain preparations. This approach allows revealing submillimetric tissue
3 structure differences, particularly in the GM, which are difficult to detect *in vivo* [21]. As a trade-off,
4 fixation process may decrease brain water content reducing ADC absolute values, although
5 diffusion anisotropy is preserved [51].

6
7
8
9
10
11 In growth restricted pups, global decreased FA values were demonstrated in both whole
12 brain and WM mask analysis. Findings are similar to those observed in acute hypoxic-ischemic
13 injury models [52] and perinatal asphyxia in humans [23] demonstrating decreased values in FA
14 particularly in WM areas. Aside from acute models, preliminary evidence in neonates with cyanotic
15 congenital heart defects suggests also the presence of brain FA changes [53,54]. FA indicates the
16 degree of anisotropic diffusion and typically increases in WM areas during brain maturation, being
17 closely related with myelination processes [23]. After acute hypoxic-ischemic injury in rat pups,
18 decreased values of FA have been related with decreased myelin content in WM areas [55].
19 Consistently with decreased FA, the findings demonstrated that IUGR had a significant decrease in
20 linearity and a significant increase in sphericity, changes that have been related with reduced
21 organization of WM tracts [41]. Therefore, the results of the study are consistent with the presence
22 of decreased WM myelination and brain reorganization after exposure to IUGR in the rabbit model.

23
24
25
26
27
28
29
30
31
32
33
34
35
36
37
38 Global diffusivity analysis revealed a non-significant trend for increased ADC in the IUGR
39 group. ADC is directly related with the overall magnitude of water diffusion, typically decreasing as
40 brain maturation occurs [23]. In addition, after perinatal acute hypoxic-ischemic event, it shows a
41 dynamic process with a quickly decrease followed by a pseudo-normalization to finally increase to
42 higher values than normal [27]. In humans, ADC values have been demonstrated to be increased in
43 multiple brain regions after chronic fetal conditions including IUGR [30] and fetal cardiac defects
44 [29,53,54]. In addition, increased ADC values have been reported after prenatal acute hypoxic-
45 ischemic injury in hypertonic rabbits [52]. We found a non-significant trend to increased ADC values
46 in IUGR. We acknowledge that sample size may have prevented to detect subtle differences in
47 ADC. In any event, the lack of remarkable differences in ADC is possibly a reflection of the
48 abovementioned notion that IUGR results in delayed brain maturation and reorganization rather

1 than in significant brain injury [22,56]. Further histological studies may help to clarify essential
2 information about microstructural changes and allow correlations with findings in diffusion
3 parameters here reported.

4 **MRI regional analysis**

5 Regional analysis of diffusivity parameters may provide information of the anatomical pattern
6 of brain microstructural changes in IUGR. As expected, manual brain segmentation showed limited
7 results and significant differences in a few brain areas. As shown in previous studies this approach
8 has limitations in small structures, due to the difficulty in obtaining accurate delineations [57] and to
9 the partial volume effects [37]. Since these limitations were known, a VBA strategy was applied.
10 VBA approach performs the analysis of the whole brain voxel-wise avoiding the need of *a priori*
11 hypothesis or previous delineation [38], and allowed to localize regional differences between cases
12 and controls in FA distribution.

13 Cortical and subcortical GM areas were the most altered regions and as expected regional
14 reductions in FA showed high correlations with functional impairment. Cortical changes are a
15 feature of IUGR, as suggested by decreased cortical volume [13] and discordant patterns of
16 gyrification due to pronounced reduction in cortical expansion in neonates [15] and differences in
17 GM brain structure in infants [16] suffering this condition. Our results support the notion that these
18 changes are based on microstructural differences. In line with this contention, microstructural
19 changes in cortical regions have previously been demonstrated in a sheep model of IUGR, including
20 cortical astrogliosis, fragmentation of fibers and thinner subcortical myelin sheaths [58]. Importantly,
21 these histological features have been shown to correlate with decreased FA in cortex [28] and
22 subcortical WM [59]. Regional analysis demonstrated that among GM affected regions, the
23 hippocampus showed the highest number of correlations with neurobehavioral domains. The
24 hippocampus is known for its crucial role in cognitive function such as memory and learning. In
25 human IUGR neonates, a reduction in neonatal hippocampal volume was associated with poor
26 neurofunctional outcomes in neonatal period including autonomic motor state, attention-interaction,
27 self-regulation and examiner facilitation [14]. Additionally, previous experimental data have
28 demonstrated reduced number of neurons in hippocampus [60] and alterations in the dendritic

1 morphology of pyramidal neurons [61] after IUGR. In summary, the findings support that impaired
22 neurocognition in IUGR is mediated by microstructural changes in cortical and subcortical areas
43 detectable with diffusion MRI, with hippocampus playing an important role.

74 Regional analysis revealed changes in multiple WM structures. The most pronounced
95 differences were found in the internal capsule, anterior commissure and fimbria of hippocampus,
16 which showed significant correlations with locomotion parameters and posture. Changes in WM
147 structures have also been reported in human fetuses, with increased ADC in pyramidal tract in
168 IUGR [30] and increased ADC in multiple WM in areas in fetuses [29] and newborns [53,54] with
189 congenital cardiac defects. Consistently with our results, prenatal chronic hypoxia models have
210 demonstrated inflammatory microgliosis, mild astrogliosis [62], and a delay in the maturation of
211 oligodendrocytes leading to a transient delay in myelination [56]. These changes result in global
212 reduction in axonal myelination in absence of overt WM damage [63] which in turn is reflected by
213 decreased values of FA [59] as observed in this study. Interestingly, anterior commissure and
214 fimbria of hippocampus, WM structures with significant differences in FA distribution demonstrated
215 by VBA, were the WM structures correlated with more altered neurobehavioral items, especially
216 locomotion parameters and posture. Of note, these two WM tracks connect GM structures that also
217 presented significantly decreased FA demonstrated by VBA. Anterior commissure contains axonal
218 tracts connecting temporal lobes and fimbria of hippocampus contains efferent fibers from
219 hippocampus. Finally, changes in olfactory tract and lateral lemniscus WM tracts, which are closely
220 related with olfaction, were significantly correlated with smelling test results. This finding was
221 consistent with previous data demonstrating that neurons of the olfactory epithelium in rabbit are
222 sensitive to global acute hypoxia-ischemia [50]. In summary, this study characterized regional
223 alterations in WM diffusion parameters, findings which were in line with GM data and further suggest
224 the presence of microstructural regional changes underlying brain reorganization in IUGR.
225 Furthermore, reduced WM FA could indicate connectivity changes and a role for MRI diffusion
226 connectomics for the development of more robust biomarkers of brain injury in IUGR, which deserve
227 investigation in future studies.

Strengths and limitations

Some issues must be noted concerning the methodology followed. Firstly, the absolute values of ADC obtained in this study were lower than those previously reported in neonatal rabbit brain [52,64]. As abovementioned, that could be explained by the fact that brain fixation decreases water content in the brain reducing ADC values [51]. However, in order to preserve diffusion contrast we used high b-values as previously suggested [65]. In addition, all the brains followed the same fixation process and, theoretically, must be affected in a similar way. Secondly, in the global analysis, a FA thresholding approach was used to identify the voxels belonging to the WM. Although this thresholding has usually been described in order to segment the WM in human brains [66], to the best of our knowledge, it has not been defined for perinatal rabbit brain. Therefore, different thresholds were analyzed, showing that the differences between controls and IUGR are preserved for a wide range of values of the FA threshold (Figure 2 and Figure S2). Thirdly, regional analysis of the images has been performed by means of VBA technique in order to overcome manual delineation limitations. However, the use of VBA implies weaker statistical power due to the large number of voxels tested [45], increasing type I error rate even after smoothing diffusion related measures volumetric maps. Another issue concerning VBA is that the method requires registration of all the subjects in the dataset to a template volume, and therefore the arbitrary choice of this template could bias the result [45]. To avoid such a bias, the VBA procedure was repeated taking all subjects as template. Similar results were obtained with each template, and there was a high consistency among repeated tests for the regional changes identified. Finally, this work is based on diffusion related parameters, which measure either the amount of diffusivity or the anisotropy of the diffusion, but do not provide information about diffusion direction and therefore, about the fiber bundles trajectories. Further connectivity studies, where WM tracts connecting different areas are identified, will permit a better understanding of the consequences of IUGR in the brain development.

Conclusions

In conclusion, we developed a fetal rabbit model reproducing neurobehavioral and neurostructural consequences of IUGR. Diffusion MRI in whole organ preparations allowed showing differences on global and regional diffusion related parameters, revealing in detail the pattern of

1 brain microstructural changes produced by IUGR already at birth and their functional correlates in
2
3 early neonatal life. The results illustrate that sustained intrauterine restriction of oxygen and nutrient
4
5 induces a complex pattern of maturational changes, in both GM and WM areas. The model here
6
7 described allowed to characterize the most significantly affected regions. These anatomical findings
8
9 could be of help in multi-scale studies to advance in the understanding of the mechanisms
10
11 underlying abnormal neurodevelopment of prenatal origin. In addition, MRI diffusion changes can be
12
13 used to monitor the impact of interventions. WM changes warrant the development of further studies
14
15 for the development of imaging biomarkers of brain reorganization in IUGR and other fetal chronic
16
17 conditions.
18
19
20
21
22
23
24
25
26
27
28
29
30
31
32
33
34
35
36
37
38
39
40
41
42
43
44
45
46
47
48
49
50
51
52
53
54
55
56
57
58
59
60
61
62
63
64
65

1 REFERENCES

- 1
22 1. Walker DM, Marlow N (2008) Neurocognitive outcome following fetal growth restriction. Arch Dis
3
43 Child Fetal Neonatal Ed 93: F322-325.
5
- 6
74 2. Baschat AA (2004) Pathophysiology of fetal growth restriction: implications for diagnosis and
8
95 surveillance. Obstet Gynecol Surv 59: 617-627.
- 10
116 3. Rees S, Harding R, Walker D (2007) An adverse intrauterine environment: implications for injury
12
137 and altered development of the brain. Int J Dev Neurosci 26: 3-11.
14
- 158 4. Bassan H, Stolar O, Geva R, Eshel R, Fattal-Valevski A, et al. (2011) Intrauterine growth-
16
179 restricted neonates born at term or preterm: how different? Pediatr Neurol 44: 122-130.
18
- 19
210 5. Figueras F, Oros D, Cruz-Martinez R, Padilla N, Hernandez-Andrade E, et al. (2009)
21
211 Neurobehavior in term, small-for-gestational age infants with normal placental function. Pediatrics
23
241 124: e934-941.
25
- 26
2713 6. Eixarch E, Meler E, Iraola A, Illa M, Crispi F, et al. (2008) Neurodevelopmental outcome in 2-
28
2914 year-old infants who were small-for-gestational age term fetuses with cerebral blood flow
30
315 redistribution. Ultrasound Obstet Gynecol 32: 894-899.
32
- 3316 7. Feldman R, Eidelman AI (2006) Neonatal state organization, neuromaturation, mother-infant
34
3517 interaction, and cognitive development in small-for-gestational-age premature infants. Pediatrics
36
3718 118: e869-878.
38
- 39
409 8. Geva R, Eshel R, Leitner Y, Fattal-Valevski A, Harel S (2006) Memory functions of children born
41
420 with asymmetric intrauterine growth restriction. Brain Res 1117: 186-194.
43
- 44
4521 9. Geva R, Eshel R, Leitner Y, Valevski AF, Harel S (2006) Neuropsychological outcome of children
46
4722 with intrauterine growth restriction: a 9-year prospective study. Pediatrics 118: 91-100.
48
- 4923 10. Leitner Y, Fattal-Valevski A, Geva R, Eshel R, Toledano-Alhadeif H, et al. (2007)
50
5124 Neurodevelopmental outcome of children with intrauterine growth retardation: a longitudinal, 10-year
52
5325 prospective study. J Child Neurol 22: 580-587.
54
- 55
5626 11. McCarton CM, Wallace IF, Divon M, Vaughan HG, Jr. (1996) Cognitive and neurologic
57
5827 development of the premature, small for gestational age infant through age 6: comparison by birth
59
6028 weight and gestational age. Pediatrics 98: 1167-1178.
61
62
63
64
65

1 12. Scherjon S, Briet J, Oosting H, Kok J (2000) The discrepancy between maturation of visual-
2 evoked potentials and cognitive outcome at five years in very preterm infants with and without
3 hemodynamic signs of fetal brain-sparing. *Pediatrics* 105: 385-391.

4 13. Tolsa CB, Zimine S, Warfield SK, Freschi M, Sancho Rossignol A, et al. (2004) Early alteration
5 of structural and functional brain development in premature infants born with intrauterine growth
6 restriction. *Pediatr Res* 56: 132-138.

7 14. Lodygensky GA, Seghier ML, Warfield SK, Tolsa CB, Sizonenko S, et al. (2008) Intrauterine
8 growth restriction affects the preterm infant's hippocampus. *Pediatr Res* 63: 438-443.

9 15. Dubois J, Benders M, Borradori-Tolsa C, Cachia a, Lazeyras F, et al. (2008) Primary cortical
10 folding in the human newborn: an early marker of later functional development. *Brain* 131: 2028-
11 2041.

12 16. Padilla N, Falcón C, Sanz-Cortés M, Figueras F, Bargallo N, et al. (2011) Differential effects of
13 intrauterine growth restriction on brain structure and development in preterm infants: A magnetic
14 resonance imaging study. *Brain research* 1382: 98-108.

15 17. Esteban F, Padilla N, Sanz-Cortés M, de Miras J (2010) Fractal-dimension analysis detects
16 cerebral changes in preterm infants with and without intrauterine growth restriction. *NeuroImage* 53:
17 1225-1232.

18 18. Jiang S, Xue H, Counsell S, Anjari M, Allsop J, et al. (2009) Diffusion tensor imaging (DTI) of the
19 brain in moving subjects: application to in-utero fetal and ex-utero studies. *Magn Reson Med* 62:
20 645-655.

21 19. Kasprian G, Brugger PC, Weber M, Krssak M, Krampfl E, et al. (2008) In utero tractography of
22 fetal white matter development. *Neuroimage* 43: 213-224.

23 20. Pallotto EK, Kilbride HW (2006) Perinatal outcome and later implications of intrauterine growth
24 restriction. *Clin Obstet Gynecol* 49: 257-269.

25 21. D'Arceuil H, Liu C, Levitt P, Thompson B, Kosofsky B, et al. (2008) Three-dimensional high-
26 resolution diffusion tensor imaging and tractography of the developing rabbit brain. *Dev Neurosci*
27 30: 262-275.

- 1 22. Rees S, Harding R, Walker D (2011) The biological basis of injury and neuroprotection in the
1 fetal and neonatal brain. *Int J Dev Neurosci*: in press.
- 3
43 23. Neil J, Miller J, Mukherjee P, Huppi PS (2002) Diffusion tensor imaging of normal and injured
5 developing human brain - a technical review. *NMR Biomed* 15: 543-552.
- 6
74 24. Basser PJ, Pierpaoli C (1996) Microstructural and physiological features of tissues elucidated by
8 quantitative-diffusion-tensor MRI. *J Magn Reson B* 111: 209-219.
- 95
10
116 25. Merino JG, Warach S (2010) Imaging of acute stroke. *Nat Rev Neurol* 6: 560-571.
- 12
137 26. Rivers CS, Wardlaw JM (2005) What has diffusion imaging in animals told us about diffusion
14 imaging in patients with ischaemic stroke? *Cerebrovasc Dis* 19: 328-336.
- 158
16 27. Lodygensky GA, Inder TE, Neil JJ (2008) Application of magnetic resonance imaging in animal
17 models of perinatal hypoxic-ischemic cerebral injury. *Int J Dev Neurosci* 26: 13-25.
- 189
19
20 28. Sizonenko SV, Camm EJ, Garbow JR, Maier SE, Inder TE, et al. (2007) Developmental
21 changes and injury induced disruption of the radial organization of the cortex in the immature rat
22 brain revealed by in vivo diffusion tensor MRI. *Cereb Cortex* 17: 2609-2617.
- 23
24
25
26
27
28
29
30
315 29. Berman JI, Hamrick SE, McQuillen PS, Studholme C, Xu D, et al. (2011) Diffusion-weighted
32 imaging in fetuses with severe congenital heart defects. *AJNR Am J Neuroradiol* 32: E21-22.
- 336
34
35
36
37
38 30. Sanz-Cortes M, Figueras F, Bargallo N, Padilla N, Amat-Roldan I, et al. (2010) Abnormal brain
39 microstructure and metabolism in small-for-gestational-age term fetuses with normal umbilical artery
40 Doppler. *Ultrasound Obstet Gynecol* 36: 159-165.
- 41
42
43
44
45 31. Bassan H, Trejo LL, Kariv N, Bassan M, Berger E, et al. (2000) Experimental intrauterine growth
46 retardation alters renal development. *Pediatr Nephrol* 15: 192-195.
- 47
48
49
50
51
52 32. Eixarch E, Figueras F, Hernandez-Andrade E, Crispi F, Nadal A, et al. (2009) An experimental
53 model of fetal growth restriction based on selective ligation of uteroplacental vessels in the pregnant
54 rabbit. *Fetal Diagn Ther* 26: 203-211.
- 55
56
57
58 33. Eixarch E, Hernandez-Andrade E, Crispi F, Illa M, Torre I, et al. (2011) Impact on fetal mortality
59 and cardiovascular Doppler of selective ligation of uteroplacental vessels compared with
60 undernutrition in a rabbit model of intrauterine growth restriction. *Placenta* 32: 304-309.
- 61
62
63
64
65

- 1 34. Derrick M, Drobyshevsky A, Ji X, Tan S (2007) A model of cerebral palsy from fetal hypoxia-
1 ischemia. Stroke 38: 731-735.
22
3
- 43 35. Derrick M, Luo NL, Bregman JC, Jilling T, Ji X, et al. (2004) Preterm fetal hypoxia-ischemia
5 causes hypertonia and motor deficits in the neonatal rabbit: a model for human cerebral palsy? J
6
74 Neurosci 24: 24-34.
8
95
- 116 36. Zhan L, Chiang M-C, Barysheva M, Toga AW, McMahon KL, et al. (2008) How Many Gradients
12 are Sufficient in High-Angular Resolution Diffusion Imaging (HARDI)? 13th Annual Meeting of the
137 Organization for Human Brain Mapping (OHBM). Melbourne, Australia.
14
158
- 189 37. Van Camp N, Blockx I, Verhoye M, Casteels C, Coun F, et al. (2009) Diffusion tensor imaging in
19 a rat model of Parkinson's disease after lesioning of the nigrostriatal tract. NMR Biomed 22: 697-
210 706.
21
211
- 24 38. Snook L, Plewes C, Beaulieu C (2007) Voxel based versus region of interest analysis in
25 diffusion tensor imaging of neurodevelopment. Neuroimage 34: 243-252.
26
2713
- 28 39. Tyszka JM, Readhead C, Bearer EL, Pautler RG, Jacobs RE (2006) Statistical diffusion tensor
29 histology reveals regional dysmyelination effects in the shiverer mouse mutant. Neuroimage 29:
315 1058-1065.
32
3316
- 35 40. Toussaint N, Souplet J-C, Fillard P (2007) MedINRIA: Medical Image Navigation and Research
36 Tool by INRIA. Proc of MICCAI'07 Workshop on Interaction in medical image analysis and
37
388 visualization. Brisbane, Australia.
39
409
- 420 41. Westin CF, Maier SE, Mamata H, Nabavi A, Jolesz FA, et al. (2002) Processing and
43 visualization for diffusion tensor MRI. Med Image Anal 6: 93-108.
44
4521
- 46 42. Jones DK, Griffin LD, Alexander DC, Catani M, Horsfield MA, et al. (2002) Spatial normalization
47 and averaging of diffusion tensor MRI data sets. Neuroimage 17: 592-617.
48
4923
- 50 43. Mattes D, Haynor D, Vesselle H, Lewellwn T, Eubank W (2001) Non-rigid multi-modality image
51 registration. Medical Imaging 2001: Image Processing: 1609-1620.
52
5325
- 54 44. Vercauteren T, Pennec X, Perchant A, Ayache N (2009) Diffeomorphic demons: efficient non-
55
5626 parametric image registration. Neuroimage 45: S61-72.
57
5827

- 1 45. Lee JE, Chung MK, Lazar M, DuBray MB, Kim J, et al. (2009) A study of diffusion tensor
1
22 imaging by tissue-specific, smoothing-compensated voxel-based analysis. *Neuroimage* 44: 870-
3
43 883.
5
- 6 46. Royston P (1993) A pocket-calculator algorithm for the Shapiro-Francia test for non-normality:
7
8 an application to medicine. *Stat Med* 12: 181-184.
9
- 10 47. Val-Laillet D, Nowak R (2008) Early discrimination of the mother by rabbit pups. *Applied Animal*
116
12 *Behaviour Science* 111: 173-182.
13
- 14 48. Saadani-Makki F, Kannan S, Lu X, Janisse J, Dawe E, et al. (2008) Intrauterine administration
15
16 of endotoxin leads to motor deficits in a rabbit model: a link between prenatal infection and cerebral
17
18 palsy. *Am J Obstet Gynecol* 199: 651 e651-657.
19
20
- 21 49. Derrick M, Drobyshevsky A, Ji X, Chen L, Yang Y, et al. (2009) Hypoxia-ischemia causes
22
23 persistent movement deficits in a perinatal rabbit model of cerebral palsy: assessed by a new swim
24
25 test. *Int J Dev Neurosci* 27: 549-557.
26
27
- 28 50. Drobyshevsky A, Robinson AM, Derrick M, Wyrwicz AM, Ji X, et al. (2006) Sensory deficits and
29
30 olfactory system injury detected by novel application of MEMRI in newborn rabbit after antenatal
31
32 hypoxia-ischemia. *Neuroimage* 32: 1106-1112.
33
34
- 35 51. Sun SW, Neil JJ, Song SK (2003) Relative indices of water diffusion anisotropy are equivalent in
36
37 live and formalin-fixed mouse brains. *Magn Reson Med* 50: 743-748.
38
39
- 40 52. Drobyshevsky A, Derrick M, Wyrwicz AM, Ji X, Englof I, et al. (2007) White matter injury
41
42 correlates with hypertonia in an animal model of cerebral palsy. *J Cereb Blood Flow Metab* 27: 270-
43
44 281.
45
- 46 53. Shedeed S, Elfaytouri E (2011) Brain Maturity and Brain Injury in Newborns With Cyanotic
47
48 Congenital Heart Disease. *Pediatric Cardiology* 32: 47-54.
49
50
- 51 54. Miller SP, McQuillen PS, Hamrick S, Xu D, Glidden DV, et al. (2007) Abnormal Brain
52
53 Development in Newborns with Congenital Heart Disease. *New England Journal of Medicine* 357:
54
55 1928-1938.
56
- 57 55. Wang S, Wu EX, Tam CN, Lau HF, Cheung PT, et al. (2008) Characterization of white matter
58
59 injury in a hypoxic-ischemic neonatal rat model by diffusion tensor MRI. *Stroke* 39: 2348-2353.
60
61
62
63
64
65

1 56. Tolcos M, Bateman E, O'Dowd R, Markwick R, Vrijisen K, et al. (2011) Intrauterine growth
 1 restriction affects the maturation of myelin. *Experimental Neurology* In Press, Uncorrected Proof.
 22
 3
 43 57. Abe O, Takao H, Gonoj W, Sasaki H, Murakami M, et al. (2010) Voxel-based analysis of the
 5
 6 diffusion tensor. *Neuroradiology* 52: 699-710.
 7
 8
 95 58. Mallard E, Rees S, Stringer M, ML C, Harding R (1998) Effects of chronic placental insufficiency
 10
 116 on brain development in fetal sheep. *Pediatr Res* 43: 262-270.
 12
 137 59. Kochunov P, Williamson DE, Lancaster J, Fox P, Cornell J, et al. (2010) Fractional anisotropy of
 14
 158 water diffusion in cerebral white matter across the lifespan. *Neurobiology of Aging* In Press.
 16
 17
 189 60. Mallard C, Loeliger M, Copolov D, Rees S (2000) Reduced number of neurons in the
 19
 200 hippocampus and the cerebellum in the postnatal guinea-pig following intrauterine growth-
 21
 211 restriction. *Neuroscience* 100: 327-333.
 23
 24
 25 61. Dieni S, Rees S (2003) Dendritic morphology is altered in hippocampal neurons following
 26
 27 prenatal compromise. *J Neurobiol* 55: 41-52.
 28
 29
 30 62. Olivier P, Baud O, Bouslama M, Evrard P, Gressens P, et al. (2007) Moderate growth restriction:
 31
 32 deleterious and protective effects on white matter damage. *Neurobiol Dis* 26: 253-263.
 33
 34
 35 63. Nitsos I, Rees S (1990) The effects of intrauterine growth retardation on the development of
 36
 37 neuroglia in fetal guinea pigs. An immunohistochemical and an ultrastructural study. *Int J Dev*
 38
 39 *Neurosci* 8: 233-244.
 40
 41
 42 64. Saadani-Makki F, Kannan S, Makki M, Muzik O, Janisse J, et al. (2009) Intrauterine endotoxin
 43
 44 administration leads to white matter diffusivity changes in newborn rabbits. *J Child Neurol* 24: 1179-
 45
 46 1189.
 47
 48
 49 65. Miller KL, Stagg CJ, Douaud G, Jbabdi S, Smith SM, et al. (2011) Diffusion imaging of whole,
 50
 51 post-mortem human brains on a clinical MRI scanner. *Neuroimage* 57: 167-181.
 52
 53
 54 66. Mori S, Zhang J (2006) Principles of diffusion tensor imaging and its applications to basic
 55
 56 neuroscience research. *Neuron* 51: 527-539.
 57
 58
 59
 60
 61
 62
 63
 64
 65

1 **Legends to figures**

2
3
4
5 **Figure 1. Schematic and graphical representation of study design and methods.**

6
7
8
9
10
11
12
13
14
15
16
17
18
19
20
21
22
23
24
25
26
27
28
29
30
31
32
33
34
35
36
37
38
39
40
41
42
43
44
45
46
47
48
49
50
51
52
53
54
55
56
57
58
59
60
61
62
63
64
65

PANEL 1: (A) Illustrative image of unilateral ligation of 40-50% of uteroplacental vessels at 25 days of pregnancy (B) Scheme of surgical procedures and study groups.

PANEL 2: Illustrative pictures of neurobehavioral evaluation of locomotion (C), tone (D), smelling test (E), righting reflex (F) and sucking and swallowing (G) performed at +1 postnatal day.

PANEL 3: MRI acquisition. Fixed brains (H) were scanned to obtain a high resolution T1 weighted (I) image and diffusion weighted images (J).

PANEL 4a: MRI global analysis. After masking brain volume, global analysis is performed to obtain average DTI parameters (FA, ADC, radial diffusivity, axial diffusivity, linearity, planarity and sphericity).

PANEL 4b: Voxel based analysis was performed by elastic registration to a reference FA map. Once subject brains were registered and smoothed, FA values distribution for each voxel was analyzed to identify areas with statistically significant different distribution in IUGR and the correlation of changes with neurobehavioral tests.

Figure 2. FA thresholds in the global analysis.

(A) Control and IUGR group distribution of average FA on the mask of WM computed with different FA thresholds. Error bar depicts ± 1 SD.

(B) Representative axial and coronal slices of WM mask based on different FA thresholds of a control subject of the study. The mask obtained with a 0.2 FA threshold was found to most accurately discriminate white matter areas.

FA: Fractional Anisotropy, IUGR: intrauterine growth restriction, WM: white matter,

* $p < 0.05$

Figure 3. Fractional anisotropy values: regions showing statistically significant differences between cases and controls.

1 Slices of the smoothed reference FA image. Red areas have a significance of $p < 0.01$, green areas
1
22 have a significance of $p < 0.05$. The slices displayed contain representative anatomical structures.
3
43 Slice locations are shown in the T1-weighted MRIs in the right. (A) Coronal slices from anterior to
5
6
74 posterior. (B) Axial slices from superior to inferior.
8
95

10
116 **Figure 4. Correlation maps between neurobehavioral test items and fractional anisotropy**
12
137 **values.**
14

158 Coronal slices (from anterior to superior) of the smoothed reference FA image. Colormap highlights
16
17 the areas where the correlation coefficient is higher than 0.2.
189

19
200 (A) Posture, (B) Righting reflex, (C) Tone, (D) Locomotion, (E) Circular motion, (F) Intensity, (G)
21
221 Duration, (H) lineal movement, (I) Fore-hindpaw distance, (J) Sucking and swallowing, (K) Head
23
2412 turn, (L) Smelling test, (M) Smelling test time
25

26
27
28
294 **Figure S1. Apparent Diffusion Coefficient values: regions showing statistically significant**
30
315 **differences between cases and controls.**
32

3316 Slices of the smoothed reference ADC image. Red areas have a significance of $p < 0.01$, green
34
35 areas have a significance of $p < 0.05$. The slices have been chosen because they contained the most
36
37 representative anatomical structures. Slice locations are shown in the T1-weighted MRIs in the
3818 right. (A) Coronal slices from anterior to posterior. (B) Axial slices from superior to inferior.
39
409
41

42
43
44
45 **Figure S2. Influence of the FA thresholds in the global analysis off DTI parameters on the**
46
47 **mask of WM computed with different FA thresholds.**
48

49
50 Control and IUGR average (A) Apparent Diffusion Coefficient, (B) Axial Diffusivity, (C) Radial
5123 Diffusivity, (D) Linearity, (E) Sphericity, (F) Planarity.
52

53
54 Error bars depict standard deviation. * $p < 0.05$
55

56
57
58 **Video S1. Illustrative video of neurobehavioral tests in cases and controls.**
59
60
61
62
63
64
65

Figure 1

[Click here to download high resolution image](#)

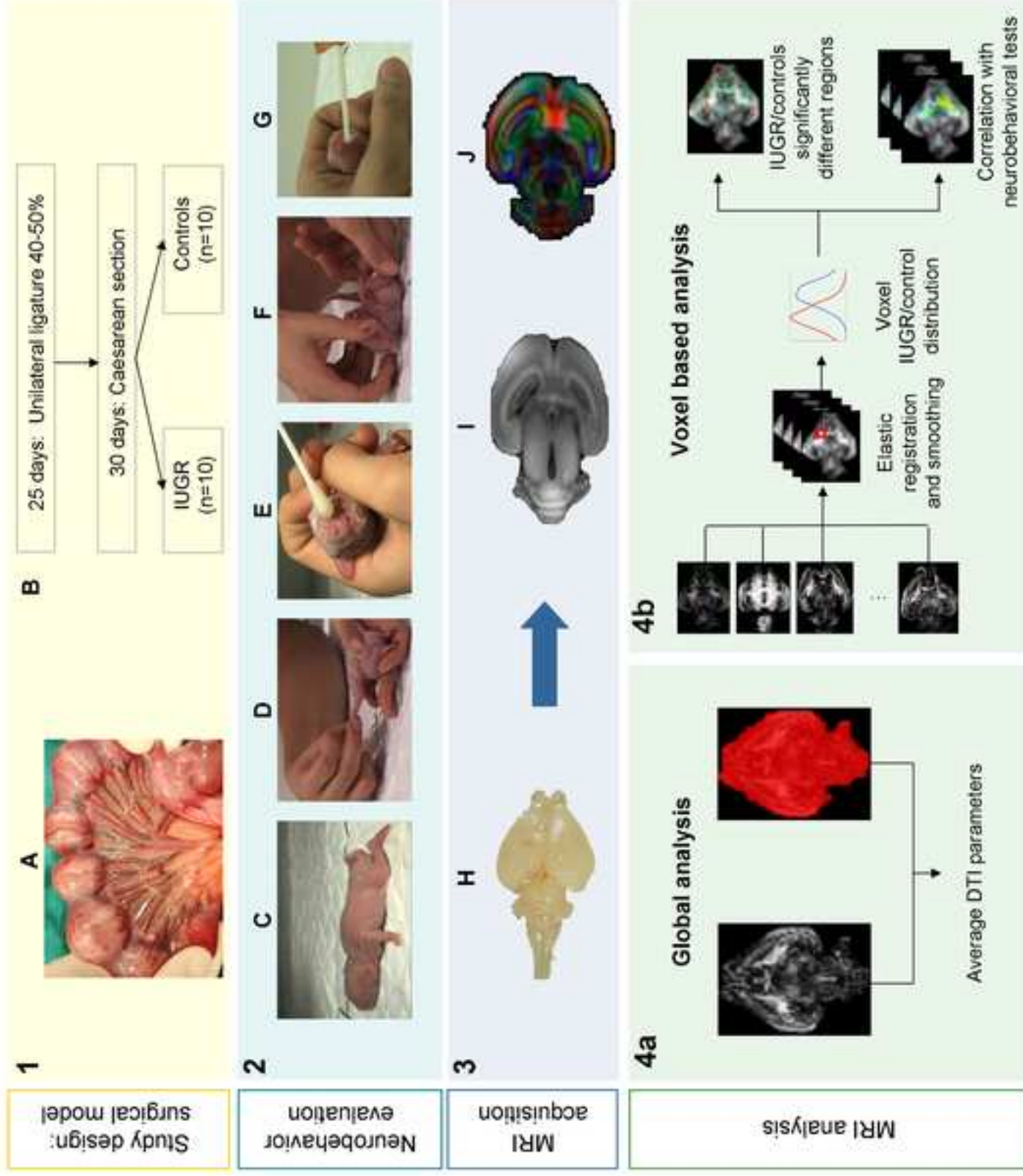


Figure 2
[Click here to download high resolution image](#)

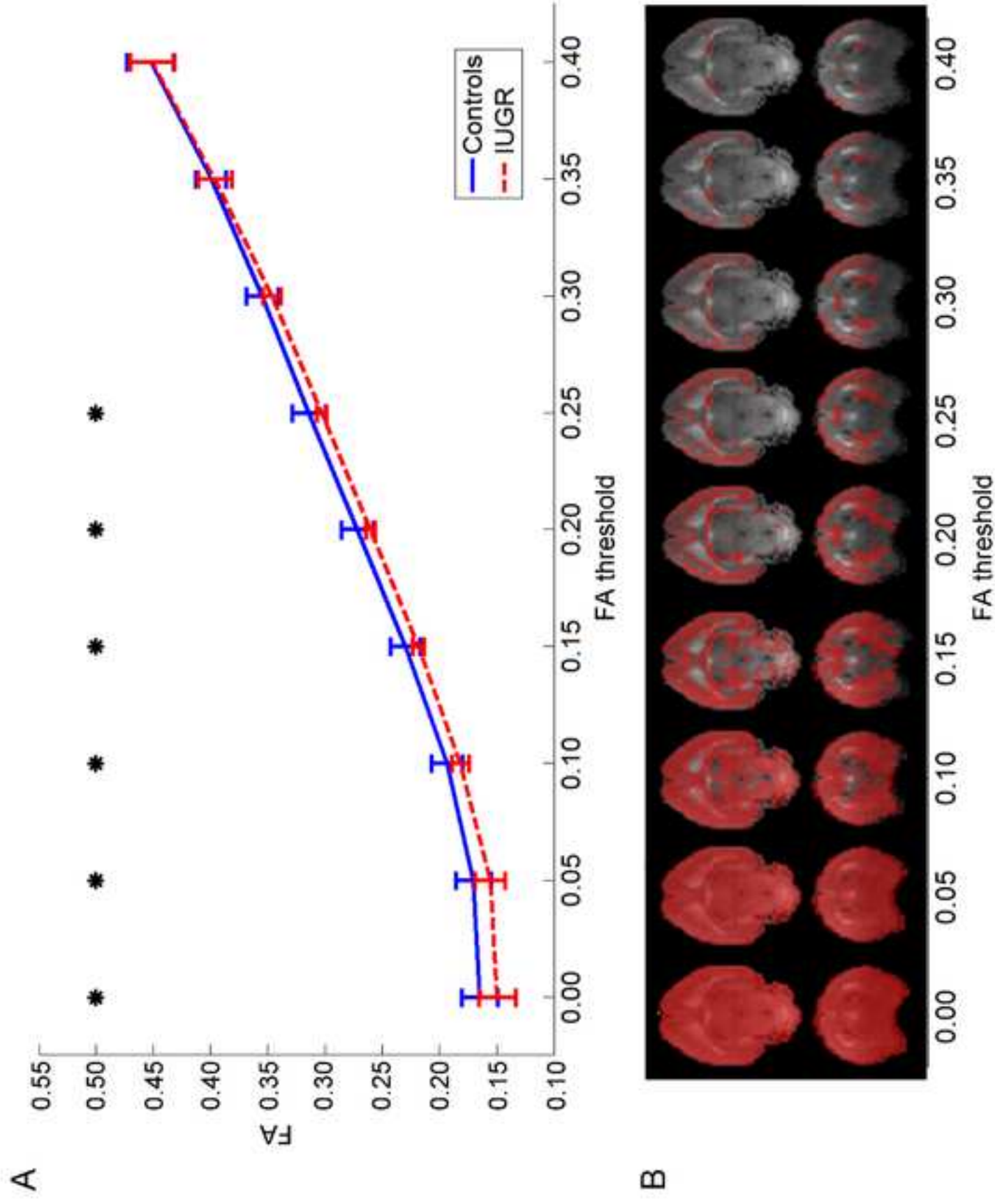


Figure 3
[Click here to download high resolution image](#)

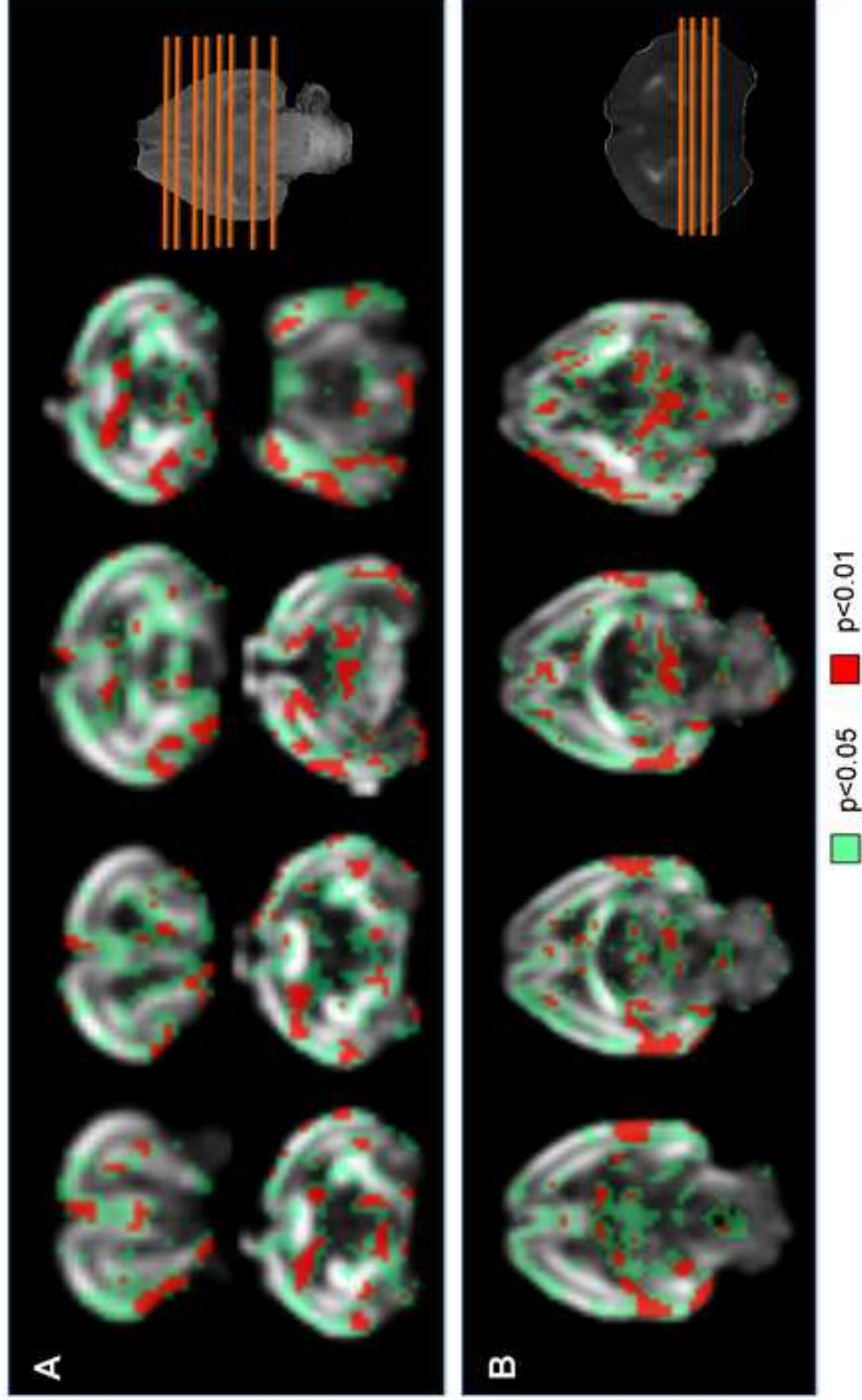
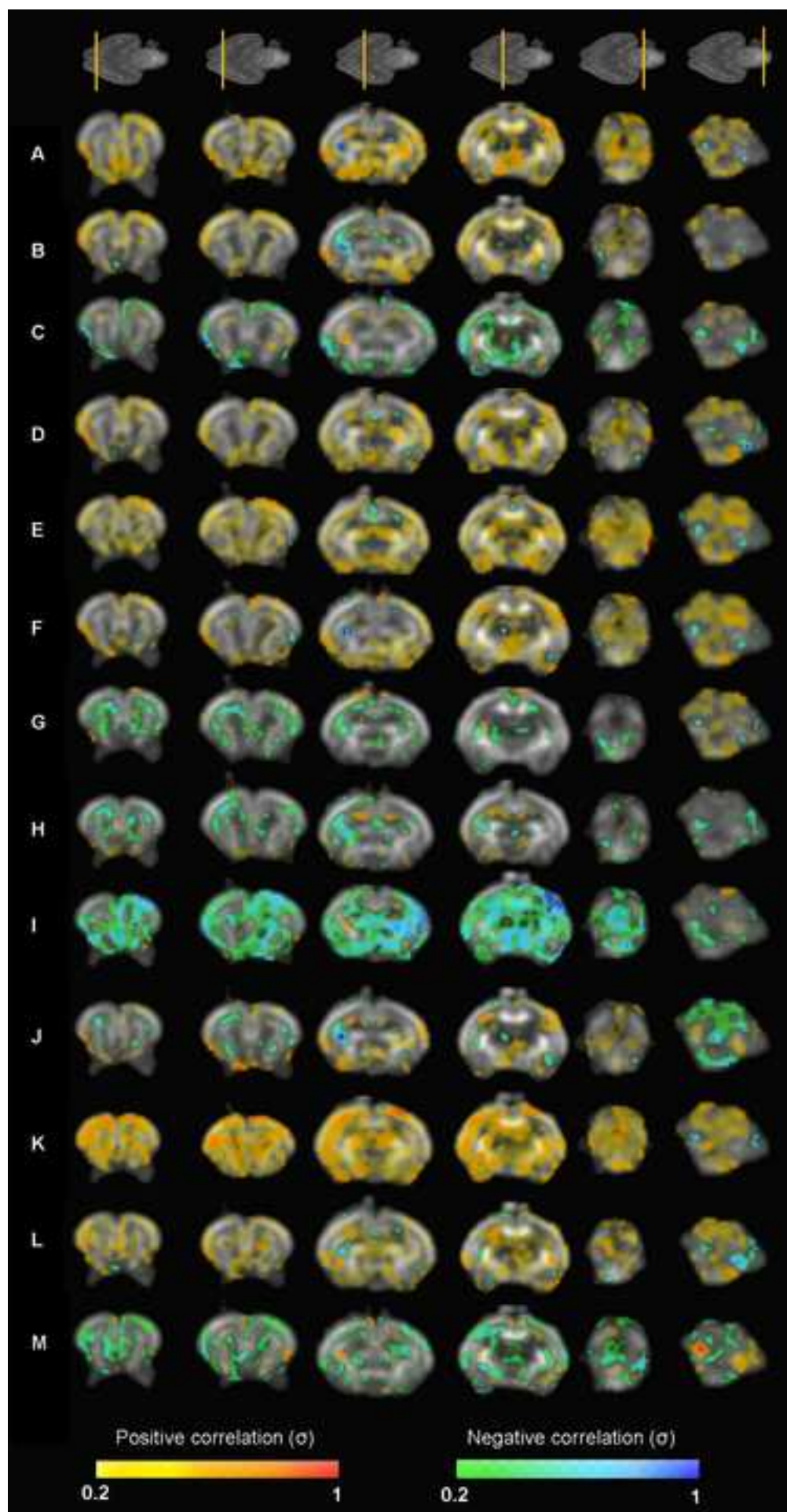


Figure 4

[Click here to download high resolution image](#)



1 **Table 1. Neurobehavioral test results in study groups.**

	<i>Control</i> <i>n=10</i>	<i>IUGR</i> <i>n=10</i>	<i>p</i>
Posture, score*	3.0 (0)	3.0 (1)	0.143
Righting reflex, number of turns	8.7 (1.5)	6.3 (3.0)	0.035
Tone, score*	0 (0)	1.0 (1.5)	0.019
Locomotion, score*	3.0 (0)	2.0 (2)	0.005
Circular motion, score*	2.0 (1)	2.0 (1)	0.247
Intensity, score*	3.0 (0)	2.5 (2)	0.089
Duration, score*	2.0 (0)	1.5 (1)	0.052
Lineal movement, line crosses in 60 sec	2.8 (1.4)	1.1 (1.1)	0.009
Fore–hindpaw distance, mm †	0.7 (1.9)	7.6 (5.4)	0.007
Sucking and swallowing, score*	3.0 (1)	1 (2)	0.075
Head turn, score*	3.0 (1)	2.0 (1)	0.043
Smelling test, score *†	3.0 (1)	1.0 (0)	0.006
Smelling test time, sec †	4.0 (1)	8.5 (5)	0.021

2

3 IUGR: intrauterine growth restriction; sec: seconds; mm: millimetres.

4 Values are mean and standard deviation (mean (sd)) or median and interquartile
5 range (median (IQ)) when appropriate.

6 *U Mann-Whitney

7 †Data available for 7 controls and 8 cases.

Table 2[Click here to download Table: Table 2.doc](#)

1 **Table 2. Whole brain and white matter global analysis of diffusion parameters in**
 2 **study groups.**

	<i>Control n=10</i>	<i>IUGR n=10</i>	<i>p</i>
Whole brain			
Fractional anisotropy	0.16 (0.02)	0.15 (0.02)	0.048
Apparent Diffusion Coefficient ($\times 10^{-3}\text{mm}^2/\text{s}$)*	0.44 (0.08)	0.47 (0.10)	0.353
Axial diffusivity ($\times 10^{-3}\text{mm}^2/\text{s}$)*	0.52 (0.10)	0.54 (0.11)	0.393
Radial diffusivity ($\times 10^{-3}\text{mm}^2/\text{s}$)*	0.41 (0.07)	0.43 (0.10)	0.393
Sphericity (C_s)	0.74 (0.02)	0.76 (0.02)	0.061
Linearity (C_l)	0.16 (0.02)	0.15 (0.02)	0.044
Planarity (C_p)	0.10 (0.01)	0.10 (0.01)	0.368
White matter (threshold $FA > 0.2$)			
Fractional anisotropy	0.27 (0.01)	0.26(0.00)	0.019
Apparent Diffusion Coefficient ($\times 10^{-3}\text{mm}^2/\text{s}$)*	0.42(0.08)	0.44(0.11)	0.353
Axial diffusivity ($\times 10^{-3}\text{mm}^2/\text{s}$)*	0.55 (0.10)	0.58 (0.15)	0.393
Radial diffusivity ($\times 10^{-3}\text{mm}^2/\text{s}$)*	0.36 (0.06)	0.38 (0.09)	0.247
Sphericity (C_s)	0.60 (0.02)	0.61 (0.01)	0.033
Linearity (C_l)	0.29 (0.02)	0.28 (0.02)	0.201
Planarity (C_p)	0.11 (0.02)	0.11 (0.03)	0.877

3

4 Values are mean and standard deviation (mean (sd)) or median and interquartile
 5 range (median (IQ)) when appropriate.

6 *U Mann-Whitney

1 **Table 3. Mean correlation coefficients between diffusion parameters and**
 2 **neurobehavioral test results (Pearson's r correlation)**
 3

	<i>Fractional Anisotropy</i>	<i>Apparent Diffusion Coefficient</i>	<i>Fractional Anisotropy (FA>0.2)</i>	<i>Apparent Diffusion Coefficient (FA>0.2)</i>
Posture	0.260	0.007	0.242	-0.042
Righting reflex	0.043	0.098	0.172	0.035
Tone	0.092	-0.110	0.238	-0.105
Tone2	-0.092	0.110	-0.238	0.105
Locomotion	0.206	-0.265	0.213	-0.315
Circular motion	0.382	-0.153	0.342	-0.213
Intensity	0.241	-0.135	0.266	-0.148
Duration	-0.081	-0.234	0.011	-0.272
Lineal movement	0.018	0.198	0.035	0.182
Fore–hindpaw distance	-0.458	0.181	-0.448	0.240
Sucking and swallowing	0.150	0.118	0.446	0.096
Head turn	0.540*	-0.158	0.619**	-0.135
Smelling test	0.287	-0.428	0.200	-0.365
Smelling test time	-0.091	-0.013	-0.314	0.007

4 * p<0.05, **p<0.001

1 **Table 4. Correlations between neurobehavioral domains and fractional anisotropy in brain**
 2 **regions**

		Positive correlation	Negative correlations
Posture	Cx:	Frontal*, occipital*, temporal*	
	GM:	Brain stem, thalamus*	
	WM:	Anterior commissure*, corona radiata, fimbria of hippocampus*, olfactory tract*, Optic tract	
Righting reflex	Cx:	Frontal, occipital*, temporal*	
	GM:		Caudate nucleus*
	WM:	Anterior commissure*, olfactory tract	
Tone	Cx:		Frontal*, occipital*, temporal*
	GM:	Caudate nucleus*	
	WM:		Optic tract*
Locomotion	Cx:	Insular*, frontal*, prefrontal, occipital*, temporal*	
	GM:	Clastrum, hippocampus*, thalamus	
	WM:	Anterior commissure, fimbria of hippocampus*, lateral lemniscus*, olfactory tract	
Circular motion	Cx:	Frontal*, occipital*, temporal*	
	GM:	Brain stem, hippocampus*, thalamus*	
	WM:	Corona radiata*, fimbria of hippocampus*	
Intensity	Cx:	Insular*, temporal*	
	GM:	Clastrum*, hippocampus*, inferior colliculus	
	WM:	Olfactory tract*, optic tract*	
Duration	GM:	Brain stem	
	WM:		Corona radiata
Lineal movement	GM:	Hippocampus*	Caudate nucleus*, claustrum*
Fore–hindpaw distance	Cx:		Frontal*, occipital*, temporal*
	GM:	Caudate nucleus*	Hippocampus*, thalamus
	WM:	Corona radiata, olfactory tract	Fimbria of hippocampus*, internal capsule*, lateral lemniscus*
Sucking and swallowing	Cx:	Frontal*, Occipital*, Temporal*	
	WM:	Corpus callosum, fimbria of hippocampus*, lateral and medial lemniscus, olfactory tract	
Head turn	Cx:	Frontal*, Occipital*, Temporal*	
	GM:	Brain stem, caudate nucleus*, claustrum, hippocampus*, putamen*, thalamus*, vermis	
	WM:	Anterior comissure*, corona radiata*, internal capsule*, fimbria of	

Smelling test	Cx:	hippocampus*, olfactory tract	Cerebellar hemisphere and vermis, hippocampus Corpus callosum, corona radiata, olfactory tract Prefrontal, temporal*
	GM:	Prefrontal*, temporal*	
	WM:	Hippocampus, thalamus	
Smelling test time	Cx:	Olfactory tract*	Vermis Lateral lemniscus*
	GM:	Caudate nucleus*, hippocampus	
	WM:	Corona radiata, corpus callosum	

1

2 Cx: cortex, GM: gray matter; WM: white matter. *p<0.05

Figure S1

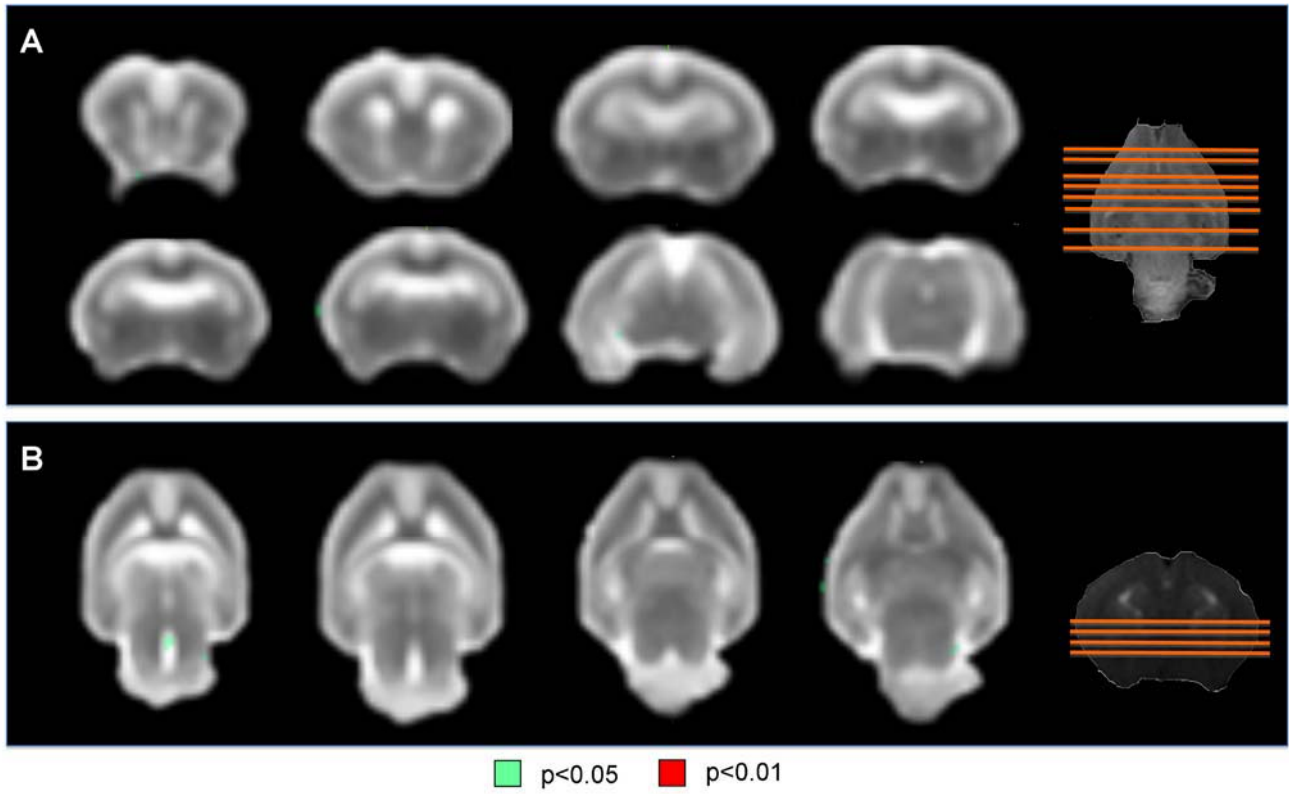


Figure S2

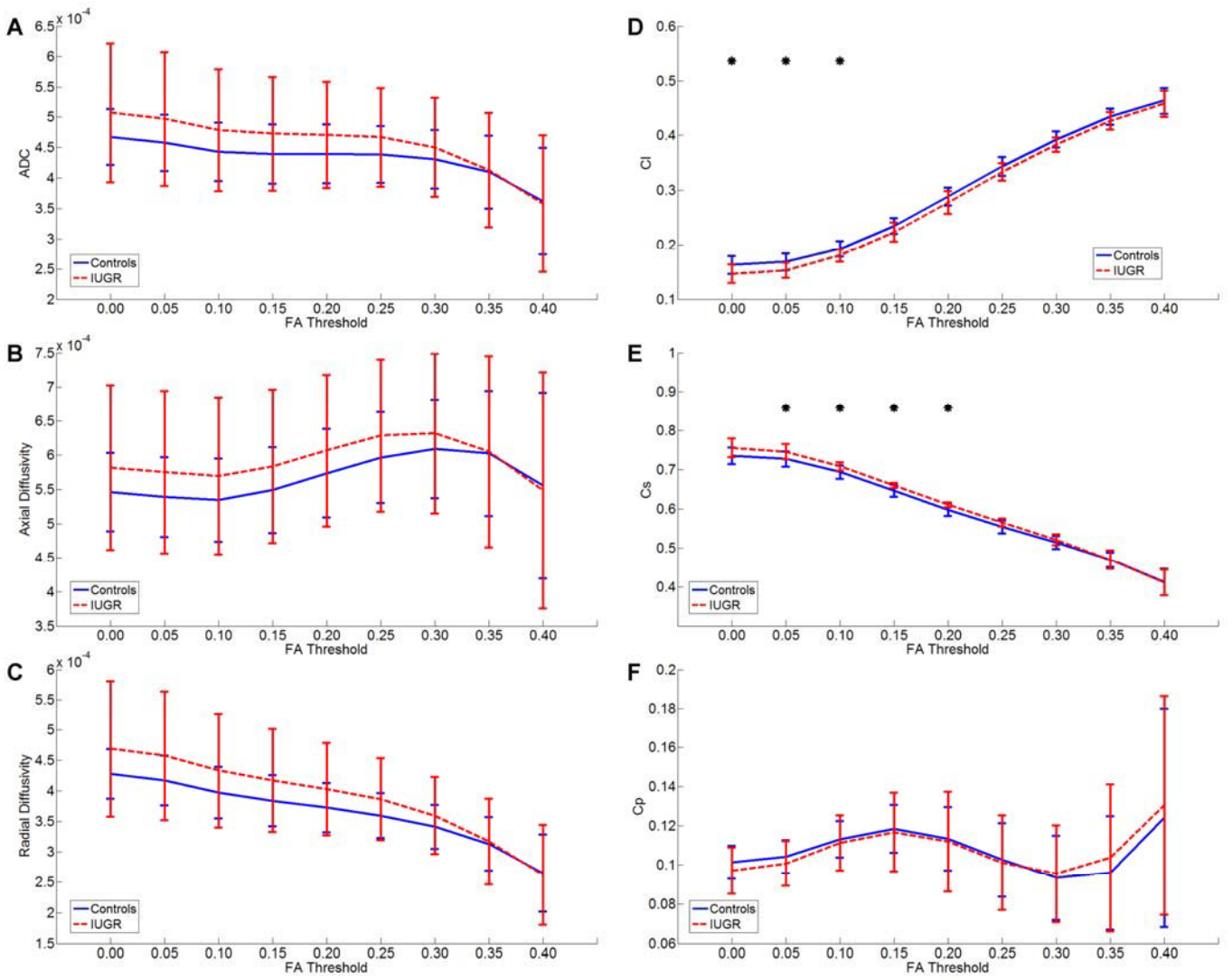


Table S1— Regional analysis of diffusion parameters in study groups.

	Fractional Anisotropy			Apparent Diffusion Coefficient ($\times 10^{-3} \text{mm}^2/\text{s}$)		
	Control n=10	IUGR n=10	p	Control n=10	IUGR n=10	p
White matter structures						
Corpus callosum	0.29 (0.04)	0.28 (0.03)	n.s.	0.35 (0.07)	0.34 (0.11)	n.s.
Left internal capsule	0.26 (0.03)	0.27 (0.04)	n.s.	0.37 (0.09)	0.37 (0.08)	n.s.
Right internal capsule	0.27 (0.02)	0.25 (0.03)	n.s.	0.36 (0.10)	0.38 (0.13)	n.s.
Left fimbria of hippocampus	0.37 (0.05)	0.35 (0.04)	n.s.	0.40 (0.09)	0.40 (0.05)	n.s.
Right fimbria of hippocampus	0.40 (0.04)	0.36 (0.02)	0.048	0.40 (0.10)	0.36 (0.07)	n.s.
Left corona radiata	0.23 (0.04)	0.23 (0.04)	n.s.	0.40 (0.10)	0.39 (0.12)	n.s.
Right corona radiata	0.23 (0.04)	0.24 (0.04)	n.s.	0.41 (0.11)	0.40 (0.08)	n.s.
Grey matter structures						
Cerebellar vermis	0.13 (0.02)	0.13 (0.02)	n.s.	0.47 (0.21)	0.48 (0.15)	n.s.
Left cerebellar hemisphere	0.11 (0.02)	0.11 (0.03)	n.s.	0.57 (0.26)	0.57(0.24)	n.s.
Right cerebellar hemisphere	0.11 (0.02)	0.12 (0.02)	n.s.	0.53 (0.19)	0.54 (0.21)	n.s.
Left putamen	0.18 (0.02)	0.17 (0.02)	n.s.	0.39 (0.11)	0.69 (0.10)	n.s.
Left caudate nucleus	0.18 (0.02)	0.17 (0.04)	n.s.	0.46 (0.10)	0.46 (0.10)	n.s.
Left thalamus	0.15 (0.02)	0.14 (0.02)	n.s.	0.41 (0.11)	0.41 (0.10)	n.s.
Right putamen	0.20 (0.02)	0.20 (0.03)	n.s.	0.38 (0.10)	0.37 (0.10)	n.s.
Right caudate nucleus	0.14 (0.02)	0.13 (0.02)	n.s.	0.50 (0.18)	0.51 (0.10)	n.s.
Right thalamus	0.15 (0.03)	0.14 (0.01)	n.s.	0.40 (0.09)	0.41 (0.08)	n.s.
Left prefrontal cortex	0.22 (0.03)	0.20 (0.02)	n.s.	0.54 (0.17)	0.52 (0.12)	n.s.
Right prefrontal cortex	0.17 (0.03)	0.17 (0.04)	n.s.	0.63 (0.15)	0.62 (0.14)	n.s.

IUGR: intrauterine growth restriction. Values are mean and standard deviation